UTILIZATION OF THE PRAIRIE DOG (CYNOMYS SP.) ANIMAL MODEL FOR THE STUDY OF MONKEYPOX VIRUS: PATHOGENICITY DIFFERENCES BETWEEN VIRAL CLADES AND THE EFFECT OF ANALGESICS ON VIRAL INFECTION IN VIVO

by

CHRISTINA LEIGH HUTSON

(Under the Direction of Tamas Nagy)

ABSTRACT

Since smallpox eradication, monkeypox virus (MPXV) became the most important human health-threat within genus *Orthopoxvirus*. Previous work demonstrated the prairie dog (PD) MPXV model closely mimics human disease, including development of skin rash. Additionally the model can be used to study pathogenicity differences between the more virulent Congo Basin (CB) MPXV and less virulent West African (WA) MPXV. The goal of this work was to utilize this animal model to further characterize differences in MPXV clade pathogenesis (including apoptosis and NFkB inhibition), and additionally to compare viral pathogenesis/disease presentation in MPXV challenged PDs treated with analgesics. In initial studies, PDs were intranasally infected ($8x10^3$p.f.u.) with CB or WA MPXV, and tissues were harvested on subsequent days. Virus was recovered from tissues earlier in CB challenged animals (day 4) than WA challenged animals (day 6). CB MPXV spread more rapidly,

accumulated to greater levels, and caused greater morbidity. Further analysis on these tissues was done to determine levels of apoptosis and NFkB activation. In our study, CB MPXV was able to inhibit NFkB in more tissues compared to WA MPXV, but resulted in increased apoptosis. This indicates that circumventing the NFkB pathway may be more important in resulting virulence/pathogenicity than apoptosis inhibition. Additional studies to look at the effect of two common analgesics on MPXV disease progression were done. Understanding whether analgesic agents would affect disease progression is critical when planning animal challenge studies. To investigate this, PDs were challenged with WA MPXV ($4X10^3$ pfu) and treated with Metacam (NSAID) or Buprenorphine (opioid). MPXV controls and treatment controls were compared to challenged/treated animals. Disease progression was similar in challenged animals; with the exception of two deaths in the Metacam-treated group. Only subtle differences were seen comparing Buprenorphine-treated MPXV infected animals to controls. Taken together, these findings allow for further characterization of differences between MPXV clade pathogenesis, including identifying early sites during viral replication, cellular response to viral infection and mechanisms the virus uses to evade the immune response. Additionally, we showed that the PD-MPXV model may receive Buprenorphine for short-term pain relief, however NSAIDs should be avoided during challenge studies.

INDEX WORDS: Orthopoxvirus; Monkeypox; Pathogenesis; Animal model; In vivo; NFkB; Apoptosis; Analgesic

UTILIZATION OF THE PRAIRIE DOG (CYNOMYS SP.) ANIMAL MODEL FOR THE STUDY OF MONKEYPOX VIRUS: PATHOGENICITY DIFFERENCES BETWEEN VIRAL CLADES AND THE EFFECT OF ANALGESICS ON VIRAL INFECTION IN VIVO

by

CHRISTINA LEIGH HUTSON

BS, Berry College, 2001

MS, The University of Georgia, 2003

A Dissertation Submitted to the Graduate Faculty of The University of Georgia in Partial Fulfillment of the Requirements for the Degree

DOCTOR OF PHILOSOPHY

ATHENS, GEORGIA

2015

UTILIZATION OF THE PRAIRIE DOG (CYNOMYS SP.) ANIMAL MODEL FOR THE STUDY OF MONKEYPOX VIRUS: PATHOGENICITY DIFFERENCES BETWEEN VIRAL CLADES AND THE EFFECT OF ANALGESICS ON VIRAL INFECTION IN VIVO

by

CHRISTINA LEIGH HUTSON

Major Professor:	Tamas Nagy
Committee:	Corrie C. Brown
	Darin S. Carroll
	Zhen Fu
	Robert J. Hogan

Electronic Version Approved:

Julie Coffield
Interim Dean of the Graduate School
The University of Georgia
May 2015

DEDICATION

Loving thanks has to be given to my sweet kids, who sometimes had to deal with a stressed-out Mommy. Hadlee and Tanner, I love you so much and am so grateful for you. I hope you know that everything that I do is always for you. I hope that you will always be proud of me and my accomplishments, just as I am always so proud of you both. To my husband Travis, who was so simply supportive. You picked up the slack when needed so that I could finish my degree without complaint or ill-will and I hope you know how much I love you for that gift. To my parents Jim and Velma, who have always been the most supportive, incredible parents any person could ask for. Thank you for supporting me, encouraging me, and always being in my corner no matter what. For all of the support and encouragement from my other friends and family: Sheila, Drew, Jason, Anne, Cody, and Shaye, as well as all of the other family and friends who have wished me encouragement, thank you!!

ACKNOWLEDGEMENTS

I first must thank Dr. Darin Carroll, Dr. Victoria Olson and Dr. Kevin Karem. Without your support and encouragement, I would not have begun the journey to attain my PhD. Thanks to you all for ALWAYS being in my corner! A sincere thank you to my major professor, Dr. Tamas Nagy for allowing me the opportunity to work on my degree under his mentorship. To my committee members, thanks so much for your guidance, support, input and suggestions. To all of the co-authors on the three manuscripts that form the body of my dissertation, thank you for all of your assistance, input and support, especially Dr. Nadia Gallardo-Romero, who was an invaluable right-hand woman and cheerleader for me during some of the trying times. Dr. Russ Regnery, thank you for giving me the opportunity to work under your mentorship when I first came to CDC. And a special thanks to all those other Pox peeps who always made my time in the lab enjoyable!

TABLE OF CONTENTS

Page

LIST OF TABLES

Page

LIST OF FIGURES

Page

CHAPTER 1

INTRODUCTION AND LITERATURE REVIEW

Monkeypox virus (MPXV) and variola virus (the causative agent of smallpox) are members of the genus *Orthopoxvirus*. While smallpox has been eradicated from the human population and viral isolates only remain in secure Biosafety Level 4 laboratories; MPXV is a zoonotic pathogen endemic to Central and Western Africa where it can cause human infection and even mortality, and is maintained in the wild by undetermined rodent reservoir(s) [1–3]. In 2003 MPXV caused the first outbreak of human disease outside of Africa within the United States [4]. The virus was introduced due to importation of infected rodents destined for the pet trade industry; human disease resulted from the subsequent infection of pet North American black-tailed prairie dogs (*Cynomys ludovicianus)* which in turn efficiently transmitted disease to humans [5,6]. Anecdotally, it appeared prairie dogs transmitted MPXV within households, pet store, or other settings. Previous studies have defined two distinct MPXV clades, West African and Congo Basin [7,8]; the U.S. outbreak was due to an importation of the West African clade MPXV. In humans, West African MPXV causes a milder disease, <1% mortality and is rarely associated with person to person transmission [9,10]. However, Congo Basin MPXV causes approximately 10% mortality and human to human transmission has been observed; up to six sequential interhuman transmission events have been laboratory-documented [11]. The reasons for the differences in MPXV clade pathogenicity have not yet been explained.

As evidenced by the 2003 US outbreak, as well as the ongoing outbreaks of MPXV within Africa, there is a continued need to study this important human health threat.

Additionally, MPXV provides a surrogate for the study of related orthopoxviruses including variola virus. An ideal animal model is one that would emulate key features of human disease including: utilizing a route of infection that mimics the natural transmission of the pathogen in humans; the ability to obtain disease with an infectious dose equivalent to that causing disease in humans; as well as having a disease course, morbidity and mortality similar to what is observed with human disease. The development of small animal models for the study of MPXV has been quite extensive for the relatively short period of time this pathogen has been known, although most of these animal models have not proven to be good representatives of monkeypox disease within humans [12]. MPXV causes human disease characterized by an approximately 13 day incubation period (average of 12-14 days) followed by a prodrome of fever for 1-3 days [13]. Following the prodrome, disseminated skin lesions begin to appear; developing first as macules, then papules to vesicles to pustules. The pustules begin to scab approximately 4 weeks after initial infection. Previous studies of the prairie dog MPXV model showed after intranasal or scarification challenge with a reasonable challenge dose, animals developed disease that closely resembled human monkeypox, including an incubation period of approximately 10-13 days followed approximately 2 days later by generalized cutaneous lesions [14,15]. It has been challenging to truly identify a fever stage simply due to difficulties in temperature monitoring of the animals and their normal variations; however, a prodrome characterized by inappetence is consistently observed with this animal model. Skin lesions begin to scab approximately 24 days after onset. This model has allowed for the characterization of monkeypox disease including virus shedding (from the oral cavity shedding begins prior to lesion onset), the occurrence of viremia, and finally the serologic detection of anti-orthopoxvirus antibodies at or near the onset of lesion formation. Additionally, the prairie dog MPXV model has been utilized to describe

observed differences between disease manifestations of the viral clades as well as comparisons of transmissibility of the 2 clades within this animal model [14,16,17]. We have also utilized the prairie dog MPXV model for the study of vaccine efficacy and antiviral benefit as well as for the study of potential pathogenic viral genes [18–20]. Therefore having a complete description of the viral kinetics and pathology of MPXV within this model is critical when evaluating efficacy of potential therapeutic agents. Additionally the model may be useful for elucidating the reason(s) for the differences in pathogenicity between the MPXV clades.

One possible explanation for the increased virulence of the Congo Basin MPXV clade, is that the virus may be better equipped at evading the host's immune response after infection. Orthopoxviruses, including MPXV, appear to have acquired several mechanisms to evade the hosts' immune system. One of these evasion techniques is the inhibition of nuclear factor kappa-light-chain-enhancer of activated B cells (NF-κB) activation. Orthopoxviruses, have been shown to encode multiple proteins that act in various ways to prevent NF-κB activity [21,22]. NF-κB is a mammalian transcription factor that regulates stress, immune response, and is an important component in the progression of inflammatory diseases. Viral inhibition of apoptosis, or programmed cell death has also been implicated as a possible mechanism of viral evasion of the host immune response [22]. Apoptosis, or programmed cell death, is used by the cell to protect itself after injury, including when viral invasion occurs. As the Congo Basin Clade MPXV is more virulent than West African MPXV in both humans and animal models, it is possible that this increased virulence is at least in part due to differences in the ability of these viruses to inhibit the innate immune system, including these two critical pathways, NFkB activation and apoptosis.

The nuclear factor KappaB (NF-κB) is a mammalian transcription factor that regulates stress, immune response, and is an important component in the progression of inflammatory diseases. The NF- κB family is composed of homo- and heterodimers of Rel proteins; these include NF- κB1 (p105/p50), NF- κB2 (p100/p52), RelA (p65), RelB, and c-rel (Rel). RelA (p65) and p50 exist in the majority of mammalian tissue types, while RelB expression is limited to sites such as the thymus, Peyer's patches and lymph nodes [23]. There are two main mechanisms known to activate the NF- κB signaling pathway which are termed the classic pathway or the alternate pathway. These pathways can be activated simultaneously, or at separate times; however they are mediated by different regulatory functions. The classic pathway involves the subunits p50 and p65 and IkB as its cytoplasmic inhibitor. This heterodimer p50/p65 is considered an anti-apoptotic gene regulator. The alternate pathway involves the activation of subunits p50 and RelB. Under normal conditions, NF- κB complex resides in the cytoplasm, most often in its p50/p65 heterodimer form where it is tethered by a family of inhibitors of κB (IκB) proteins. Upon intra or extra cellular stimulation of the cells by an assortment of stressors, including inflammation caused by viral agents (such as poxviruses) [24], IκB is phosphorylated on two serine residues, which triggers its degradation [25]. After the degradation of IκB, NF- κB is free to enter the nucleus where it is involved in the transcription of many pro-inflammatory and anti-apoptotic genes. In the nucleus, the p65 subunit is a strong activator for a wide variety of genes.

Apoptosis is a complex signaling pathway that can be triggered by different stimuli, including viral invasion. There are 2 main pathways that result in apoptosis, the intrinsic (mitochondrial) and extrinsic (death receptor) pathways; it is possible for both the intrinsic and extrinsic pathways to be activated simultaneously within tissues [26]. Because apoptosis, or

programmed cell death, is used by the cell to protect itself after injury, including when viral invasion occurs viral inhibition of apoptosis has also been implicated as a possible mechanism of viral evasion of the host immune response by different viruses, including poxviruses [22].

Understanding how the virus is able to inhibit certain pathways such as NFkB and apoptosis, is important when planning animal challenge studies. Although much work has been done looking at how poxviruses inhibit the host immune system *in vitro*, there is less data from *in vivo* studies. Because the ability of orthopoxviruses to modulate NF-κB activation likely plays an important role in the ability of these viruses to cause disease, the utilization of substances that inhibit NF-κB activation (such as non-steroidal anti-inflammatory drugs (NSAIDS)) would very likely change the normal virus. However, different drugs have been shown to inhibit NF- κB via different mechanisms and therefore may have a different effect on the viral life cycle [27]. Aspirin, salicylates and NSAID drugs have all been shown to inhibit NF-κB activity [19]. Opiates do not affect the NF- κB pathway. However, tramadol (opiate) has been suggested to have immune enhancing effect in-vitro, while morphine (also classified as an opiate) is believed to suppress the immune response [28]. For these reasons, many animal studies involving orthopoxviruses do not utilize pain relieving drugs and are categorized as "class E pain" protocols. Understanding how these substances affect the NF-kB activity and resulting MPXV disease progression is critical when planning animal studies as well as making recommendations for pain-relieving agents during a human MPXV infection.

Human patients with MXPV infection report painful signs during the course of disease including headache, sore throat, back pain and mouth sores [29]. Therefore it is likely that animals infected with MXPV experience some degree of pain, especially during robust infections. However analgesics are often withheld during challenge studies with the reasoning

that viral disease course might be altered. Non-steroidal anti-inflammatory drugs (NSAIDs) are commonly prescribed to alleviate pain. These include salicylates, NSAIDs, and glucocorticoids to name a few. Metacam is commonly prescribed by veterinarians and falls into the NSAID category. However NSAIDs have been shown to inhibit the NF-κB which is the primary regulator of inflammation and plays a key role in regulating the immune response to different types of infection, including viral infection [30]. Opioids are also a common pain-reliving type of drug used to alleviate human and animal suffering. The justification for not using opioids during a viral challenge study is that these drugs have been shown to have multiple adverse effects that may exacerbate the morbidity of infected animals and may complicate the assessment of the immune response to the virus in an animal model. MPXV infection can cause respiratory distress which could be confused with the depression of respiratory function which can occur with opioid analgesics. In addition, opioid analgesics in rats have been shown to cause temperature deregulation and respiratory depression which could affect the safety of the animals during anesthesia and would also affect the behavior and eating habits of the animals. Because these animal experiments also seek to understand the immune response of the animals to the viral infection and opioid based analgesics could compromise the analysis of the immune response. Lastly, MPXV can affect liver function and this could be exacerbated by opioid use as many of these drugs are metabolized in the liver.

Previous work demonstrated the prairie dog MPXV model mimics human disease more closely than previous models, including the development of skin rash. Thus unlike other small animal models, utilizing the prairie dog MPXV model, therapeutics can be tested at time of rash onset. Additionally the model can be used to study differences in pathogenicity between the more virulent Congo Basin MPXV and the less virulent West African MPXV clade. The prairie

dog model will continue to be important in the testing of novel therapeutics and next generation vaccines and thus complete characterization of the model is necessary. The goal of this work was to utilize this animal model to further characterize differences in MPXV clade pathogenesis, compare levels of apoptosis and NFkB activation between clades in vivo, and additionally to compare viral pathogenesis and disease presentation in MPXV challenged prairie dogs treated with analgesics.

Specific Aim 1. The overreaching goal of this work was to fully characterize the viral kinetics and pathology of each of the MXPV clades within the prairie dog MPXV model. To do this, we challenged groups of prairie dogs with Congo Basin MPXV or West African MPXV (each at 8 X 10^3 PFU), animals were then sacrificed at early time points after infection, as well as once symptomatic, in order to infer distribution of virus and characterize tissue pathology. Viral loads in 28 different tissues from animals were collected and prepared for pathology or routine tissue culture. Molecular assays including histologic examination, immunohistochemistry, PCR, virologic titer, and immune response were completed for each animal and comparisons made between the MPXV clades.

Specific Aim 2. One possible explanation for the increased virulence of the Congo Basin MPXV clade, is that the virus may be better equipped at evading the host's immune response after infection. Orthopoxviruses, including MPXV, appear to have acquired several mechanisms to evade the hosts' immune system, including suppression of the NFkB and apoptosis pathways. Our second aim was designed to look at the amount of apoptosis and NFkB activation during an *in vivo* MPXV challenge, and to compare the activation levels between MXPV clades. Utilizing tissues collected during the prairie dog MPXV serial sacrifice study, we analysed spleen, kidney, liver and gallbladder for activation state levels of key proteins involved in the NF-κB pathway.

These tissues were chosen as they represented early, intermediate and late viral kinetics during a MPXV infection. Western blotting using standard techniques were completed with antibodies to examine the activation state and total protein levels of key proteins in the NF-κB pathway: IKKα, NF-κB p65/RelA and IκBα. For comparison purposes, tissues from PBS non-infected control animals were also analysed. Two cellular pathways that are upstream of NFkB activity include receptors that are termed Rig-I like receptors (RLRs) and Toll-like receptors (TLRs). These pathways are an important component of the innate immune response and have been shown to be important in detection of viral invasion and result in the translocation of NFkB subunits. Therefore, activation state and total protein levels of key proteins in both of these pathways (Rig-I, MyD88, TBK, IRAK4) were also examined via Western blot assays in spleen and liver from infected animals. Additionally, spleen and liver sections were fixed and analysed using immunohistochemistry analysis to look at levels of apoptosis in both the spleen and liver tissues from West African and CB MPXV infected prairie dogs.

Specific Aim 3. Human patients with MPXV infection report painful signs during the course of the disease; it is therefore reasonable to assume that animals infected with the virus experience some degree of pain. However, analgesics are often withheld during challenge studies with the reasoning that viral disease course might be altered. Understanding how analgesic agents affect MPXV disease progression is critical when planning animal studies as well as making recommendations for human infections. To complete aim 3, prairie dogs were challenged with a low dose ($4X10^3$ pfu) of West African MPXV and treated with Metacam (NSAID) or Buprenorphine (opioid). Another group of animals were challenged with MPXV and not treated. Additional groups of animals were treated with Metacam or Buprenorphine, but were not challenged with MPXV. Subsets of animals from each group were serially sacrificed

during the course of the study and samples obtained. By comparing disease progression, pathology, and molecular markers (blood chemistries, PCR, viral load, immune response) we sought to determine whether Metacam or Buprenorphine changed the disease course of MPXV infected prairie dogs.

Reference List

1. Breman JG, Nakano JH, Coffi E, Godfrey H, Gautun JC (1977) Human poxvirus disease after smallpox eradication. Am J Trop Med Hyg 26: 273-281.

2. Hutin YJ, Williams RJ, Malfait P, Pebody R, Loparev VN, Ropp SL, Rodriguez M, Knight JC, Tshioko FK, Khan AS, Szczeniowski MV, Esposito JJ (2001) Outbreak of human monkeypox, Democratic Republic of Congo, 1996 to 1997. Emerg Infect Dis 7: 434-438.

3. Khodakevich L, Szczeniowski M, Manbu mD, Jezek Z, Marennikova S, Nakano J, Messinger D (1987) The role of squirrels in sustaining monkeypox virus transmission. Trop Geogr Med 39: 115-122.

4. Centers for Disease Control and Prevention (2003) Update: multistate outbreak of monkeypox--Illinois, Indiana, Kansas, Missouri, Ohio, and Wisconsin, 2003. MMWR Morb Mortal Wkly Rep 52: 561-564.

5. Hutson CL, Lee KN, Abel J, Carroll DS, Montgomery JM, Olson VA, Li Y, Davidson W, Hughes C, Dillon M, Spurlock P, Kazmierczak JJ, Austin C, Miser L, Sorhage FE, Howell J, Davis JP, Reynolds MG, Braden Z, Karem KL, Damon IK, Regnery RL (2007) Monkeypox

zoonotic associations: insights from laboratory evaluation of animals associated with the multi-state US outbreak. Am J Trop Med Hyg 76: 757-768.

6. Reed KD, Melski JW, Graham MB, Regnery RL, Sotir MJ, Wegner MV, Kazmierczak JJ, Stratman EJ, Li Y, Fairley JA, Swain GR, Olson VA, Sargent EK, Kehl SC, Frace MA, Kline R, Foldy SL, Davis JP, Damon IK (2004) The detection of monkeypox in humans in the Western Hemisphere. N Engl J Med 350: 342-350.

7. Chen N, Li G, Liszewski MK, Atkinson JP, Jahrling PB, Feng Z, Schriewer J, Buck C, Wang C, Lefkowitz EJ, Esposito JJ, Harms T, Damon IK, Roper RL, Upton C, Buller RM (2005) Virulence differences between monkeypox virus isolates from West Africa and the Congo basin. Virology 340: 46-63.

8. Likos AM, Sammons SA, Olson VA, Frace AM, Li Y, Olsen-Rasmussen M, Davidson W, Galloway R, Khristova ML, Reynolds MG, Zhao H, Carroll DS, Curns A, Formenty P, Esposito JJ, Regnery RL, Damon IK (2005) A tale of two clades: monkeypox viruses. J Gen Virol 86: 2661-2672.

9. Breman JG, Kalisa R, Steniowski MV, Zanotto E, Gromyko AI, Arita I (1980) Human monkeypox, 1970-79. Bull World Health Organ 58: 165-182.

10. Foster SO, Brink EW, Hutchins DL, Pifer JM, Lourie B, Moser CR, Cummings EC, Kuteyi OE, Eke RE, Titus JB, Smith EA, Hicks JW, Foege WH (1972) Human monkeypox. Bull World Health Organ 46: 569-576.

11. Learned LA, Reynolds MG, Wassa DW, Li Y, Olson VA, Karem K, Stempora LL, Braden ZH, Kline R, Likos A, Libama F, Moudzeo H, Bolanda JD, Tarangonia P, Boumandoki P, Formenty P, Harvey JM, Damon IK (2005) Extended interhuman transmission of monkeypox in a hospital community in the Republic of the Congo, 2003. Am J Trop Med Hyg 73: 428-434.

12. Hutson CL, Damon IK (2010) Monkeypox Virus Infections in Small Animal Models for Evaluation of Anti-Poxvirus Agents. Viruses 2: 2763-2776.

13. Henderson DA (2002) Smallpox: clinical and epidemiologic features. Med Health R I 85: 107-108.

14. Hutson CL, Olson VA, Carroll DS, Abel JA, Hughes CM, Braden ZH, Weiss S, Self J, Osorio JE, Hudson PN, Dillon M, Karem KL, Damon IK, Regnery RL (2009) A prairie dog animal model of systemic orthopoxvirus disease using West African and Congo Basin strains of monkeypox virus. J Gen Virol 90: 323-333.

15. Hutson CL, Carroll DS, Self J, Weiss S, Hughes CM, Braden Z, Olson VA, Smith SK, Karem KL, Regnery RL, Damon IK (2010) Dosage comparison of Congo Basin and West African strains of monkeypox virus using a prairie dog animal model of systemic orthopoxvirus disease. Virology 402: 72-82.

16. Hutson CL, Gallardo-Romero N, Carroll DS, Clemmons C, Salzer JS, Nagy T, Hughes CM, Olson VA, Karem KL, Damon IK (2013) Transmissibility of the monkeypox virus clades via respiratory transmission: investigation using the prairie dog-monkeypox virus challenge system. PLoS One 8: e55488. 10.1371/journal.pone.0055488 [doi];PONE-D-12-23800 [pii].

17. Hutson CL, Carroll DS, Gallardo-Romero N, Weiss S, Clemmons C, Hughes CM, Salzer JS, Olson VA, Abel J, Karem KL, Damon IK (2011) Monkeypox disease transmission in an experimental setting: prairie dog animal model. PLoS One 6: e28295. 10.1371/journal.pone.0028295 [doi];PONE-D-11-17293 [pii].

18. Keckler MS, Carroll DS, Gallardo-Romero NF, Lash RR, Salzer JS, Weiss SL, Patel N, Clemmons CJ, Smith SK, Hutson CL, Karem KL, Damon IK (2011) Establishment of the black-tailed prairie dog (Cynomys ludovicianus) as a novel animal model for comparing smallpox

vaccines administered preexposure in both high- and low-dose monkeypox virus challenges. J Virol 85: 7683-7698. JVI.02174-10 [pii];10.1128/JVI.02174-10 [doi].

19. Smith SK, Self J, Weiss S, Carroll D, Braden Z, Regnery RL, Davidson W, Jordan R, Hruby DE, Damon IK (2011) Effective antiviral treatment of systemic orthopoxvirus disease: ST-246 treatment of prairie dogs infected with monkeypox virus. J Virol 85: 9176-9187. JVI.02173-10 [pii];10.1128/JVI.02173-10 [doi].

20. Hudson PN, Self J, Weiss S, Braden Z, Xiao Y, Girgis NM, Emerson G, Hughes C, Sammons SA, Isaacs SN, Damon IK, Olson VA (2012) Elucidating the role of the complement control protein in monkeypox pathogenicity. PLoS One 7: e35086. 10.1371/journal.pone.0035086 [doi];PONE-D-11-15032 [pii].

21. Moss B, Shisler JL (2001) Immunology 101 at poxvirus U: immune evasion genes. Semin Immunol 13: 59-66. 10.1006/smim.2000.0296 [doi];S1044-5323(00)90296-3 [pii].

22. Seet BT, Johnston JB, Brunetti CR, Barrett JW, Everett H, Cameron C, Sypula J, Nazarian SH, Lucas A, McFadden G (2003) Poxviruses and immune evasion. Annu Rev Immunol 21: 377-423. 10.1146/annurev.immunol.21.120601.141049 [doi];120601.141049 [pii].

23. Li Q, Verma IM (2002) NF-kappaB regulation in the immune system. Nat Rev Immunol 2: 725-734. 10.1038/nri910 [doi];nri910 [pii].

24. Barnes PJ, Karin M (1997) Nuclear factor-kappaB: a pivotal transcription factor in chronic inflammatory diseases. N Engl J Med 336: 1066-1071. 10.1056/NEJM199704103361506 [doi].

25. Delhalle S, Blasius R, Dicato M, Diederich M (2004) A beginner's guide to NF-kappaB signaling pathways. Ann N Y Acad Sci 1030: 1-13. 1030/1/1 [pii];10.1196/annals.1329.002 [doi].

26. Strasser A, O'Connor L, Dixit VM (2000) Apoptosis signaling. Annu Rev Biochem 69: 217-245. 69/1/217 [pii];10.1146/annurev.biochem.69.1.217 [doi].

27. D'Acquisto F, May MJ, Ghosh S (2002) Inhibition of nuclear factor kappa B (NF-B): an emerging theme in anti-inflammatory therapies. Mol Interv 2: 22-35. 10.1124/mi.2.1.22 [doi];2/1/22 [pii].

28. Liu Z, Gao F, Tian Y (2006) Effects of morphine, fentanyl and tramadol on human immune response. J Huazhong Univ Sci Technolog Med Sci 26: 478-481.

29. Huhn GD, Bauer AM, Yorita K, Graham MB, Sejvar J, Likos A, Damon IK, Reynolds MG, Kuehnert MJ (2005) Clinical characteristics of human monkeypox, and risk factors for severe disease. Clin Infect Dis 41: 1742-1751.

30. Kopp E, Ghosh S (1994) Inhibition of NF-kappa B by sodium salicylate and aspirin. Science 265: 956-959.

CHAPTER 2

COMPARISON OF MONKEYPOX VIRUS CLADE KINETICS AND PATHOLOGY WITHIN THE PRAIRIE DOG ANIMAL MODEL USING A SERIAL SACRIFICE STUDY DESIGN[1]

[1] Christina L. Hutson, Darin S. Carroll, Nadia Gallardo-Romero, Clifton Drew, Sherif R. Zaki, Tamas Nagy, Christine Hughes, Victoria A. Olson, Jeanine Sanders, Nishi Patel, Scott K. Smith, M. Shannon Keckler, Kevin Karem,[a] Inger K. Damon. Submitted to BioMed Research International: Virology 2/1/2015.

Abstract

Monkeypox virus (MPXV) infection of the prairie dog is valuable to study systemic orthopoxvirus disease. To further characterize differences in MPXV clade pathogenesis, groups of prairie dogs were intranasally infected ($8x10^3$p.f.u.) with Congo Basin (CB) or West African (WA) MPXV, and 28 tissues were harvested days 2, 4, 6, 9, 12, 17 and 24 post infection. Samples were evaluated for the presence of virus, gross and microscopic lesions. Virus was recovered from nasal mucosa, oropharyngeal lymph nodes and spleen earlier in CB challenged animals (day 4) than WA challenged animals (day 6). For both groups, primary viremia (indicated by viral DNA) was seen days 6-9 through day 17. CB MPXV spread more rapidly, accumulated to greater levels, and caused greater morbidity in animals compared to WA MPXV. Histopathology and immunohistochemistry (IHC) findings, however, were similar. Two animals that succumbed to disease demonstrated abundant viral antigen in all organs tested, except for brain. These findings allow for further characterization of differences between MPXV clade pathogenesis, including identifying sites important during early viral replication and cellular response to viral infection.

Introduction

Orthopoxvirus members of the family *Poxviridae* include important current, or eradicated, human pathogens such as *monkeypox virus* (MPXV) and *variola virus* (the causative agent of smallpox). These viruses are closely related and disease progression and presentation during human infections are clinically similar with the exception of lymphadenopathy associated with human MPXV infections. Smallpox was solely a human pathogen, and an intense international campaign using surveillance, containment and vaccination, led to eradication of disease. However MPXV is a zoonosis, and remains endemic to the rain forests of Central and

Western Africa, with reports of sporadic human outbreaks and areas of prevalent disease. In the era post- eradication of smallpox and with the subsequent cessation of routine vaccination, there is a rising population of unvaccinated people with little to no protection against *Orthopoxvirus* infections, including MPXV [14]. Additionally, there is a concern, due to the waning population immunity, that either *variola virus* or MPXV could potentially be used as a bioterrorist weapon. Notably, MPXV caused an outbreak in the United States in 2003 due to importation of infected African rodents, which transmitted virus to pet black-tailed prairie dogs (*Cynomys ludovicianus)*, causing human infection, and demonstrating the ability of the disease to emerge outside of its normal ecological range [5,6].

Based on clinical presentation, epidemiologic characteristics, geographic location and genotyping, prior studies have identified 2 distinct MPXV clades, WA and CB [7,8]. CB MPXV is associated with approximately 10% mortality and can be transmit between humans; up to 6 sequential inter-human transmission events have been documented [11]. In comparison, WA MPXV is associated with milder disease, and person to person transmission has never been documented as the sole mode of transmission [9,10].

Although our understanding of this important human pathogen continues to increase, the disease pathogenesis is still only partially described. MPXV causes human disease characterized by an approximately 13 day incubation period (average of 12-14 days) followed by a prodrome of fever for 1-3 days [15]. Following the prodrome, disseminated skin lesions begin to appear; developing first as macules, then papules to vesicles to pustules. The pustules begin to scab approximately 4 weeks after initial infection. As seen in this study as well as previous prairie dog MPXV challenges, the prairie dog animal model also displays an incubation period of approximately 10-13 days followed approximately 2 days later by generalized cutaneous lesions

[12,13]. It has been challenging to truly identify a fever stage simply due to difficulties in temperature monitoring of the animals and their normal variations; however, a prodrome characterized by inappetence is consistently observed with this animal model. Skin lesions begin to scab approximately 24 days after onset. This model has allowed for the characterization of monkeypox disease including virus shedding (from the oral cavity shedding begins prior to lesion onset), the occurrence of viremia, and finally the serologic detection of anti-orthopoxvirus antibodies at or near the onset of lesion formation. Additionally, the prairie dog MPXV model has been utilized to describe observed differences between disease manifestations of the viral clades as well as comparisons of transmissibility of the 2 clades within this animal model [12,16,17]. We have also utilized the prairie dog MPXV model for the study of vaccine efficacy and antiviral benefit as well as for the study of potential pathogenic viral genes [18–20]

In the current study we challenged animals intranasally with an equivalent amount of Congo Basin (CB) or West African (WA) clade virus designed to cause symptomatic disease (8 X 10^3 p.f.u.). Animals were then sacrificed at early time points after infection, as well as once symptomatic, in order to infer distribution of virus and characterize tissue pathology. Viral dissemination/loads and tissue pathology in 28 different tissues on days 2, 4, 6, 9, 12, 17 and 24 were analyzed and compared. Antigen distribution utilizing IHC and virologic analyses of these samples has confirmed differences in disease progression between the 2 clades of MPXV, and identified sites important during early viral replication and cellular response to viral infection.

Materials and Methods

Animals

Wild-caught, juvenile black-tailed prairie dogs (PDs ;*Cynomys ludovicianus*) were obtained from Colorado. At time of infection, animals were approximately 10 months old and had been prescreened by a veterinarian, determined to be in good health status and found negative for the presence of anti-orthopoxvirus antibodies. A sterile passive integrated transponder (PIT) tag was injected subcutaneously at the base of the neck for animal identification and non-invasive recording of body temperature. The average starting weight for animals challenged with WA MPXV was 781 grams (range 488-965), and the average for CB MPXV challenged animals was 740 grams (range 549-899). During experimental infections animals were housed individually in large (12.13" x 23.38" x209.00") rat cages with aerosol filter tops. Cages were kept in a Duo-Flow biosafety cabinet in an animal Biological Safety Level-3 (ABSL-3) animal room. Animals were cared for in accordance with CDC Institutional Animal Care and Use Committee (IACUC) guidelines under an approved protocol (1683DAMPRAC). In addition to PD chow and hay, animals were provided with monkey biscuits for added dietary enrichment.

Viruses

The WA MPXV strain, MPXV-USA-2003-044, was isolated during the 2003 U.S. outbreak [6,8] and the CB MPXV strain, MPXV-ROC-2003-358, was collected from a 2003 outbreak of MPXV in the Republic of Congo (ROC) [8]. Both viruses have been fully sequenced and underwent 2 passages in African green monkey kidney cells (BSC-40) prior to seed pool production. The seed pool preparations were then grown in BSC-40 cells and sucrose-cushion purified prior to being used for animal challenges.

Animal inoculation

Inocula dosages ($8X10^3$ plaque forming units [p.f.u.]) were calculated based on the morbidity and mortality rates observed in the author's previous study. Briefly, a challenge dose of $6X10^3$ p.f.u. WA MPXV or $8X10^3$ p.f.u. CB MPXV resulted in disease morbidity including skin lesions and viral shedding identified in oral cavity samples in 100% of animals challenged [13]. Both virus strain stocks were diluted in phosphate-buffered saline (PBS). Inocula titers were immediately re-confirmed by standard plaque assay (as described below). Animals were infected by an intranasal (IN) route of inoculation while under general anesthesia using 5% isoflurane administered through a VetEquip Incorporated vaporizer. For each virus strain, animals were inoculated with 1 of the virus clades in a total volume of 10ul (5ul in each nostril). Additionally, 7 animals were mock infected with PBS.

Observations and sampling

Two animals challenged with virus from each MPXV clade as well as 1 PBS animal were pre-selected for euthanasia on days 2, 4, 6, 9, 12, 17 or 24 post infection (p.i.). For all 24 days of study post-infection, individual animals were observed for signs of morbidity, fever, malaise (inappetence, decreased activity, recumbent with reluctance to move, etc.) and clinical lesions, including rash. On scheduled euthanasia days (see above); oropharyngeal swabs, weights, and lesion counts were collected from all animals while under general anesthesia (as described above), before subsets of animals were sacrificed by humane euthanasia. For those animals euthanized, blood and necropsy samples were also collected. Additionally, 1 animal from each MPXV clade was serially bled throughout the study for determination of antibody kinetics. Strict euthanasia criteria were applied throughout the study as follows: any animal that became unresponsive to touch, lost 25% or more starting body weight, or accrued a total score of 10 on

the following scale was humanely euthanized; decreased activity (2 points); lethargy, unsteady gait, inappetence (3 points each); labored breathing and recumbence (5 points each).

Necropsy and tissue specimen collection

Necropsies on all animals were performed according to IACUC standards in an ABSL-3 laboratory and utilizing full ABSL-3 personal protective equipment (PPE). Samples taken during necropsy included: eyelid, eye, inner cheek tissue, tongue, nasal cavity tissue, tonsils, submandibular lymph nodes/salivary glands, mesentery lymph nodes, oropharynx tissue, trachea, gallbladder, lungs, heart, spleen, pancreas, kidney, liver, duodenum, jejunum, ileum, stomach, brain, gonad, belly skin, lesion if present, feces, urine or bladder tissue, oral swab, ocular swab, and blood. Instruments were cleaned and decontaminated with 5% Microchem and 70% ethanol between collections of each tissue. Tissues were frozen at -70°C prior to further processing. Oral and ocular swabs were collected with sterile individual Dacron swabs and stored frozen without diluent. Serum was separated from whole blood and processed for serology and clinical chemistry levels (see below). Tissues and swabs were subsequently processed and further prepared for DNA analysis, virus isolation, histopathology and immunohistochemistry (see below).

Sample preparation for PCR and viral growth

Sample processing was performed under BSL-2 conditions with BSL-3 work practices. The BioRobot EZ-1 Workstation (Qiagen) was used for genomic DNA extraction of all blood, swab and tissue samples. Samples were incubated with Qiagen buffer and proteinase K at 55ºC for an hour to degrade tissue and inactivate viable virus particles prior to DNA extraction. For whole blood samples, 100ul was used for DNA extraction, and the remaining blood was used for tissue culture propagation. For each swab collected, 400ul of PBS was added. The swab

extraction tube systems (SETS) (Roche) protocol was used to recover sample from the swab. DNA was extracted from 100ul of the swab lysate. The remaining swab eluate was used for virus isolation. For tissue preparation, 1ml aliquots of PBS and SPEX bead (SPEX Sample Prep) were prepared. The PBS/bead aliquot was then poured into a tube containing the individual tissue sample. The GenoGrinder 2000 (SPEX Sample Prep) was used following the manufacturer's instructions to create a tissue homogenate. 100ul of the homogenate was extracted for DNA isolation. The remaining homogenate was used for virus isolation.

Real-time PCR analysis

Samples were tested by real-time PCR using forward and reverse primers and probes complimentary to the conservednon-variola orthopoxvirus (OPXV) E9L (DNA polymerase) gene [21]. Purified MPXV DNA (10fg – 1ng) was used as standard controls to allow quantification of viral DNA. A sample was considered positive if duplicate reactions showed amplification crossing the threshold at cycle (CT) of 37 or earlier. A weakly positive sample displayed CT values 38-39 (duplicates).

Virus-tissue infectivity

All samples were stored at -70°C until virus isolation was attempted. Previous analyses demonstrated that real-time PCR detection is more sensitive than viability assays due to the ability to detect trace amounts of MPXV DNA in samples without viable virus [5]. Therefore, specimens were first tested for presence of OPXV DNA by PCR and, if positive, were subsequently evaluated for viable virus by tissue culture propagation. Each swab or tissue sample was titrated in duplicate using 10 fold dilutions of swab eluate or tissue slurry on BSC-40 cell monolayers, incubated at 35.5° C and 6% CO_2 for 72 hours, and subsequently stained with

crystal violet and formalin to visualize plaques. Titers were expressed as p.f.u. per milliliter of blood or swab eluate; or p.f.u. per gram of tissues.

Serologic analysis

A modified ELISA was used for analysis of anti-OPXV immunoglobulin types M and G in separated serum as previously described in detail [12,22] .

High content screening-green fluorescent protein (HCS-GFP) neutralization assay

All serum samples that were considered negative by ELISA were further tested with the HCS-GFP neutralization assay as described in Keckler et al. In brief, serum samples were serially diluted from 1:40 to 1:1280 and then neutralizing antibody (NAb) titers against vaccinia virus were measured using a GFP based assay. The HCS-GFP assay detects the percentage of GFP-producing responder cells (R), and this value is then normalized to control wells to produce the relative percent responders (RPR) titer. The reported values in this manuscript are 50% RPR titers that are equivalent to the serum dilution that neutralizes 50% of viral infection (ID_{50}) in a traditional plaque reduction neutralization titer (PRNT) assay. The 50% RPR titer was calculated using a modified variable slope sigmoidal equation (Hill equation, Levenberg Marquardt algorithm) and Prism 5.0 software (GraphPad) with goodness of fit to this sigmoidal curve (represented by R^2; all R^2 values considered positive were above 0.9000) calculated by the least-squares method.

Blood chemistry analysis

Serum was separated from whole blood, transferred to a clean tube and stored at -20ºC prior to analysis. The Piccolo blood chemistry analyzer (Abaxis) was utilized to determine the following blood chemistry profiles: sodium
(NA), potassium (K), total carbon dioxide (Tco2), chloride (CL), glucose (GLU), calcium (CA),

blood urea nitrogen (BUN), creatinine (CRE), alkaline phosphatase (ALP), alanine aminotransferase (ALT), aspertate aminotransferase (AST), total bilirubin (TBIL), albumin (ALB), and total protein (TP).

Histopathologic, immunohistochemical, and electron microscopy studies

After euthanasia, a necropsy was performed and tissues were taken as described above. Pieces of each tissue were fixed in 10% neutral-buffered formalin for at least 48 hours and then transferred to 70% ethanol for routine processing to create paraffin block which were subsequently sectioned at 3 μm. Routine hematoxylin-eosin (H&E) stains were performed for histopathological evaluation. Immunohistochemical tests using a multi-step immunoalkaline phosphatase technique were performed on sections using a previously described technique [23]. The primary antibody used for this test was a rabbit polyclonal anti-monkeypox or anti-smallpox antibody. For ultrastructural analysis, hematoxylin and eosin stained sections were processed for thin-section electron microscopy (EM). Briefly, sections were prepared on-slide and processed through a graded ethanol series to rehydrate the tissue for osmium tetroxide fixation. Tissue was then block stained with uranyl acetate and rinsed with water. The sample was microwave processed with ethanol to dehydrate, followed by acetone to prepare the tissue for resin infiltration. Following 4exchanges of resin, the tissue was polymerized in a final exchange of resin at 60ºC. Thin sections were cut and stained with uranyl acetate and lead citrate before viewing sections at the electron microscope (Tecnai Spirit, FEI, Hillsboro, OR).

Data analyses

As data were not normally distributed, nonparametric statistical analyses were used (Lehman, 1975). The Wilcoxon rank-sum test was utilized to compare the blood chemistry percent change (Percent change from day zero value to necropsy day value) for the WA MPXV,

CB MPXV, and PBS control animals, controlling for necropsy day. The p.f.u. value for each tissue type was compared between the CB MPXV and WA MPXV infected prairie dogs, controlling for day of necropsy using the Wilcoxon rank-sum test. A p-value of <= 0.05 was considered statistically significant. Data analysis was performed using SAS v9.3

Results

Clinical Observations and Gross Necropsy Findings

WA MPXV Clade

Animals appeared healthy, without objective signs or signs of illness until day 9. Gross observations of tissues from animals sacrificed on days 2, 4, and 6 were similarly indistinguishable from the control animals (Table 1.1). Beginning on day 9, the majority of infected animals displayed respiratory depression while under anesthesia. Other clinical signs and signs observed included inappetence, maculopapular cutaneous lesions forming on the medial aspect of the pelvic limbs of 2 animals, and nasal discharge in 1animal. During necropsy of PD15 on day 9, the kidneys were pale; the other animal euthanized at this time (PD16) was grossly normal. All remaining animals challenged with WA MPXV were observed to have disseminated cutaneous papules and/or vesicles by day 12 p.i (Table 1.1). Unexpectedly on day 12 p.i., PD21 expired from infection; this animal was noted to have nasal discharge and inappetence prior to death. During necropsy of PD21, hepatomegaly was noted as was bilateral hemorrhage on the horns of the uterus and the adipose tissue associated with the round ligament. Additionally, there were hyperemic foci associated with the ovaries and oviducts. On day 12, PDs 17 and 18 presented with submandibular lymphadenopathy and additionally, for PD17, hyperemic foci associated with the oviducts. PD 19 was necropsied on day 17 p.i.; inappetence

had been noted during infection but the activity of this animal appeared normal. Gross observations included lymphadenopathy, hemorrhagic foci in the adipose tissue associated with lymph nodes and multiple, smallfoci of hemorrhage on the visceral pleura of the lungs. On day 24, all cutaneous lesions had resolved at the time of necropsy for PD22 and PD20; however, pericarditis was observed in PD22. With the exception of disseminated skin lesions, morbidity for these 2 animals during the course of the study was not observed.

CB MPXV Clade

Clinically, all animals were healthy without discernible signs and signs of illness until day 9 (Table 1.2); in contrast, animals euthanized on scheduled day 4 manifest withfoci of serosal congestion in the stomach and colon (PD25), or foci of pleural congestion and serosal congestion in the stomach (PD 26). On day 6p.i. all animals were asymptomatic and grossly normal. As seen with the WA MPXV challenged animals, beginning on day 9 the majority of infected animals displayed respiratory depression while under anesthesia. Also observed on this sample day, 3 animals developed disseminated maculopapular cutaneous lesions and inappetence was noted for 1 animal. PD29 was necropsied on day 9 and was asymptomatic with no gross abnormalities. PD30 had developed cutaneous lesions (maculopapular or papular) and had nasal discharge; this animal died while under anesthesia. During necropsy, the lungs had multiple, randomly distributed foci of parenchymal hemorrhage. By day 12 p.i., 5/6 of the remaining animals had developed papular and/or vesicular cutaneous lesions; lesions were observed on the sixth animal by day 16 p.i. PD32 expired due to infection on day 12. This animal had developed inappetence, facial edema and cutaneous lesions before death. Necropsy of this animal revealed multiple hemorrhagic foci in the jejunum and submandibular lymphadenopathy . The other animal necropsied on this day (PD31) also had facial edema and disseminated papular cutaneous

lesions; necropsy results of internal organs were grossly normal. On day 13 p.i., PD36 had to be euthanized before the preselected euthanasia date due to measures of morbidity. This animal had nasal discharge and inappetence beginning on day 10 p.i. By day 12, the animal presented with papular/vesicular cutaneous lesions, periocular erythema and epiphora associated with 1 eye, purulent discharge from the nares, and a distended abdomen. During necropsy, gastrointestinal tract gas distention was observed. The uterus had foci of serosal hemorrhage; multiple hemorrhagic foci were observed in the periovarian adipose tissue. Mucosal associated lymphoid tissue (MALT) was hemorrhagic. Additionally, the cardia of the stomach showed mucosal hemorrhage. Both animals necropsied on day 17 (PDs 33 and 34) had facial edema that was diminishing at time of necropsy, purulent nasal discharge as well as crusted cutaneous lesions. Necropsy of PD33 revealed a focus of hemorrhage in the jejunum and multiple hemorrhagic foci were observed in the periovarian adipose tissue. PD34 appeared grossly normal. On the final time point, day 24 p.i., PD35 was recovering from infection. All cutaneous lesions were healing at time of necropsy and no abnormalities involving internal organs were seen during necropsy of this animal.

PBS Control animals

In regards to the 7 animals that were mock infected with PBS, 1 control animal was euthanized at each time point. None of these animals showed clinical signs indicative of MPXV infection during the course of the study. Additionally, gross necropsy observations did not indicate viral infection and all 7 animals were negative for viral DNA and OPXV antibodies.

Blood Chemistry Results

The mean percent value change from day zero to necropsy for each blood chemistry was compared between WA MPXV infected animals, CB MPXV infected animals and PBS controls,

controlling for day of necropsy (data not shown). No significant changes were observed in these blood chemistry values (p-values range 0.1-1). Sera from the 2 animals that died due to MPXV infection during the study were not available for analysis (PDs 21 and 32). However, when comparing pre and post-blood chemistry values in the animal euthanized on day 13 p.i. (PD36) liver enzyme levels were abnormal (increased alanine aminotransferase, decreased albumin and alkaline phosphatase), as we have seen in previous studies ([13,24]). Additionally glucose levels were elevated in PD36 most likely due to stress and/or the moribund state of the animal and blood urea nitrogen and sodium levels were increased

Immune Response

All serum samples collected from prairie dogs were negative by ELISA until day 12/13 p.i., at which time all 4 sacrificed animals had detectable orthopoxvirus antibodies (PDs 21 and 32 did not have serum available for analysis) (Figure 1.1a/b). Two animals that were serially bled throughout the study are used to illustrate the dramatic increase in antibody titer between days 12 and 17; levels appear to be beginning to plateau on day 24 p.i. Figure (Figure 1.1c). Although no antibodies were detected by ELISA before day 12, 2 animals sacrificed on day 9 (PD15 [WA MPXV] and PD29 [CB MPXV]) were shown to have neutralizing antibodies (Figure 1.1d). Antibody titers and neutralizing antibody levels were similar when comparing animals challenged with the 2 MPXV clades.

Kinetics of Viral Spread

Viremia

Viral DNA in blood samples was detectable from 3/4 animals on day 6 (2 CB MPXV and 1 WA MPXV infected animals) and all 4 euthanized animals on day 9 p.i. (Figure 1.2). The highest loads of viral DNA in the blood were seen on day 12; by day 24 p.i. viral DNA was

undetectable in all blood samples tested. Viable virus was only detected from 2 blood samples collected on day 12 from the 2 animals that perished due to infection (PDs 21 [WA MPXV] and 32 [CB MPXV]; Figure 1.2). Both of these animals had values of approximately $2X10^6$ p.f.u./mL of blood, suggesting that when viral loads are below this amount, we are unable to detect viable virus. A previous study has indicated that the methods utilized may not be sensitive enough to detect low levels of intact virions within blood samples [17].

WA MPXV Clade

On day 2 p.i. viral DNA was only detected in the submandibular lymph node/salivary gland from those animals challenged with WA MPXV. By day 4 additional tissues were positive for viral DNA including the tongue, nasal cavity, tonsils, oropharynx, lungs, heart, spleen, liver ileum, and stomach in at least 1 animal necropsied (Table 1.3). However, viable virus was not detected in any tissues until day 6 from those animals challenged with WA MPXV (Figure 1.3, Figure 1.4 and Table 1.3). Those tissues positive beginning on day 6 included nasal cavity, submandibular lymph nodes, spleen, tonsils as well as additional tissues as summarized (Figure 1.3). Of the sacrifice days chosen for this study, all tissues tested from the WA MPXV challenged animals were classified by onset of detectable viable virus: day 6, day 9 or day 12. The majority of tissues were positive for virus beginning on day 6 (Figure 1.3, Figure 1.4). Viral loads tended to be highest from tissues taken on day 12 p.i.; however nasal cavity yielded the highest level of virus ($7.7X10^8$pfu/gram (g)) compared to all other tissues on day 9, followed closely by liver ($5.7X10^8$pfu/g) and spleen ($4.9X10^8$pfu/g) tissues on day 12 (Table 1.3). Figure 1.4 illustrates the tissues that were positive for virus on each sample day for both MPXV clades. Noticeably, the mesenteric lymph nodes, stomach, heart and pancreas were only positive on day

12 p.i. for WA MPXV challenged animals, unlike the CB MPXV challenged animals. Urine/bladder tissue and feces were also analyzed for virus, and the WA MPXV challenged animals seem to shed virus longer from these samples compared to CB MXPV (Figure 1.4). On the last sample day (day 24 p.i.), 80% of the tissues were still positive for viral DNA, but only the lesion and fecal samples yielded viable virus (Table 1.3, Figure 1.4).

CB MPXV Clade

Beginning on day 2 p.i., low levels of viral DNA were detected from 1 animal in eyelid, nasal cavity, oropharynx and liver samples (Table 1.3). By day 4 p.i., 57.9% of tissues tested were positive for viral DNA, and unlike WA MPXV challenged animals in which no samples yielded viable virus on day 4 p.i., the nasal cavity, submandibular lymph node/salivary gland tissue, and spleen samples yielded viable virus from CB MPXV challenged animals (Figures 1.4, 1.5, Table 1.3). Therefore for the CB MXPV challenged animals, samples were classified into day 4, day 6, day 9 or day 12 viable virus onsets. As was seen for WA MXPV challenged animals, the majority of tissues were positive beginning on day 6. The majority of tissues had the highest viral load on day 12 similar to WA MXPV infected animals; for CB MPXV infected animals the liver ($2.9X10^9$) yielded the highest load followed by spleen, nasal cavity and lesion all on day 12 p.i. respectively ($7.5X10^8$, $2.6X10^8$, and $2.3X10^8$) (Table 1.3). At study end (day 24 p.i.), less than half of the tissues had detectable levels of viral DNA, and no samples were positive for viable virus from those animals challenged with CB MPXV.

Pathology Findings

Histopathologic, Immunohistochemical, and Electron Microscopy Findings

MPXV infected prairie dogs exhibited histologic changes attributable to viral infection beginning on day 6. Early changes for both MPXV clades were seen within the spleen which had prominent neutrophils within red pulp and increased apoptotic or necrotic cells in all 4 euthanized animals. Apoptotic or necrotic cells were seen in the lung from 1CB MPXV infected animal; 1 WA MPXV infected animal had prominent bronchus associated lymphoid tissue within the lung on day 6 p.i. Beginning on day 9 p.i., histopathologic changes attributable to viral infection were observed in 1or more animal at each time point and those data were compiled in the text below for each day and clade of virus. Additionally, IHC positive results were not obtained until day 9 p.i. from any infected animals and are summarized in Tables 1.1 and 1.2.

WA MPXV Clade

On day 9 p.i. dermal lesions characterized by epidermal spongiosis and vacuolation predominantly in the basal layer were observed. Superficial and mid dermal inflammation was composed predominantly of neutrophils and surrounding vessels had reactive endothelium and walls with edema, fibrin and acute inflammatory infiltrates. Small dermal vessels were occasionally obscured by necrotic debris admixed with fibrin. Lymph nodes had superficial cortical and subcapsular necrosis that variably extended into adjacent soft tissues, which were edematous with small numbers of neutrophils and immature or reactive fibrosis. Necropsy results for animals on day 12 p.i. revealed cutaneous lesions characterized by small foci of epidermal vacuolation with minimal exocytosis of neutrophils. Oral and pharyngeal mucosal epithelia had small foci of acute necrosis. The soft tissues adjacent to the uterus of 2 animals showed necrosis within or adjacent to early fibrosis. One animal also had accompanying myometrial necrosis.

The liver had multiple foci of randomly distributed, occasionally coalescing foci of necrosis accompanied by neutrophilic inflammation. Hepatocytes frequently had intracytoplasmic, amphophilic inclusion bodies that were round and ranged from 3-6 micrometers in diameter. Regional necrotizing enteritis, multiple foci of splenitis and a focal keratitis were observed. On day 17 p.i., animals infected with WA MPXV had cutaneous lesions characterized by multiple foci in the dermis composed of necrotic cellular debris. Peritesticular soft tissues had foci of necrosis with minimal fibrosis and chronic-active inflammation. At the last time point, day 24 p.i., the skin of 1 animal showed focal dermal fibrosis covered by a hyperkeratotic epidermis.

CB MPXV Clade

Animals euthanized on day 9 p.i. had cutaneous lesions characterized by small foci of epidermal cell vacuolation. Multiple dermal foci showed acute inflammation that was predominantly perivascular. The small intestinal lymphoid tissue (MALT) showed focal necrosis. The spleen had multiple, discrete necrotic foci. Interstitial edema with minimal hemorrhage was observed in the lungs. On day 12 and 13, animals had cutaneous lesions characterized by foci of epidermal necrosis with serocellular crusts. The dermis showed acute, predominantly perivascular inflammation. The rostral nasal cavity had epithelial necrosis and ulceration with acute inflammatory infiltrates and abundant luminal necrotic debris. The oral and pharyngeal mucosa had multiple foci of epithelial necrosis and ulceration with acute inflammation in the adjacent submucosa. The liver had multiple foci of randomly distributed, occasionally coalescing foci of necrosis accompanied by neutrophilic inflammation. Hepatocytes frequently had intracytoplasmic, amphophilic inclusion bodies that were round and ranged from 3-6 micrometers in diameter. Lymph nodes were diffusely necrotic and surrounding soft tissues had early fibrosis. On day 17, resolving foci of superficial dermatitis and foci of epidermal

necrosis was observed**.** Chronic sinusitis was observed in the rostral nasal cavity. Similar to WA MPXV infected animals, on day 24 p.i. cutaneous lesions were the predominant finding and characterized by dermal fibrosis, hyperkeratosis and crusting.

Comparing pathology of 2 animals that succumbed to disease on day 12 from each MPXV clade, both animals demonstrated abundant viral antigen (indicated by red chromogen) in all organs except the brain. Liver sections from PD21 that died from WA MPXV had typical intracytoplasmic basophilic inclusions and multifocal staining of orthopoxvirus antigens in hepatocytes (Figure 1.6a and 1.6b). Extensive staining of orthopoxvirus antigens was seen in the spleen, salivary gland and lung (Figure 1.6 c-d). Additionally, mesenchymal cells in the myometrium and broad ligament were positive for antigen as was the small intestinal staining in lamina propria fibroblasts and epithelial cells (Table 1.1). PD32 which died after CB MPXV challenge similarly had prominent inclusions within the liver (Figure 1.7a). Thin section EM of liver from this animal showed oval and brick shaped MPX virions, with dense dumb-bell shaped cores within hepatocytes (Figure 1.7b). The urinary bladder showed desquamated epithelial lining cells (arrows) containing poxvirus antigens (Figure 1.7c) and the submandibular lymph node had abundant macrophages and vascular (arrows) poxvirus antigens seen by IHC (Figure 1.7d). Orthopoxvirus IHC showed typical intracytoplasmic inclusions (arrows) by H&E (Figure 1.7e) and extensive staining of orthopoxvirus antigens within the oropharynx (Figure 1.7f).

Co-infection with Giardia or Coccidia

Although animals were inspected by a licensed veterinarian, as well as treated for fleas and intestinal worms upon capture and arrival at CDC facilities, it was noted during histological examination that a portion of the animals were infected with either of 2 protozoan parasites;

giardia (n=9/33) or coccidia (n=3/34). Both of these organisms are common parasites found in many wild rodents [25–29]; and likely this is also the case for wild prairie dogs. Our data does not suggest that infection with either giardia or coccida had a negative impact on the health of the animals or the disease progression of MPXV. The range in starting weights of the WA MPXV challenged animals was 488-965 grams; CB MPXV starting range was 549-899 grams. In comparison, the 9 animals that were positive for giardia had a starting weight range of 538-965 grams. The weight range for the 3 animals that were positive for coccidia was 748-802 grams. Thus, the animals with parasites did not have appreciably low weights compared to parasite-free animals. The 2 animals that unexpectedly perished from MPXV infection as well as the prairie dog that had to be euthanized due to morbidity criteria (PDs 21, 32 and 36) were negative for both giardia and coccidia. Additionally, there were no observed differences in the development of antibody titers between animals co-infected with parasites and those that were parasite free. Furthermore, no noticeable signs were observed in the animals that were found to be positive for coccidia or giardia such as diarrhea during the course of the study.

Discussion

Similar onset and range of clinical signs were observed in animals challenged with virus representatives of the WA and CB MPXV clades. Although we used the same inoculum for each MPVX clade ($8X10^3$ p.f.u.), it is worth noting that we previously determined that CB MPXV has approximately a hundred times lower LD50 value than the WA MPXV clade (5.9×10^3 vs. 1.29×10^5 respectively) with this animal model [13]. The 2 unscheduled deaths in the CB MPXV group compared to the 1 unscheduled WA MPXV death is explained by this difference. However, because the current study was designed to look at kinetics of viral spread in vivo using

a serial sacrifice technique; the study was not designed to determine differences in mortality between the clades.

By day 9 p.i.; respiratory depression while under anesthesia, as well as inappetence, formation of cutaneous poxvirus-lesions and nasal discharge occurred within multiple animals. These clinical signs, including respiratory depression under anesthesia were only seen with infected animals and not with the PBS controls. Inhalation anesthetics are eliminated from an animal primarily from the lungs, liver and kidneys and injury to these organs, such as through viral infection, many result in dose-related complications, including respiratory depression. As by day 9 p.i., the kidney, liver and lung tissues of infected animals had high loads of virus, it is possible that the viral induced organ damage resulted in decreased clearance of the anesthetic and respiratory depression of the animal and resulting respiratory depression. During peak infection (day 12 p.i.) however, CB MPXV challenged animals developed more pronounced signs of morbidity including facial edema, gastrointestinal distention, and ocular erythema and epiphora. Blood chemistry results did not display significant changes throughout the study, however the animal that was euthanized had abnormalities suggesting liver injury and dehydration. Based on the extremely high loads of virus recovered from the liver tissue, it is reasonable to assume there was viral-induced tissue injury. The earlier viral kinetics of CB MPXV as well as the increased tissue burden of virus in these infected animals compared to WA MPXV infected animals could account for the increased morbidity and mortality associated with the CB clade of MPXV.

When comparing peak mean viral loads in the tissues harvested, 74% of tissues had higher peak loads from the CB infected animals compared to WA infected animals (Table 3). However p-values for these comparisons were not statistically significant when comparing each tissue type (CB vs. WA) and controlling for day of necropsy (p-value range of 0.21-1; data not shown). Of

note, animals infected with virus from either clade, day 12 p.i. seems to be a pivotal time in this animal model. On day 12/13 p.i. unexpected deaths were observed, antibody production was uniformly observed, peak virus levels are seen, and the highest percent of viral isolates from tissues are obtained. Furthermore this was also the only point at which viable virus was recovered from blood samples.

Viremia as detected in the form of viral DNA was first detected on day 6; this was after the detection of viral DNA/ infectious virus within nasal cavity, submandibular lymph nodes and the spleen in those animals challenged with CB MPXV suggesting initial replication within the primary site of infection (nasal cavity) followed closely by lymphatic spread. Although viral DNA was detected in the blood after that of the spleen and submandibular lymph node, it is possible that a primary, transient viremia occurred but was not captured. The temporal similarity of viral detection in nasal cavity, submandibular lymph nodes, tonsils, spleen, and liver, within the WA MXPV infected animals supports the supposition that virus initially spread simultaneously through lymphatics (lymph nodes and tonsils)and blood stream (spleen and liver).

As seen within this and other MPXV animal models, detection of antibodies for all animals occurred at the same time or shortly after cutaneous lesion presentation (Wenner et al. 40-44). However, sera from 2 animals were able to neutralize on day 9, before lesion onset. Most likely this neutralization is due to IgM antibodies, which we have hypothesized our ELISA assay does not adequately capture (unlike IgG antibodies). Therefore we are likely missing the initial rise in immunoglobulins.

Neutrophils were prominent within the red pulp of the spleen early in infection with both MPXV clades. Pathological changes were similar between the clades as the study progressed.

Day 9 changes included dermal lesions characterized by epidermal vacuolation and inflammation along with varying lymphoid tissue necrosis. Additionally for CB MPXV infected animals, splenic necrosis was observed. Day 12 animals had more appreciable pathological changes including multifocal necrosis in the oral and pharyngeal mucosal epithelia, liver, nasal cavity, uterus, spleen small intestines, lymph nodes and uterus. By study end, dermal fibrosis, hyperkeratosis and crusting were the only findings. Comparing 2 animals (1 animal from each MPXV clade) that succumbed to disease on day 12, both animals demonstrated abundant viral antigen in all organs except the brain.

Although our understanding of MPXV pathogenesis *in vivo* continues to increase, there is still much to learn. In early studies, a model based on MPXV challenge of cynomolgus monkeys was used to describe the viral pathogenesis after infection. The investigators hypothesized that after a primary route of infection (intramuscular inoculation mimicking a bite from an infected animal), virus multiplies at this primary site leading to virus multiplication occurring simultaneously in the lymphatics and blood stream (primary viremia) followed by the draining lymph nodes, spleen and tonsils [30]. This is followed by virus release into systemic lymph nodes and a secondary viremia. The secondary viremia results in skin and other organs infection leading to clinical signs of disease including cutaneous lesion presentation. Our studies utilizing intranasal inoculation to mimic respiratory exposure suggests a similar time course within the prairie dog MPXV model. Our data suggests that the virus replicates at the primary site of infection (nasal cavity) followed closely by regional lymphatic tissues. This results in a transient viremia leading to viral spread and replication in target organs followed by a secondary viremia leading to characteristic disseminated cutaneous lesions. Our proposed pathogenesis model for MPXV within the prairie dog has been depicted within Figure 1.8. These findings allow for the

better understanding of the pathogenesis of MPXV within a relevant animal model, including identifying sites important during early viral replication and cellular response to viral infection. This data could prove useful in understanding the disease differences observed between the MPXV clades, understanding the risk of viral transmissions and development of therapeutic and biologic agents that could halt transmission between hosts.

Although we have shown with this and previous studies utilizing the prairie dog MXPV model that there are indeed differences in the pathogenicity between the two MPXV clades (similar to that seen during human MPXV infections), we have not determined the cause of these differences. CB MPXV causes increased morbidity and mortality, as well as a higher rate of transmission within humans as well as in our animal model. We have shown through the current and previous studies that CB MPXV infected prairie dogs consistently shed slightly larger loads of viable virus compared to WA MXPV. Additionally through the current study, we see that CB MXPV infected animals have a slightly earlier viral kinetics time-line, however WA MXPV infected prairie dogs seem to shed virus for a slightly longer period of time. Although we have not yet identified the cause(s) of the differences in MPXV clade pathogenicity, we consistently show that through utilization of the prairie dog MPXV model, we may yet understand why these genetically similar viruses result in different disease presentation and pathogenicity within humans.

Acknowledgements

The authors would like to thank Cynthia Goldsmith for taking EM pictures, Erin McDowell and Sonja Weiss for technical support for immune assays, Jason Abel for assistance with animal handling, and Nelva Bryant for processing tissues for pathology assays.

Reference List

1. Breman JG, Nakano JH, Coffi E, Godfrey H, Gautun JC (1977) Human poxvirus disease after smallpox eradication. Am J Trop Med Hyg 26: 273-281.

2. Hutin YJ, Williams RJ, Malfait P, Pebody R, Loparev VN, Ropp SL, Rodriguez M, Knight JC, Tshioko FK, Khan AS, Szczeniowski MV, Esposito JJ (2001) Outbreak of human monkeypox, Democratic Republic of Congo, 1996 to 1997. Emerg Infect Dis 7: 434-438.

3. Khodakevich L, Szczeniowski M, Manbu mD, Jezek Z, Marennikova S, Nakano J, Messinger D (1987) The role of squirrels in sustaining monkeypox virus transmission. Trop Geogr Med 39: 115-122.

4. Centers for Disease Control and Prevention (2003) Update: multistate outbreak of monkeypox--Illinois, Indiana, Kansas, Missouri, Ohio, and Wisconsin, 2003. MMWR Morb Mortal Wkly Rep 52: 561-564.

5. Hutson CL, Lee KN, Abel J, Carroll DS, Montgomery JM, Olson VA, Li Y, Davidson W, Hughes C, Dillon M, Spurlock P, Kazmierczak JJ, Austin C, Miser L, Sorhage FE, Howell J, Davis JP, Reynolds MG, Braden Z, Karem KL, Damon IK, Regnery RL (2007) Monkeypox zoonotic associations: insights from laboratory evaluation of animals associated with the multi-state US outbreak. Am J Trop Med Hyg 76: 757-768.

6. Reed KD, Melski JW, Graham MB, Regnery RL, Sotir MJ, Wegner MV, Kazmierczak JJ, Stratman EJ, Li Y, Fairley JA, Swain GR, Olson VA, Sargent EK, Kehl SC, Frace MA, Kline R, Foldy SL, Davis JP, Damon IK (2004) The detection of monkeypox in humans in the Western Hemisphere. N Engl J Med 350: 342-350.

7. Chen N, Li G, Liszewski MK, Atkinson JP, Jahrling PB, Feng Z, Schriewer J, Buck C, Wang C, Lefkowitz EJ, Esposito JJ, Harms T, Damon IK, Roper RL, Upton C, Buller RM (2005) Virulence differences between monkeypox virus isolates from West Africa and the Congo basin. Virology 340: 46-63.

8. Likos AM, Sammons SA, Olson VA, Frace AM, Li Y, Olsen-Rasmussen M, Davidson W, Galloway R, Khristova ML, Reynolds MG, Zhao H, Carroll DS, Curns A, Formenty P, Esposito JJ, Regnery RL, Damon IK (2005) A tale of two clades: monkeypox viruses. J Gen Virol 86: 2661-2672.

9. Breman JG, Kalisa R, Steniowski MV, Zanotto E, Gromyko AI, Arita I (1980) Human monkeypox, 1970-79. Bull World Health Organ 58: 165-182.

10. Foster SO, Brink EW, Hutchins DL, Pifer JM, Lourie B, Moser CR, Cummings EC, Kuteyi OE, Eke RE, Titus JB, Smith EA, Hicks JW, Foege WH (1972) Human monkeypox. Bull World Health Organ 46: 569-576.

11. Learned LA, Reynolds MG, Wassa DW, Li Y, Olson VA, Karem K, Stempora LL, Braden ZH, Kline R, Likos A, Libama F, Moudzeo H, Bolanda JD, Tarangonia P, Boumandoki P, Formenty P, Harvey JM, Damon IK (2005) Extended interhuman transmission of monkeypox in a hospital community in the Republic of the Congo, 2003. Am J Trop Med Hyg 73: 428-434.

12. Hutson CL, Olson VA, Carroll DS, Abel JA, Hughes CM, Braden ZH, Weiss S, Self J, Osorio JE, Hudson PN, Dillon M, Karem KL, Damon IK, Regnery RL (2009) A prairie dog animal model of systemic orthopoxvirus disease using West African and Congo Basin strains of monkeypox virus. J Gen Virol 90: 323-333.

13. Hutson CL, Carroll DS, Self J, Weiss S, Hughes CM, Braden Z, Olson VA, Smith SK, Karem KL, Regnery RL, Damon IK (2010) Dosage comparison of Congo Basin and West

African strains of monkeypox virus using a prairie dog animal model of systemic orthopoxvirus disease. Virology 402: 72-82.

14. Reynolds MG, Carroll DS, Karem KL (2012) Factors affecting the likelihood of monkeypox's emergence and spread in the post-smallpox era. Curr Opin Virol 2: 335-343. S1879-6257(12)00031-4 [pii];10.1016/j.coviro.2012.02.004 [doi].

15. Henderson DA (2002) Smallpox: clinical and epidemiologic features. Med Health R I 85: 107-108.

16. Hutson CL, Gallardo-Romero N, Carroll DS, Clemmons C, Salzer JS, Nagy T, Hughes CM, Olson VA, Karem KL, Damon IK (2013) Transmissibility of the monkeypox virus clades via respiratory transmission: investigation using the prairie dog-monkeypox virus challenge system. PLoS One 8: e55488. 10.1371/journal.pone.0055488 [doi];PONE-D-12-23800 [pii].

17. Hutson CL, Carroll DS, Gallardo-Romero N, Weiss S, Clemmons C, Hughes CM, Salzer JS, Olson VA, Abel J, Karem KL, Damon IK (2011) Monkeypox disease transmission in an experimental setting: prairie dog animal model. PLoS One 6: e28295. 10.1371/journal.pone.0028295 [doi];PONE-D-11-17293 [pii].

18. Keckler MS, Carroll DS, Gallardo-Romero NF, Lash RR, Salzer JS, Weiss SL, Patel N, Clemmons CJ, Smith SK, Hutson CL, Karem KL, Damon IK (2011) Establishment of the black-tailed prairie dog (Cynomys ludovicianus) as a novel animal model for comparing smallpox vaccines administered preexposure in both high- and low-dose monkeypox virus challenges. J Virol 85: 7683-7698. JVI.02174-10 [pii];10.1128/JVI.02174-10 [doi].

19. Smith SK, Self J, Weiss S, Carroll D, Braden Z, Regnery RL, Davidson W, Jordan R, Hruby DE, Damon IK (2011) Effective antiviral treatment of systemic orthopoxvirus disease:

ST-246 treatment of prairie dogs infected with monkeypox virus. J Virol 85: 9176-9187. JVI.02173-10 [pii];10.1128/JVI.02173-10 [doi].

20. Hudson PN, Self J, Weiss S, Braden Z, Xiao Y, Girgis NM, Emerson G, Hughes C, Sammons SA, Isaacs SN, Damon IK, Olson VA (2012) Elucidating the role of the complement control protein in monkeypox pathogenicity. PLoS One 7: e35086. 10.1371/journal.pone.0035086 [doi];PONE-D-11-15032 [pii].

21. Li Y, Olson VA, Laue T, Laker MT, Damon IK (2006) Detection of monkeypox virus with real-time PCR assays. J Clin Virol 36: 194-203.

22. Karem KL, Reynolds M, Braden Z, Lou G, Bernard N, Patton J, Damon IK (2005) characterization of acute-phase humoral immunity to monkeypox: use of immunoglobulin M enzyme-linked immunosorbent assay for detection of monkeypox infection during the 2003 North American outbreak. Clin Diagn Lab Immunol 12: 867-872.

23. Guarner J, Johnson BJ, Paddock CD, Shieh WJ, Goldsmith CS, Reynolds MG, Damon IK, Regnery RL, Zaki SR (2004) Monkeypox transmission and pathogenesis in prairie dogs. Emerg Infect Dis 10: 426-431.

24. Hutson CL, Gallardo-Romero N, Carroll DS, Clemmons C, Salzer JS, Nagy T, Hughes CM, Olson VA, Karem KL, Damon IK (2013) Transmissibility of the monkeypox virus clades via respiratory transmission: investigation using the prairie dog-monkeypox virus challenge system. PLoS ONE 8: e55488. 10.1371/journal.pone.0055488 [doi];PONE-D-12-23800 [pii].

25. Sogayar MI, Yoshida EL (1995) Giardia survey in live-trapped small domestic and wild mammals in four regions in the southwest region of the state of Sao Paulo, Brazil. Mem Inst Oswaldo Cruz 90: 675-678.

26. Marino MR, Brown TJ, Waddington DC, Brockie RE, Kelly PJ (1992) Giardia intestinalis in North Island possums, house mice and ship rats. N Z Vet J 40: 24-27. 10.1080/00480169.1992.35693 [doi].

27. Pinter AJ, O'Dell WD, Watkins RA (1988) Intestinal parasites of small mammals from Grand Teton National Park. J Parasitol 74: 187-188.

28. Medina-Esparza L, Macias L, Ramos-Parra M, Morales-Salinas E, Quezada T, Cruz-Vazquez C (2013) Frequency of infection by Neospora caninum in wild rodents associated with dairy farms in Aguascalientes, Mexico. Vet Parasitol 191: 11-14. S0304-4017(12)00420-7 [pii];10.1016/j.vetpar.2012.08.007 [doi].

29. Ferroglio E, Pasino M, Romano A, Grande D, Pregel P, Trisciuoglio A (2007) Evidence of Neospora caninum DNA in wild rodents. Vet Parasitol 148: 346-349. S0304-4017(07)00327-5 [pii];10.1016/j.vetpar.2007.06.031 [doi].

30. Cho CT, Wenner HA (1973) Monkeypox virus. Bacteriol Rev 37: 1-18.

Table 2.1. Clinical and laboratory findings in prairie dogs intranasally challenged (8x103pfu) with West African (WA) MPXV. Groups of prairie dogs were serially sacrificed (days 2, 4, 6, 9, 12, 17 and 24) following challenge. Animals were observed for clinical signs, antibody production and lesion presentation. Gross observations were recorded and post-mortem samples were evaluated for presence of virus and histopathological changes. R.D.: respiratory

depression under anesthesia; N.O.: nothing observed; N.E. not examined.; ABs: antibodies; ǂ: Unscheduled death

Sac. Day (p.i.)	PD #	Max. # of skin lesions◊	OPX ABs	Neut. ABs	Clinical Signs	Gross Pathology	Pox IHC	Viable Virus (#positive/ #tested)
2	PD9	0	Neg.	Neg.	N.O.	N.O.	N.E.	0/28
	PD10	0	Neg.	Neg.	N.O.	N.O.	N.E.	0/28
4	PD11	0	Neg.	Neg.	N.O.	N.O.	N.O.	0/28
	PD12	0	Neg.	Neg.	N.O.	N.O.	N.O.	0/28
6	PD13	0	Neg.	Neg.	N.O.	N.O.	N.O.	10/28
	PD14	0	Neg.	Neg.	N.O.	N.O.	N.O.	10/28
9	PD15	0	Neg.	+	R.D.	Pale kidneys	LN, epithelial, dermis	15/28
	PD16	0	Neg.	Neg.	R.D.	N.O.	LN, spleen	16/28
12	PD17	20	+	N.E.	Inappetence	Lymphadenopathy, Inflamed oviducts	Buccal/caudal pharyngeal mucosa, uterus, mesenchymal cells (mononuclear inflammatory cells/reactive fibroblasts)	21/28
	PD18	12	+	N.E.	Inappetence	Lymphadenopathy	Epithelial, tonsil, fibroblasts	10/28
	PD21ǂ	3	N.E.	N.E.	Inappetence, nasal discharge	Hemorrhage of uterine horns and adipose tissue associated with the round ligament, hyperemic areas associated with the ovaries and	All tissues positive for antigen except for brain	26/28

						inflamed oviducts, and Hepatomegaly		
17	PD19	>20	+	+	Inappetence	Lymphadenopathy, hemorrhagic foci in the adipose tissue associated with lymph nodes and multiple, mild foci of serosal hemorrhage on the lungs	Peritesticular adipose tissue	14/28
24	PD20	5	+	N.E.	N.O.	N.O.	N.E.	0/28
	PD22	20	+	N.E.	N.O.	Pericarditis	N.E.	1/28

Table 2.2. Clinical and laboratory findings in prairie dogs intranasally challenged (8x103pfu) with Congo Basin (CB) MPXV. Groups of prairie dogs were serially sacrificed (days 2, 4, 6, 9, 12, 17 and 24) following challenge. Animals were observed for clinical signs, antibody production and lesion presentation. Gross observations were recorded and post-mortem samples were evaluated for presence of virus and histopathological changes. R.D.: Respiratory depression while under anesthesia; N.O.: nothing observed; N.E. not examined; ABs: antibodies

◊: Maximum number of lesion at any time-point throughout study, not restrictive to day of necropsy

ɪ: Unscheduled death

Sac. Day (p.i.)	PD #	Max. # of skin lesions◊	OPX ABs	Neut. ABs	Clinical Signs	Gross Pathology	Pox IHC	Viable Virus (#positive/ #tested)
2	PD23	0	Neg.	Neg.	N.O.	N.O.	N.E.	0/28
	PD24	0	Neg.	Neg.	N.O.	N.O.	N.E.	0/28
4	PD25	0	Neg.	Neg.	N.O.	foci of serosal congestion stomach and colon	N.O.	2/28
	PD26	0	Neg.	Neg.	N.O.	foci of serosal congestion stomach and lung	N.O.	2/28
6	PD27	0	Neg.	Neg.	N.O.	N.O.	N.O.	8/28
	PD28	0	Neg.	Neg.	N.O.	N.O.	N.O.	12/28
9	PD29	0	Neg.	+	N.O.	N.O.	Small intestine	16/28
	PD30	17	Neg.	Neg.	R.D., nasal discharge, died while under anesthesia	Multiple, randomly distributed foci of parenchymal hemorrhage on lungs	Small intestine, trachea, epithelial staining (unknown location)	25/28
12/13	PD31	5	+	N.E.	Facial edema	N.O.	Epiglottis associated with necrotic lesion, tongue, small intestine	19/28
	PD32ŧ	4	N.E.	N.E.	R.D., inappetence, facial edema	Multifocal hemorrhagic lesions in the	All tissues positive for antigen	28/28

						jejunum and lymphadenopathy /necrotic submandibular lymph nodes	except for brain	
	PD36ŧ	14	+	N.E.	Nasal discharge, inappetence, periocular erythema and epiphora, distended abdomen	Gastrointestinal distention uterus had a focal serosal hemorrhage, multifocal hemorrhagic lesions in the periovarian adipose tissue, Hemorrhagic MALT in the peritoneum, mucosal hemorrhage in stomach	Rostral nasal cavity, epidermal with some dermal mesenchymal cells	24/28
17	PD33	>20	+	N.E.	Inappetence, facial edema, bloody nose/mouth, nasal discharge	Foci of hemorrhage in the jejunum and multifocal hemorrhagic lesions in the periovarian adipose tissue	Mesenchymal cell staining in mid dermis	11/28
	PD34	6	+	+	Facial edema, nasal discharge	N.O.	N.E.	3/28

24	PD35	13	+	N.E.	Inappetence	N.O.	N.E.	0/28

Table 2.3. Viral kinetics and tissue tropism of MPXV infection within the prairie dog.

Tissue Sample	**West Africa MPXV**			**Congo Basin MPXV**		
	DNA presence (days)	**Virus presence (days)**	**Peak mean viral load and day**	**DNA presence (days)**	**Virus presence (days)**	**Peak mean viral load and day**
Nasal cavity	4-24	6-17	7.7×10^8 Day 9	2-17	4-17	2.6×10^8 Days 12/13
SM lymph nodes	2-24	6-12	6.8×10^5 Day 6	4-24	4-13	9.9×10^7 Days 6
Spleen	4-24	6-12	4.9×10^8 Day 12	4-17	4-13	7.5×10^8 Days 12/13
Tongue	4-24	6-17	2.1×10^7 Day 12	4-17	6-17	4.8×10^7 Days 12/13
Tonsils	4-24	6-12	7.7×10^7 Day 12	4-17	6-13	4.6×10^6 Days 12/13
Oropharynx	4-24	6-17	4.1×10^6 Day 12	2-24	6-17	2×10^7 Days 12/13

Inner cheek	6-24	6-17	2.4 X 10^7 Day 12	4-17	6-17	2.8 X 10^7 Days 12/13
Trachea	6-24	6-12	2.7 X10^6 Day 12	4-24	6-13	1 X 10^7 Days 9
Lungs	4-17	6-12	5.9 X 10^7 Day 12	4-24	6-13	3.9 X 10^7 Days 12/13
Liver	4-17	6-12	5.7 X10^8 Day 12	2-17	6-12	2.9 X 10^9 Days 12/13
Ileum	4-24	6-12	2.4 X10^7 Day 12	6-24	6-13	4.2 X 10^7 Days 12/13
Duodenum	6-24	6-9	6.8 X10^3 Day 9	4-24	6-13	3.9 X 10^6 Days 12/13
Jejunum	6-17	6-12	1.1 X10^7 Day 12	9-17	6-13	3.9 X 10^7 Days 12/13
Eyelid	6-24	9-17	9.7 X 10^7 Day 17	2-17	6-17	1.9 X 10^7 Days 12/13
Eye	6-24	9-17	1.2 X 10^7 Day 12	4-17	6-13	6.2 X 10^6 Days 12/13

Kidney	6-24	9-12	3.8 $X10^6$ Day 12	6-17	9-13	4 $X 10^6$ Days 12/13
Gonad	6-24	9-17	7.6 $X10^7$ Day 12	4-24	6-17	1 $X 10^7$ Days 12/13
Belly skin	6-24	9-17	3.3 $X10^5$ Day 12	4-24	9-17	3.9 $X 10^6$ Days 12/13
Mes lymph node	4-24	12	1.4$X10^7$ Day 12	6-17	9-13	1.2$X10^6$ Days 12/13
Stomach	4-24	12	4.3 $X10^5$ Day 12	4-24	9-13	3.1 $X 10^6$ Days 12/13
Brain	6-24	12-17	7.1 $X10^4$ Day 12	6-17	9-13	1.9 $X 10^5$ Days 12/13
Heart	4-24	12	1.4 $X10^6$ Day 12	4-17	9-13	7.6 $X 10^6$ Days 12/13
Pancreas	6-17	12	2.8 $X10^6$ Day 12	4-17	6-13	3.9 $X 10^7$ Days 12/13
Urine/bladder	6-24	12-17	3.5 $X10^6$ Day 12	9-24	9-13	4.9 $X 10^6$ Days 12/13
Gallbladder	6-24	12-17	3.8$X 10^4$ Day 12	4-24	12-13	2.2$X 10^6$ Days 12/13

Feces	12-24	12-24	6.5 X10^6 Day 12	12-24	12-17	1.1 X 10^7 Days 12/13
Lesion	12-24	12-24	7.8 X10^7 Day 17	12-24	12-17	2.3 X 10^8 Days 12/13

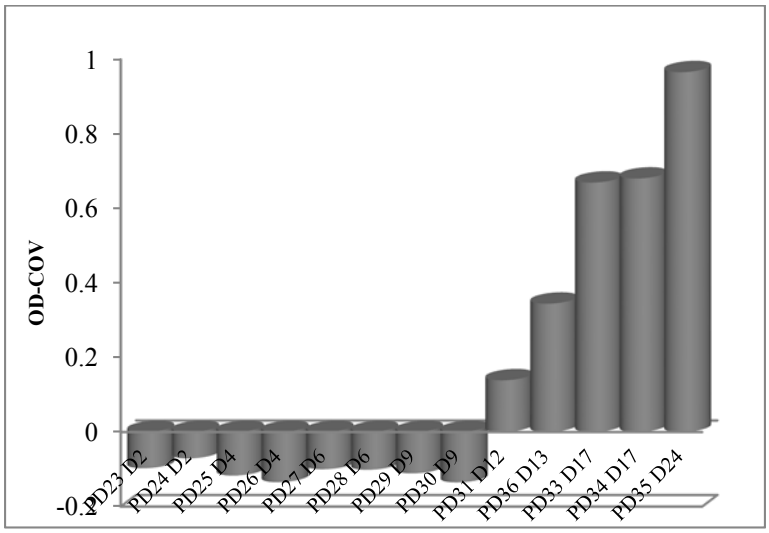

a.

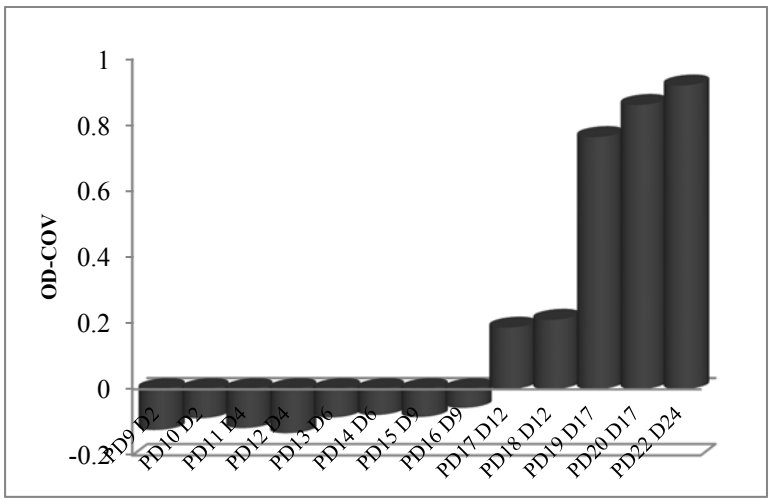

b.

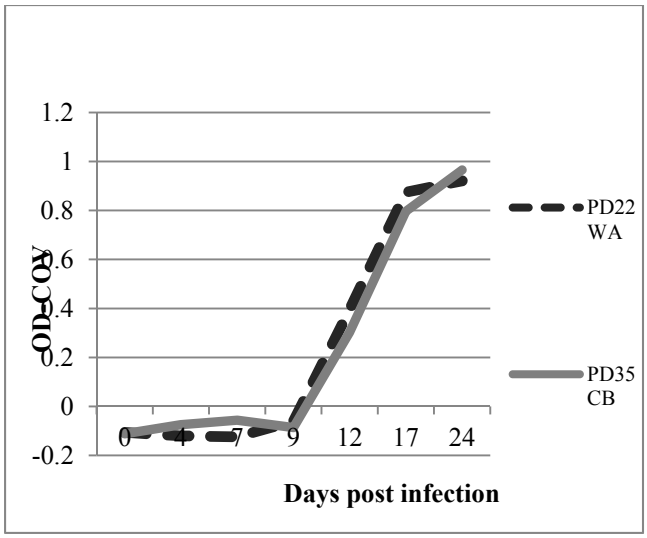

c..

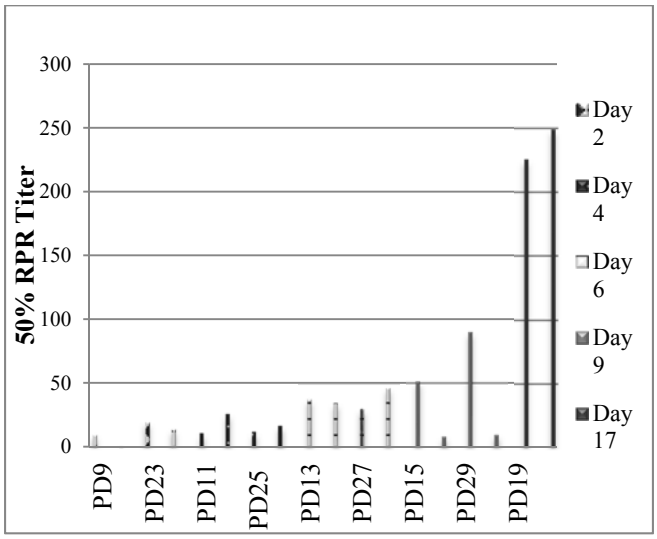

d.

Figure 2.1. Antibody response in MPXV challenged prairie dogs. Groups of prairie dogs were serially sacrificed (days 2, 4, 6, 9, 12, 17 and 24) following intranasal challenge (~7x10^3pfu) with Congo Basin (CB) or West African (WA) MPXV. Antibody response at time of sacrifice by ELISA is shown for individual MPXV infected prairie dogs (CB (a) and WA (b)). Kinetics of antibody titers for two animals that were serially bled throughout the study are

shown in c. Neutralizing titers for animals sacrificed on or before day 9 as determined by HCS-GFP are shown in d; two animals sacrificed on day 17 p.i. serve as positive controls.

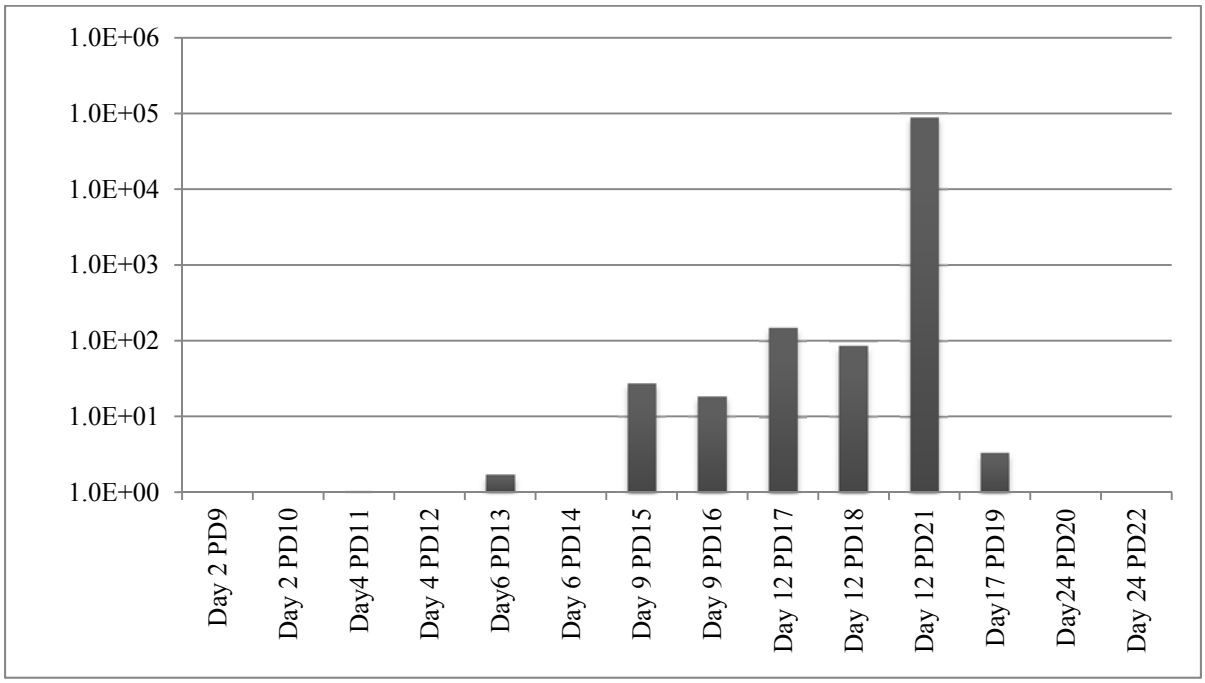

a.

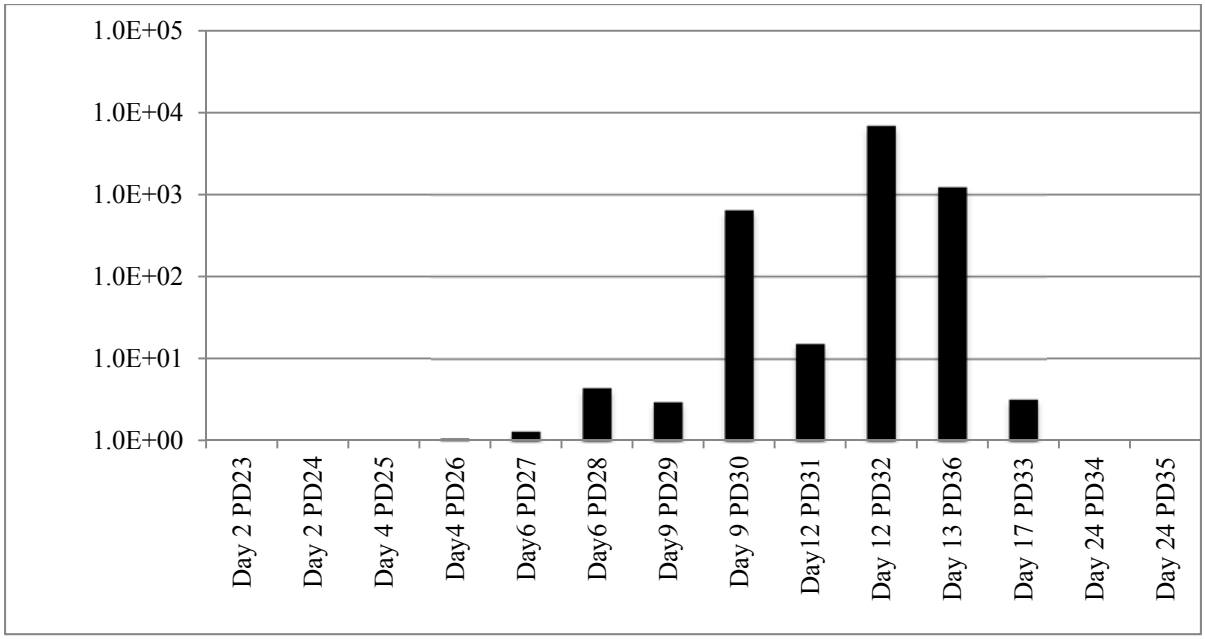

b.

Figure 2.2. MPXV challenged prairie dog viremia. Groups of prairie dogs were serially sacrificed (days 2, 4, 6, 9, 12, 17 and 24) following intranasal challenge ($8x10^3$pfu) with West African (a) or Congo Basin (b) MPXV. Viremia was determined by viral DNA in blood samples. Only blood from prairie dogs 21 and 32 were positive for viable virus (VV) ($1.8X10^6$pfu/mL and $2X10^6$pfu/mL respectively). Values are shown as DNA (fg/ul) on a log scale.

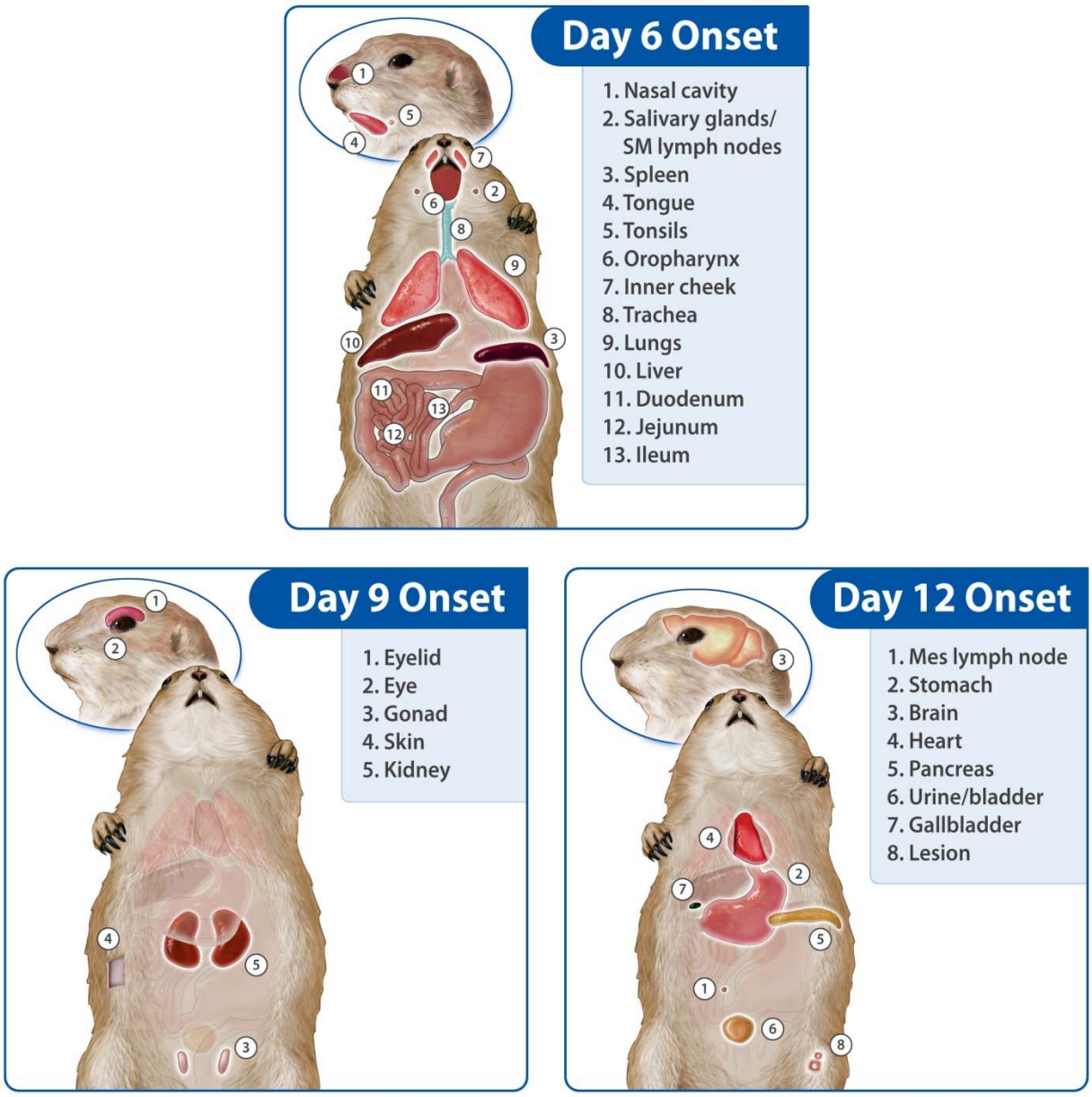

Figure 2.3. Schematic depicting WA MPXV disease progression in a prairie dog. Groups of prairie dogs were intranasally challenged (8x103p.f.u.) with West African (WA) MPXV and serially sacrificed (days 2, 4, 6, 9, 12, 17 and 24). Samples were evaluated for the presence of virus and were grouped by initial detection of viable virus (day 6 (a), 9 (b), or 12 (c) p.i.).

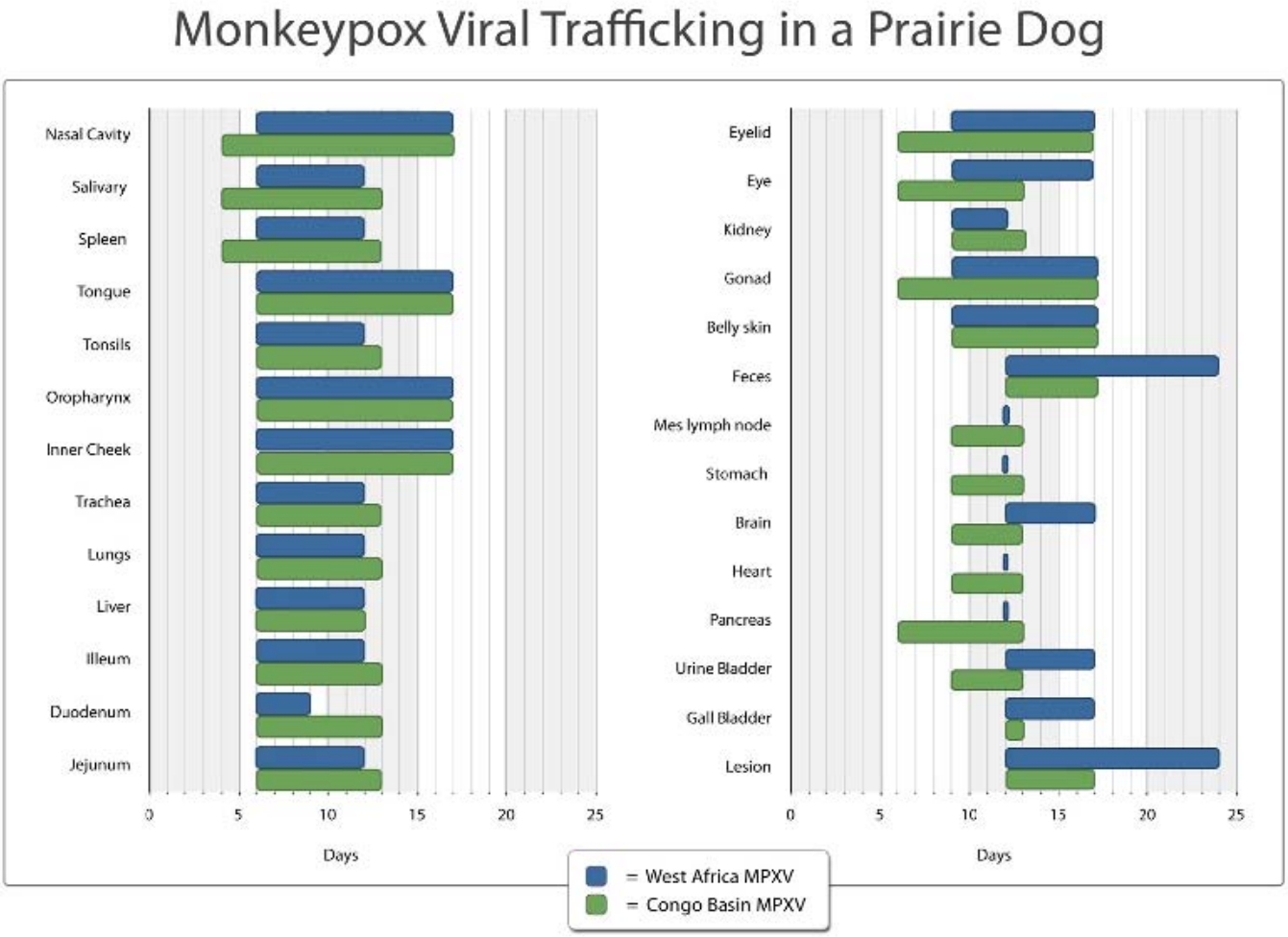

Figure 2.4. Monkeypox viral trafficking within prairie dogs. Groups of prairie dogs were serially sacrificed (days 2, 4, 6, 9, 12, 17 and 24) following intranasal challenge (8x103p.f.u.) with West African (blue) or Congo Basin (green) MPXV. Samples were evaluated for the presence of virus by tissue culture. The time courses of viral shedding from each tissue type are shown above.

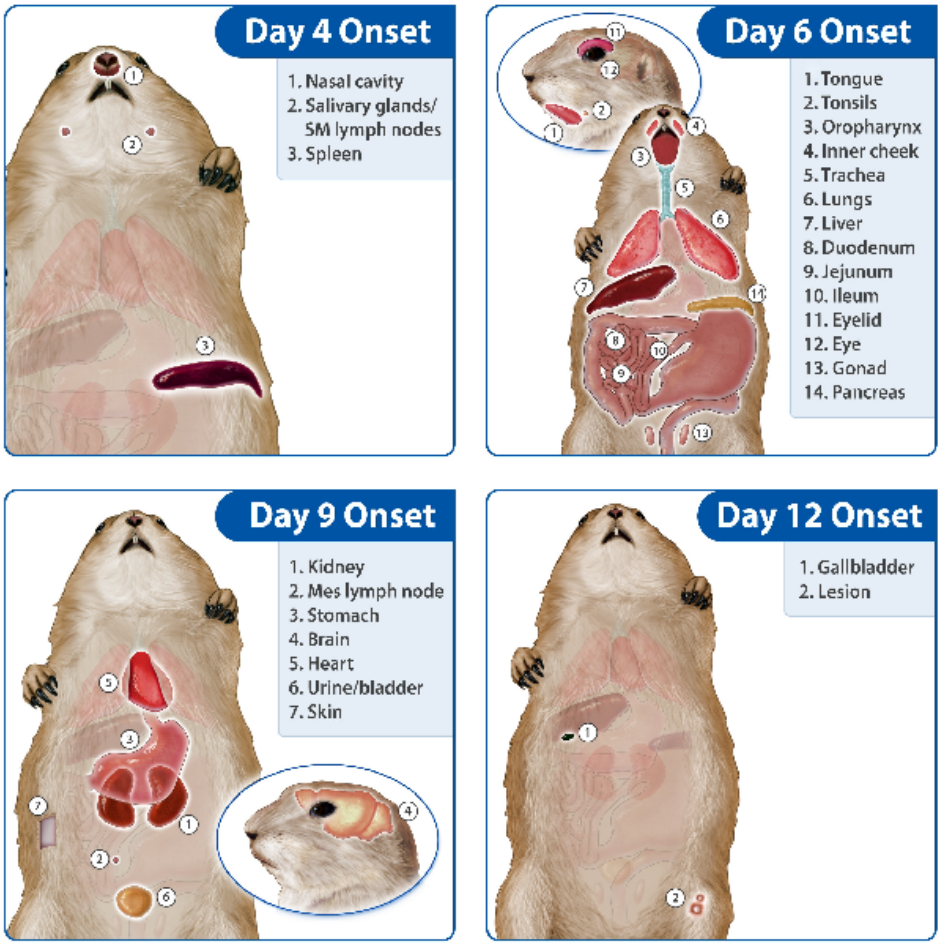

Figure 2.5. **Schematic depicting CB MPXV disease progression in a prairie dog.** Groups of prairie dogs were intranasally challenged (8x103p.f.u.) with Congo Basin (CB) MPXV. Groups of prairie dogs were serially sacrificed (days 2, 4, 6, 9, 12, 17 and 24) following challenge. Samples were evaluated for the presence of virus and were grouped by initial detection of viable virus (day 4 (a), 6 (b), 9 (c) or 12 (d) p.i.).

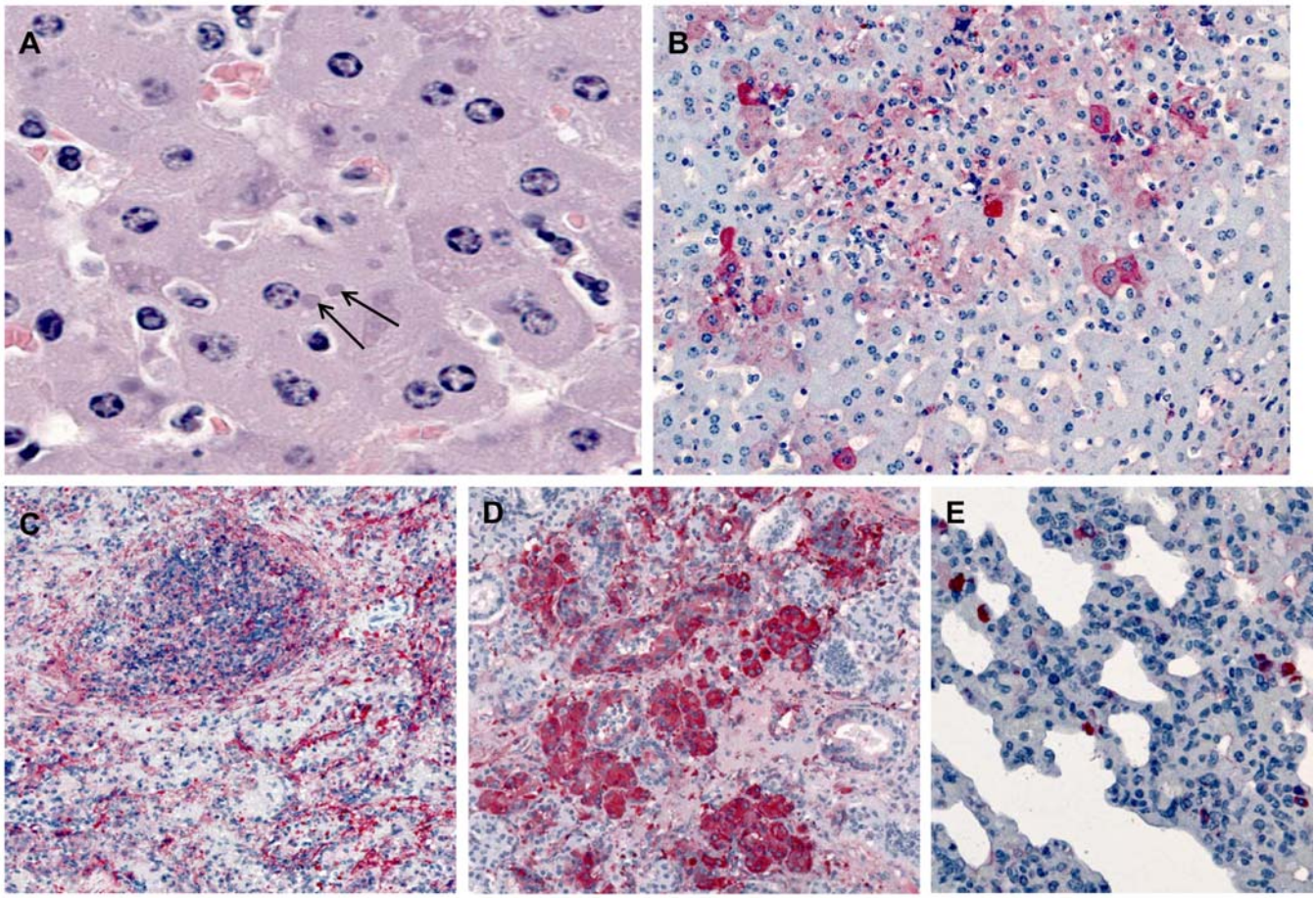

Figure 2.6. Histopathologic and immunohistochemical findings in a prairie dog that succumbed to West African MPXV (PD21). A) Liver showing typical intracytoplasmic basophilic inclusions (arrows) by H&E staining and (b) multifocal staining of orthopoxvirus antigens in hepatocytes by IHC. (C-E) Extensive staining of orthopoxvirus antigens in spleen (C), salivary gland (D) and lung (E).

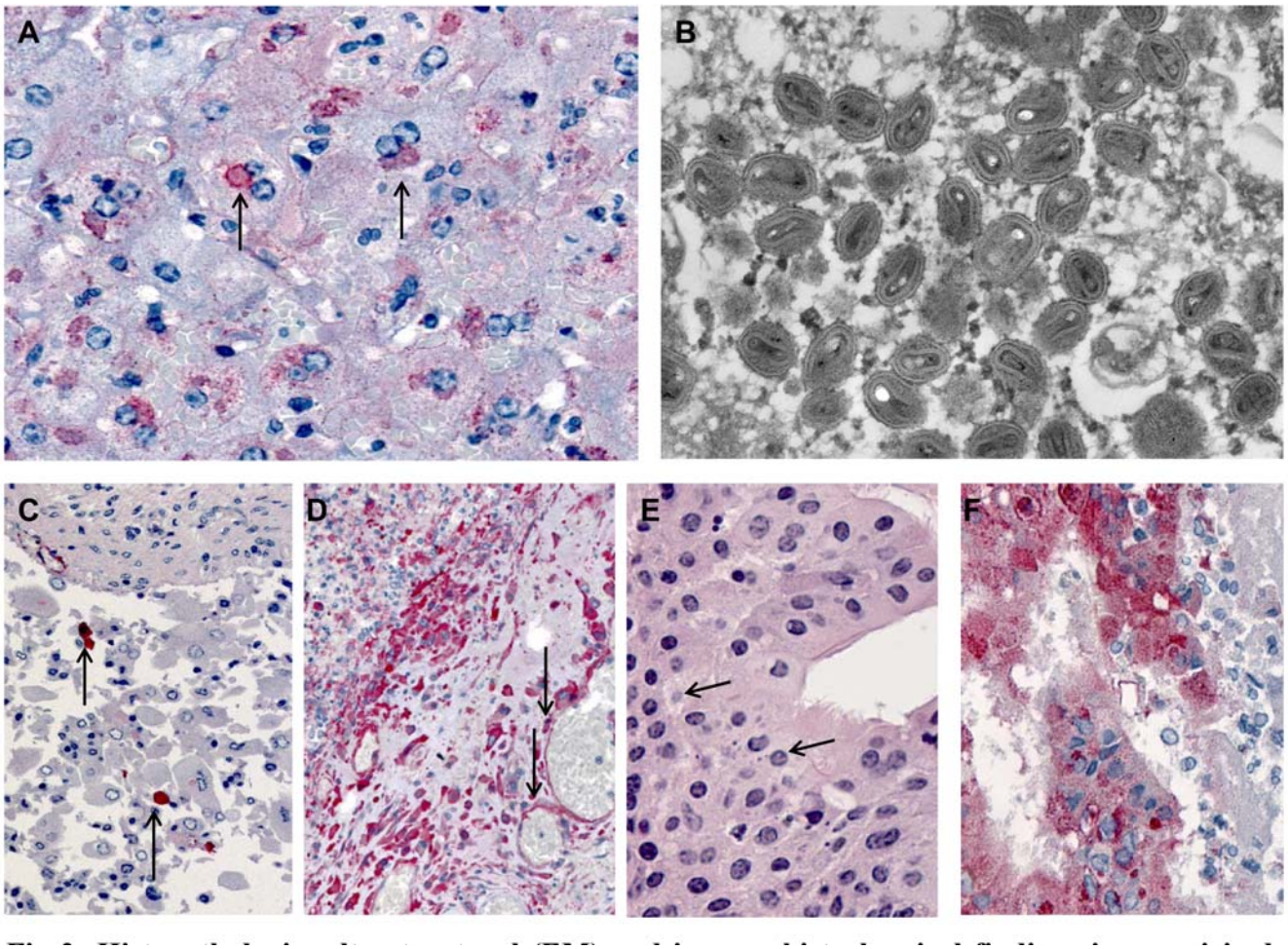

Figure 2.7: Histopathologic, ultrastructural (EM) and immunohistochemical findings in a prairie dog that succumbed to Congo Basin MPXV (PD32). A) Liver showing prominent inclusions (arrows) as seen by IHC staining of orthopoxvirus antigens. (B) Thin section EM of liver showing oval and brick shaped monkeypox virions, with dense dumb-bell shaped cores within hepatocytes. (C) Urinary bladder showing desquamated epithelial lining cells (arrows) containing poxvirus antigens as seen by IHC. (D) Submandibular lymph node showing abundant macrophages and vascular (arrows) poxvirus antigens seen by IHC. (E-F) Orthopoxvirus IHC showing typical intracytoplasmic inclusions (arrows) by H&E (E) and extensive staining of orthopoxvirus antigens as seen by IHC (F) within the oropharynx.

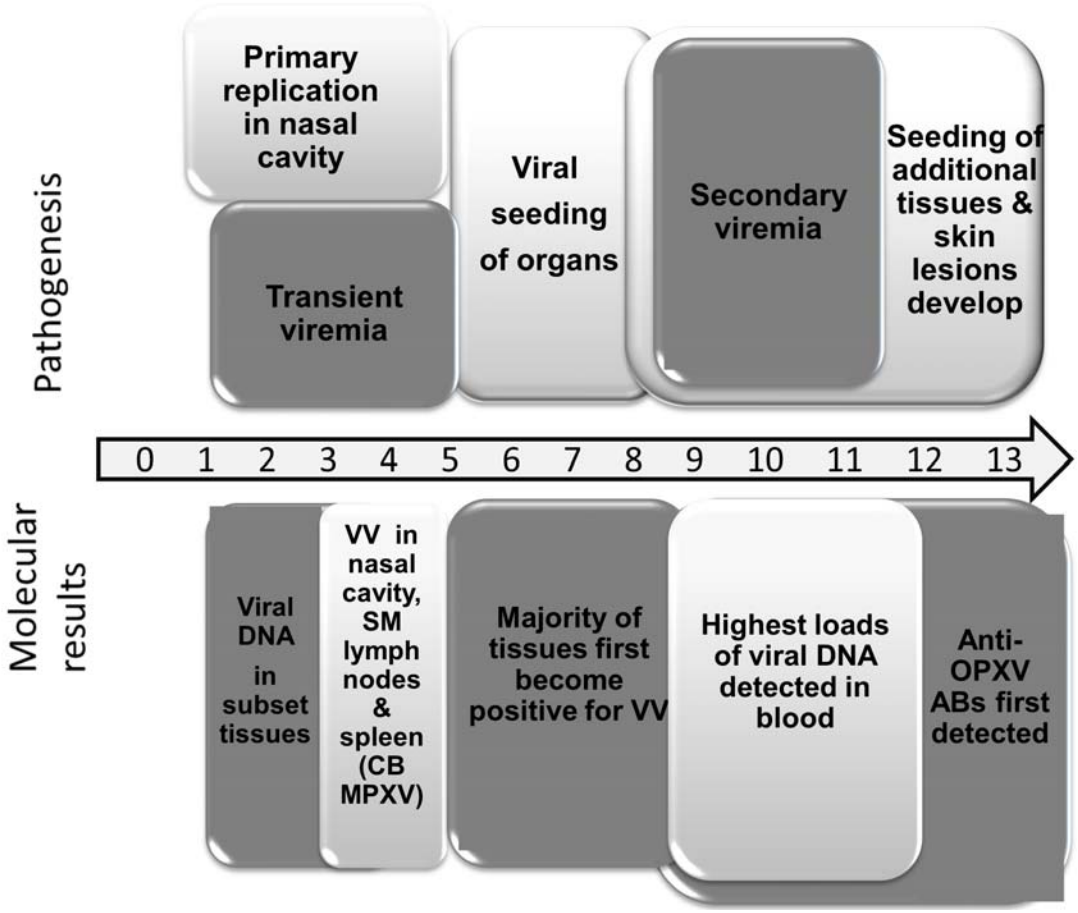

Figure 2.8. Proposed model for MPXV pathogenesis within prairie dogs. Time after infection is shown in days; VV=viable virus, SM=submandibular, CB =Congo Basin: Abs=antibodies

CHAPTER 3

COMPARISONS OF APOPTOSIS AND NUCLEAR FACTOR KAPPA B ACTIVITY DURING WEST AFRICAN AND CONGO BASIN CLADE MONKEYPOX VIRUS INFECTIONS IN VIVO

[2]Christina L. Hutson, Darin Carroll, Victoria A. Olson, Christine Hughes, Inger K. Damon, Tamas Nagy. To be submitted to BioMed Research International:Virology.

Abstract

Orthopoxviruses, including monkeypox virus (MPXV), appear to have acquired mechanisms to evade the hosts' immune system. In vitro evidence suggests that one evasion technique is modulation of NF-κB. NF- κB activation is stimulated through upstream signaling pathways such as Toll-like receptors (TLR), Retinoic acid-inducible gene 1 (RIG-1)-like receptors (RLR), and numerous other pathogen associated molecule signaling pathways. Upon activation, NF- κB serves as an important transcription factor for many pro-inflammatory molecules. Additional in vitro and in vivo evidence suggests that viral inhibition of apoptosis may also plan a role in immune evasion. Utilizing tissues from a prairie dog MPXV serial sacrifice study we analyzed spleen, kidney, liver and gallbladder for key proteins involved in NF-κB signaling via Western blot. In Congo Basin (CB) MPXV infected animals, p65 activation tended to rise on days 2-4 p.i., then drop when viable virus was present (days 6-12). At viral clearance on day 17-24 p.i., p65 activation reemerged and was higher than any other time throughout the study. This trend was not as evident in West African (WA) MPXV infected animals. For each clade and each tissue, the four animals with highest viral loads were compared to the same tissues from PBS control animals (n=5). Although viral loads reached 10^9 pfu/gram of tissue, significant differences in p65 activation were only seen in livers of animals infected with CB and WA clades and in kidney of animals infected with WA clade when compared to PBS control animals (p values=0.04, 0.04, 0.04). Other tissues in both infected groups had activation levels comparable to PBS controls. This finding suggests the virus is able to effectively inhibit NFkB activation within certain tissues. In order to identify where inhibition is occurring, upstream proteins were also analyzed including those involved in RLR and TLR signaling. These receptors are an important component of the innate immune response and

Orthopoxvirus proteins have been shown to inhibit RLR and TLR proteins during viral infection. Numbers of apoptotic cells were also compared in liver and spleen samples from WA MPXV and CB MPXV infected animals. Interestingly when comparing apoptosis levels in the liver and spleen from these animals splenocytes labelled positive for apoptosis more often than hepatocytes in both MPXV groups. Dual-IHC staining of select liver and spleen sections showed that apoptotic cells (identified by TUNEL) tended to co-localize with poxvirus antigen. Our results are important in understanding differences observed in the virulence between the two MPXV clades and how these viruses are evading the host immune response during infections.

Introduction

Orthopoxviruses, including Monkeypox virus (MPXV), appear to have acquired mechanisms to evade the hosts' immune system. One of these evasion techniques seems to be the inhibition of NF-κB activation [1,2]. NF-κB is a mammalian transcription factor that regulates stress, immune response, and is an important component in the progression of inflammatory diseases. Viral inhibition of apoptosis, or programmed cell death has also been implicated as a possible mechanism of viral evasion of the host immune response [2]. As the Congo Basin Clade MPXV is more virulent than West African MPXV in both humans and animal models, it is possible that this increased virulence is at least in part due to differences in the ability of these viruses to inhibit the innate immune system, including NFkB activation and apoptosis.

Early investigations have shown the prairie dog MPXV model to be useful for the study of systemic *Orthopoxvirus* disease. Previously we characterized the MPXV clades through a serial sacrifice study (Hutson et al. 2015 Submitted for publication). Groups of prairie dogs were intranasally infected (8x103pfu) with Congo Basin (CB) or West African (WA) MPXV, and 28

tissues were harvested days 2, 4, 6, 9, 12, 17 and 24. Presence of virus, gross and microscopic lesions were evaluated. These findings allowed for further characterization of MPXV clade pathogenesis, including identifying sites important during early viral replication and cellular response to viral infection.

Utilizing tissues collected during the prairie dog MPXV serial sacrifice study, we analysed spleen, kidney, liver and gallbladder for activation state and total protein levels of key proteins involved in the NF-κB pathway. These tissues were chosen as they represented early, intermediate and late viral kinetics during a MPXV infection. Western blotting using standard techniques were completed with antibodies to examine the activation state and total protein levels of key proteins in the NF-κB pathway: IKKα, NF-κB p65/RelA and IκBα. For comparison purposes, tissues from PBS non-infected control animals were also analysed. Two cellular pathways that are upstream of NFkB activity include receptors that are termed Rig-I like receptors (RLRs) and Toll-like receptors (TLRs). These pathways are an important component of the innate immune response and have been shown to be important in detection of viral invasion and result in the translocation of NFkB subunits. Additionally, Orthopoxvirus proteins have been shown to inhibit RLR and TLR proteins during viral infection [2] . Therefore, activation state and total protein levels of key proteins in both of these pathways (Rig-I, MyD88, TBK, IRAK4) were also examined via Western blot assays in spleen and liver from infected animals. Additionally, spleen and liver sections were fixed and analysed using immunohistochemistry analysis to look at levels of apoptosis.

Although much work has been done looking at how poxviruses inhibit the host immune system in vitro, there is less data from in vivo studies Through the current study, we were able to compare protein levels of key subunits involved in TLR and RLR pathways as well as the NFkB

pathway during *a in vivo* MPXV infection as well as the amount of apoptosis caused by each MPXV clade. The findings from our studies suggest that the ability of the virus at circumventing the NFkB pathway might be more important in the resulting virulence and pathogenicity within an animal, than the ability of the virus to inhibit apoptosis. Additional in vivo studies should be done to further look at NFkB and apoptotic response to a MPXV infection.

Materials and Methods

Animals

Wild-caught, juvenile black-tailed prairie dogs (PDs ;*Cynomys ludovicianus*) were obtained from Colorado. Information about the animal studies is described within our previous manuscript (Hutson et al. 2015. Submitted for Publication).

Viruses for Animal Inoculation

The WA MPXV strain, MPXV-USA-2003-044, was isolated during the 2003 U.S. outbreak [3,4] and the CB MPXV strain, MPXV-ROC-2003-358, was collected from a 2003 outbreak of MPXV in the Republic of Congo (ROC) [3]. Preparation of virus for animal inoculation and the subsequent experiment challenge of animals is described within our previous manuscript (Hutson et al. 2015. Submitted for Publication).

Observations and sampling

Animal observations and sampling was previously described within our previous manuscript (Hutson et al. 2015. Submitted for Publication). In brief, animals challenged with virus from each MPXV clade as well as 1 PBS animal were pre-selected for euthanasia on days 2, 4, 6, 9, 12, 17 or 24 post infection (p.i.). On scheduled euthanasia days subsets of animals were sacrificed by humane euthanasia. For those animals euthanized, blood and necropsy samples were also collected. Strict euthanasia criteria were applied throughout the study as

follows: any animal that became unresponsive to touch, lost 25% or more starting body weight, or accrued a total score of 10 on the following scale was humanely euthanized; decreased activity (2 points); lethargy, unsteady gait, inappetence (3 points each); labored breathing and recumbancy (5 points each).

Necropsy and tissue specimen collection

Necropsies on all animals were performed according to IACUC standards in an ABSL-3 laboratory and utilizing full ABSL-3 personal protective equipment (PPE) as previously described in detail (Hutson et al. 2015 Submitted for Publication). Samples taken during necropsy included: eyelid, eye, inner cheek tissue, tongue, nasal cavity tissue, tonsils, submandibular lymph nodes/salivary glands, mesentery lymph nodes, oropharynx tissue, trachea, gallbladder, lungs, heart, spleen, pancreas, kidney, liver, duodenum, jejunum, ileum, stomach, brain, gonad, belly skin, lesion if present, feces, urine or bladder tissue, oral swab, ocular swab, and blood. Instruments were cleaned and decontaminated with 5% Microchem and 70% ethanol between collections of each tissue. Tissues were frozen at -70°C prior to further processing.

Tissue preparation for immunohistochemistry analysis

After euthanasia, a necropsy was performed and tissues were taken as described above. Pieces of each tissue were fixed in 10% neutral-buffered formalin for at least 48 hours and then transferred to 70% ethanol for routine processing to create paraffin block which were subsequently sectioned at 3 μm.

Apoptosis assay

For detection of apoptosis ApopTag Peroxidase In Situ Apoptosis Detection Kit (Millipore) was used according to the manufacturers' instructions. This kit consists of terminal deoxynucleotidyl transferase mediated deoxyuridine triphosphate nick-end labeling (TUNEL)

methodology. Modifications of the manufacturers' protocol included the use of Vector NovaRed horseradish peroxidase (HRP) substrate (Vector Labs) in place of DAB as the chromogen. Counterstaining was performed with Gill's hematoxylin. Counting apoptotic cells was performed by randomly moving each slide until 10 adjacent fields were counted. These 10 fields of view were counted by 2individuals.

Double stain

For visualization of apoptosis and viral antigen co-localization, a sequential IHC protocol was followed. First, the apoptosis assay (HRP) was performed as described above. Modifications for this described assay included an additional blocking step with Dual Endogenous Block (Dako) following the hydrogen peroxidase incubation. Following incubation with the Vector NovaRed chromogen, slides were washed in ddH20. The slides were then incubated with a rabbit polyclonal anti-smallpox antibody (1:5000). The secondary antibody that was then utilized was a swine anti-rabbit alkaline phosphatase purified antibody (Dako). BCIP/NBT (Dako) was then used as the chromogen to create a blue-black color in the presence of viral antigen. Counterstaining for this double-stain IHC assay was done with a nuclei methyl green stain. Slides from PBS inoculated prairie dogs were used as negative controls.

Sample preparation for Western Blots

Sample processing was performed under BSL-2 conditions with BSL-3 work practices. For tissue homogenization, 1ml aliquots of PBS and SPEX bead (SPEX Sample Prep) were prepared. The PBS/bead aliquot was then poured into a tube containing the individual tissue sample. The GenoGrinder 2000 (SPEX Sample Prep) was used following the manufacturer's

instructions to create a tissue homogenate. 100ul of the homogenate was extracted for DNA isolation. The remaining homogenate was used for virus isolation.

Antibodies

Antibodies against phosphorylated p65, myeloid differentiation factor 88 (MyD88), tank-binding kinase (TBK), IkB-alpha, IκB kinase (IKK) IKK-epsilon, Interleukin-1 (IL-1) receptor-associated kinase (IRAK-4), and phosphorylated-IRAK4 were purchased from Cell Signal. Retinoic acid-inducible gene I (Rig-I) antibody was purchased from Santa Cruz Biotech. The antibody cytochrome c oxidase IV (COX) was used as a loading control and NF-kB control cell extracts were used as a reaction control (Cell Signal). Secondary antibodies (were anti-rabbit or anti-mouse as necessary) and were also purchased from Cell Signal.

Western Blot

Homogenized tissues were further digested with lysis buffer and protease/phosphatase inhibitor cocktail (Cell Signal), heated at 55º C for 1 hour (to inactivate virus), sonicated and protein concentrations determined with the Quibit Fluorometer (Life Technologies). Equal amounts of protein (20ug) preparations were prepared using standard Western Blot techniques and then fractioned by electrophoresis on a 3-20% gradient gel and transferred to PVDF paper, followed by probing with primary antibodies following manufacturer's recommendations. Chemiluminescent reactions were determined using the LumiGLO Peroxide Reagent (Cell Signal). Chemiluminescence was captured by the BioRad ChemiDoc instrument and band intensities were determined using the ChemiDoc software.

Statistical analyses

As data were not normally distributed, nonparametric statistical analyses were used (Lehman, 1975). The Wilcoxon rank-sum test was utilized to compare protein intensities. A p-

value of <= 0.05 was considered statistically significant. Data analysis was performed using SAS v9.3

Results

Activation levels of p65

In order to compare NFkB activation in vivo during WA and CB MPXV infections, we chose to look at phosphorylated p65 levels within the spleen, liver, kidney and gallbladder tissues from infected prairie dogs. These tissues were chosen based on viral kinetics within these animals (spleen is an early site of viral infection, liver and kidney are intermediate sites and gallbladder is a late site of viral infection). By analyzing these tissues, we hypothesized that we might observe differences in NFkB activation. By utilizing an antibody against the phosphorylated form of p65, we were looking at the activated form of this protein, which is considered the main NFkB subunit. In Congo Basin MPXV infected animals, p65 activation (band intensity) tended to rise on days 2-4 p.i., then drop when viable virus was present (days 6-12). At viral clearance on day 17-24 p.i., p65 activation reemerged (Figure 2.1). This trend was not as evident in tissues from WA MPXV animals (Figure 2.1b). For each clade and each tissue, the 4 animals with highest viral loads were compared to the same tissues from PBS control animals (n=5). Although viral loads reached 10^9 pfu/gram of tissue (Fig 2.2), significant differences in p65 activation were only seen in livers of animals infected with CB or WA clades and in kidney of animals infected with WA clade when compared to PBS control animals (p values=0.04, 0.04, 0.04; Table 2.1). Other tissues were comparable to PBS animals therefore p65 activation within those tissues was minimal. This data suggests that in those tissues (CB MPXV spleen, kidney and gallbladder and WA MPXV spleen and gallbladder) activation of NFkB is being suppressed by viral infection.

Where along pathway(s) is activation suppressed during peak MPXV infection?

The spleen and liver samples above that were analyzed for p65 activation were also analyzed for proteins via Western blot upstream of p65, including IkB-alpha and IKK-epsilon as well as key proteins involved in TLR and RLR signaling pathways (Rig-I, MyD88, TBK, IRAK4). Spleen and Liver were chosen as the spleen seems to be an early target of infection, while the liver is an intermediate/late target. Statistical comparisons of the band intensities for each protein are shown in Table 2.2. In agreement with the data we saw when analyzing the p65 activation, both WA and CB MPXV inhibited activation of most of these proteins. In fact, the only statistical significance in the spleen, occurred in the intensity of the phosphorylated IRAK4 (ph-IRAK) protein when comparing the PBS values to WA MXPV ($p=0.009$) and when comparing ph-IRAK4 intensities between CB and WA animals ($p=0.004$); WA MPXV animals were statistically higher in both of these comparisons. In all other values, both the WA and CB MXPV infected animals had similar protein levels compared to PBS control animals, suggesting in the spleen that NFkB activation at these protein levels is likely being suppressed during viral infection, supporting the data seen when looking just at ph-p65 values. Most likely this suppression in the spleen is occurring at multiple signaling pathways, based on the finding of a lack of statistical significance in the different proteins. Interestingly, there were increased numbers in the protein band intensities with significant differences in the liver of both MPXV clades, although none of these significant differences was when comparing CB tissues to PBS tissues; suggesting again that CB MXPV is better at inhibiting NFkB activation (most likely along multiple pathways) compared to WA MPXV. Although p65 activation was up-regulated in liver from infected animals, all upstream proteins in CB MPXV infected animals were similar to

PBS controls (Table 2.2). This suggests that another pathway(s) not analyzed in the current study is responsible for p65 activation within this tissue.

Virus induced apoptosis

Individual liver and spleen sections were screened for apoptosis utilizing a TUNEL assay. These tissues were chosen as the spleen seems to be an early target of infection, while the liver is an intermediate/late target. Additionally as seen in Figure 2.2 for both MPXV clades, the liver and spleen have appreciably high loads of virus during the course of infection. For both WA and CB challenged animals the amount of apoptosis within the liver only increased slightly and was comparable between the clades (Figure 2.3, Table 2.3). Kupffer cells were only observed to stain for apoptosis in the liver of 1 animal; instead hepatocytes were the predominant cell type that was positive for apoptosis. Unlike the liver, there was a noticeable trend of increased apoptosis in spleen sections (Figure 2.3) which was especially appreciable within the CB MPXV challenged animals (Table 2.3). When comparing the 2 animals that were found dead from MPXV infection on day 12 (WA MPXV PD 21 and CB MPXV PD 32), PD32 had greater than 6 times the number of apoptotic splenocytes compared to PD21.

A double IHC assay was performed on a small subset of known MPXV positive liver and spleen sections to investigate whether the virus co-localizes with the apoptotic cells. As demonstrated in Figure 2.4, we did observe co-localization of the virus (blue-black stain) in the majority of cells that were also positive for apoptosis (red-brown nuclei) in both liver and spleen sections.

Discussion

Orthopoxviruses, including MPXV are large, double-stranded DNA viruses and are considered to be mostly self-sufficient in regards to replication and transcription due to the fact

that they prepackage many of the viral proteins needed for infection. Like other members of the genus, MPXV replicates within the cytoplasm of an infected cell. Once in the cytoplasm of the cell, the virus is able to modulate host cell defenses and begins expressing early genes through the release of these prepackaged viral proteins and enzymatic factors [5–7]. Because of the large poxvirus genomes, which typically encode ~200 proteins, these viruses are primarily independent on host nuclear transcriptional machinery, therefore poxviruses are especially well suited to manipulate and evade the host immune response to viral infection. Two strategies that poxviruses have shown to modulate to evade the host immune response have been the cytoplasmic activation of NFκB, and host cell death, or apoptosis [8,9].

Although much work has been done looking at how poxviruses inhibit the host immune system *in vitro*, there is less data from *in vivo* studies. In the current study we analyzed tissues from prairie dogs infected with either WA or CB MPXV for key proteins involved in NFkB signaling, and amount of cells labelled for apoptosis. This animal model has been previously characterized and recognized as a useful model to compare differences in pathogenicity between the MXPV clades [10–12]. Through analysis of the activated state of p65, the main subunit of the NFkB pathway, we saw that NFkB activation is suppressed during MPXV infection. In the prairie dog MPXV model, peak infection with highest viral load generally occurs between days 9-13 pi [10,11]. We found that both WA and CB MPXV were able to effectively inhibit NFkB activation (p65 phosphorylation) within certain tissues during peak infection, with inhibition occurring in more tissues from CB MPXV (CB: spleen, kidney, gallbladder and WA: spleen, gallbladder).

In order to determine where p65 activation was being inhibited by the viruses, proteins upstream of p65 were analyzed (spleen and liver). Most viruses and other agents that activate NF-κB do so

through a common pathway based on phosphorylation-induced, proteasome-mediated degradation of the protein IκB. This pathway is regulated by activation of a high molecular weight IκB kinase (IKK) complex whose catalysis is generally carried out by three tightly associated IKK subunits. IKK-epsilon is a homolog of the main IKK subunit and activation of this kinase leads to NFkB activation (through degradation of IkB). Upstream of IKK degradation of IkB and NFkB stimulation, NF- κB activation is signaled through upstream pathways such as TLRs, RLRs and numerous other pathogen associated molecule signaling pathways (PAMPs). Therefore we also compared key proteins involved in RLR signaling (Rig-I) and TLR signaling (IRAK-4, TBK, MyD88). Consistent with p65 suppression in the spleen, all of the upstream proteins analyzed were inhibited by both viruses, with the exception of statistically higher expression of ph-IRAK4 in WA MPXV when compared to PBS or CB MXPV infected animals. However in the liver (in which we saw up regulation of phosphorylated p65), although tissues from WA MPXV animals were statistically higher than PBS controls in Rig-I, MyD88 and TBK proteins; the other proteins were similar to PBS controls, suggesting that the virus is inhibiting some of these upstream pathways. Additionally analysis of these proteins in CB MPXV liver samples, showed protein levels similar to PBS controls with no statistical difference, suggesting again that CB MPXV is better at inhibition of these different pathways. Since we saw inhibition of these up-stream proteins, but increased p65 phosphorylation, most likely the phosphorylation of p65 is occurring through other pathways that we did not analyze. TLR4/Trif mediated signaling may be responsible for p65 signaling in the liver. Additionally, signaling through nod-like receptors is another potential PAMP pathway that may be recognizing viral invasion and signaling the downstream NFkB pathway.

Although a large increase of apoptotic cells was seen within the spleen, the liver had only a minimal trend of increased apoptotic cells, even though these two 2 tissues had similarly high loads of viral burden in infected animals. Either the cells within the spleen are better equipped to initiate cell death when viral invasion occurs or the virus is more efficiently able to suppress apoptosis within the liver compared to the spleen; or perhaps a combination of these possibilities is the answer. Alternatively the virus may be preferentially initiating apoptosis within the spleen in order to release virions from within the cells to enhance viral spread from this lymphatic organ. In the current study we were able to show that when cells are undergoing apoptosis, they generally co-localize with the virus suggesting that the viral invasion of these cells triggers the apoptotic response. Based on our study, there is suggestion that CB MXPV causes more apoptosis within the spleen compared to WA MPXV. Our results are in contrast to *in vitro* results which showed WA MPXV caused increased apoptosis compared to CB MPXV via fluorescence-activated cell sorting analysis of AnnexinV staining [13]. This could be due to the fact that *in vitro* results are not adequately showing what is occurring *in vivo* or something specifically different within this animal model. Additional *in vivo* studies need to be performed in order to determine the cause of this discrepancy. Another interesting observation was that while there were a large number of cells labeled for apoptosis within the spleen, the liver had only a minimal trend of increased apoptotic cells, even though these 2 tissues had similarly high loads of viral burden in infected animals. Either the cells within the spleen are better equipped to initiate cell death when viral invasion occurs or the virus is more efficiently able to suppress apoptosis within the liver compared to the spleen; or perhaps a combination of these possibilities is the answer. Alternatively the virus may be preferentially initiating apoptosis within the spleen in order to release virions from within the cells to enhance viral spread from this lymphatic

organ. Apoptosis is a complex signaling pathway that can be triggered by different stimuli. There are 2 main pathways that result in apoptosis, the intrinsic (mitochondrial) and extrinsic (death receptor) pathways; it is possible for both the intrinsic and extrinsic pathways to be activated simultaneously within tissues. Interestingly, it has been reported that activation of Kupffer cells within the liver leads to secretion of the cytokine tumor necrosis factor (TNF) thereby activating the extrinsic apoptotic pathway [15–17]. Kupffer cells also express the Fas ligand which can also lead to apoptosis within hepatocytes [17]. As poxvirus proteins have been shown to inhibit both TNF and Fas receptor-induced apoptosis [18], this could explain why we did not see a dramatic increase in apoptosis within the liver as was seen in the spleen; the virus may be circumventing the host induced apoptotic response within the liver through inhibition of these specialized macrophages, Kupffer cells. The activation of apoptosis pathway(s) within different tissues as well as inhibition of these pathways in response to MPXV infection should be investigated as this may help to explain the differences in MPXV clade pathogenicity. Additional in vivo studies with more samples would be useful in elucidating the differences we observed.

Although NFkB activation and apoptosis are two different signaling cascades, there is interplay between the pathways. Generally activation of NFkB exerts anti-apoptotic influence, and this was reflected in tissues from MPXV infected animals, spleen had suppressed NFkB activation and increased apoptosis while the liver had increased NFkB activation, with minimal apoptosis. The results of our study could be unique to the prairie dog MXPV model. However, we have consistently shown that these animals have a remarkably similar disease course as humans infected with MPXV including increased virulence when infected with CB MPXV. Therefore it is important to consider our *in vivo* findings when formulating explanations for the

pathogenicity differences between the clades. In our study, CB MPXV was better able to inhibit NFkB in more tissues compared to WA MPXV, but actually resulted in increased apoptosis. This perhaps indicates that circumventing the NFkB pathway is more important in resulting virulence and pathogenicity of the virus than apoptosis. Additional *in vivo* studies should be done to further look at NFkB and apoptotic response to a MPXV infection.

Reference List

1. Moss B, Shisler JL (2001) Immunology 101 at poxvirus U: immune evasion genes. Semin Immunol 13: 59-66. 10.1006/smim.2000.0296 [doi];S1044-5323(00)90296-3 [pii].

2. Seet BT, Johnston JB, Brunetti CR, Barrett JW, Everett H, Cameron C, Sypula J, Nazarian SH, Lucas A, McFadden G (2003) Poxviruses and immune evasion. Annu Rev Immunol 21: 377-423. 10.1146/annurev.immunol.21.120601.141049 [doi];120601.141049 [pii].

3. Likos AM, Sammons SA, Olson VA, Frace AM, Li Y, Olsen-Rasmussen M, Davidson W, Galloway R, Khristova ML, Reynolds MG, Zhao H, Carroll DS, Curns A, Formenty P, Esposito JJ, Regnery RL, Damon IK (2005) A tale of two clades: monkeypox viruses. J Gen Virol 86: 2661-2672.

4. Reed KD, Melski JW, Graham MB, Regnery RL, Sotir MJ, Wegner MV, Kazmierczak JJ, Stratman EJ, Li Y, Fairley JA, Swain GR, Olson VA, Sargent EK, Kehl SC, Frace MA, Kline R, Foldy SL, Davis JP, Damon IK (2004) The detection of monkeypox in humans in the Western Hemisphere. N Engl J Med 350: 342-350.

5. Payne LG, Norrby E (1978) Adsorption and penetration of enveloped and naked vaccinia virus particles. J Virol 27: 19-27.

6. Vanderplasschen A, Hollinshead M, Smith GL (1998) Intracellular and extracellular vaccinia virions enter cells by different mechanisms. J Gen Virol 79 (Pt 4): 877-887.

7. Munyon W, Paoletti E, Grace JT, Jr. (1967) RNA polymerase activity in purified infectious vaccinia virus. Proc Natl Acad Sci U S A 58: 2280-2287.

8. Mohamed MR, McFadden G (2009) NFkB inhibitors: strategies from poxviruses. Cell Cycle 8: 3125-3132. 9683 [pii].

9. Smith GL, Benfield CT, Maluquer de MC, Mazzon M, Ember SW, Ferguson BJ, Sumner RP (2013) Vaccinia virus immune evasion: mechanisms, virulence and immunogenicity. J Gen Virol 94: 2367-2392. vir.0.055921-0 [pii];10.1099/vir.0.055921-0 [doi].

10. Hutson CL, Olson VA, Carroll DS, Abel JA, Hughes CM, Braden ZH, Weiss S, Self J, Osorio JE, Hudson PN, Dillon M, Karem KL, Damon IK, Regnery RL (2009) A prairie dog animal model of systemic orthopoxvirus disease using West African and Congo Basin strains of monkeypox virus. J Gen Virol 90: 323-333.

11. Hutson CL, Carroll DS, Self J, Weiss S, Hughes CM, Braden Z, Olson VA, Smith SK, Karem KL, Regnery RL, Damon IK (2010) Dosage comparison of Congo Basin and West African strains of monkeypox virus using a prairie dog animal model of systemic orthopoxvirus disease. Virology 402: 72-82.

12. Hutson CL, Gallardo-Romero N, Carroll DS, Clemmons C, Salzer JS, Nagy T, Hughes CM, Olson VA, Karem KL, Damon IK (2013) Transmissibility of the monkeypox virus clades via respiratory transmission: investigation using the prairie dog-monkeypox virus challenge system. PLoS One 8: e55488. 10.1371/journal.pone.0055488 [doi];PONE-D-12-23800 [pii].

13. Kindrachuk J, Arsenault R, Kusalik A, Kindrachuk KN, Trost B, Napper S, Jahrling PB, Blaney JE (2012) Systems kinomics demonstrates Congo Basin monkeypox virus infection selectively modulates host cell signaling responses as compared to West African monkeypox virus. Mol Cell Proteomics 11: M111. M111.015701 [pii];10.1074/mcp.M111.015701 [doi].

14. Strasser A, O'Connor L, Dixit VM (2000) Apoptosis signaling. Annu Rev Biochem 69: 217-245. 69/1/217 [pii];10.1146/annurev.biochem.69.1.217 [doi].

15. Kresse M, Latta M, Kunstle G, Riehle HM, van RN, Hentze H, Tiegs G, Biburger M, Lucas R, Wendel A (2005) Kupffer cell-expressed membrane-bound TNF mediates melphalan hepatotoxicity via activation of both TNF receptors. J Immunol 175: 4076-4083. 175/6/4076 [pii].

16. Malhi H, Guicciardi ME, Gores GJ (2010) Hepatocyte death: a clear and present danger. Physiol Rev 90: 1165-1194. 90/3/1165 [pii];10.1152/physrev.00061.2009 [doi].

17. Canbay A, Feldstein AE, Higuchi H, Werneburg N, Grambihler A, Bronk SF, Gores GJ (2003) Kupffer cell engulfment of apoptotic bodies stimulates death ligand and cytokine expression. Hepatology 38: 1188-1198. 10.1053/jhep.2003.50472 [doi];S0270913903008760 [pii].

18. Bertin J, Armstrong RC, Ottilie S, Martin DA, Wang Y, Banks S, Wang GH, Senkevich TG, Alnemri ES, Moss B, Lenardo MJ, Tomaselli KJ, Cohen JI (1997) Death effector domain-containing herpesvirus and poxvirus proteins inhibit both Fas- and TNFR1-induced apoptosis. Proc Natl Acad Sci U S A 94: 1172-1176.

Table 3.1: Comparison of p65 activation. For each clade and each tissue, the 4 animals with highest viral loads were compared to the same tissues from PBS control animals (n=5). Significant differences in p65 activation were seen in livers of animals infected with CB and WA clades and in kidney of animals infected with WA clade when compared to PBS control animals

Table 1	Median Band Intensity		Wilcoxon rank sun
	WA	PBS	p-value
Spleen	63650	7144	0.45
Liver	58080	0	0.04*
Kidney	96564	0	0.04*
Gallbladder	32640	17235	0.23
	Median Intensity		Wilcoxon rank sun
	CB	PBS	p-value
Spleen	27108	7144	1
Liver	39456	0	0.04*
Kidney	33689	0	0.79
Gallbladder	38073	17235	0.23

Table 3.2: Comparison of protein expression upstream of p65 activation.

Wilcoxon Rank Sum - Exact test - p-values for each comparison

Liver - Myd88	**Spleen - Myd88**

	WA	CB	WA+CB	PBS
WA	---			
CB	0.002	---		
PBS	0.03	0.54	0.44	---

	WA	CB	WA+CB	PBS
WA	---			
CB	0.94	---		
PBS	0.43	0.79	0.51	---

Liver - TBK

	WA	CB	WA+CB	PBS
WA	---			
CB	0.002	---		
PBS	0.004	0.06	0.007	---

Spleen - TBK

	WA	CB	WA+CB	PBS
WA	---			
CB	0.94	---		
PBS	0.98	0.84	0.86	---

Liver ikbalpha

	WA	CB	WA+CB	PBS
WA	---			
CB	0.7	---		
PBS	0.55	0.38	0.36	---

Spleen ikbalpha

	WA	CB	WA+CB	PBS
WA	---			
CB	0.37	---		
PBS	0.12	0.67	0.2	---

Liver kkepsilon

	WA	CB	WA+CB	PBS
WA	---			
CB	0.31	---		
PBS	0.76	0.76	0.68	---

Spleen kkepsilon

	WA	CB	WA+CB	PBS
WA	---			
CB	0.13	---		
PBS	0.45	0.17	0.23	---

Liver phirak4

	WA	CB	WA+CB	PBS
WA	---			
CB	0.015	---		
PBS	0.76	0.07	0.21	---

Spleen phirak4

	WA	CB	WA+CB	PBS
WA	---			
CB	0.004	---		
PBS	0.009	0.39	0.38	---

Liver rig1

	WA	CB	WA+CB	PBS
WA	---			
CB	0.18	---		
PBS	0.01	0.17	0.02	---

Spleen rig1

	WA	CB	WA+CB	PBS
WA	---			
CB	0.19	---		
PBS	0.32	0.76	0.84	---

Table 3.3: Number of apoptotic cells in liver and spleen from MPXV infected prairie dogs.

TMTC: too many cells to count

PD#	Day p.i	Avg # of apoptotic cells	PD#	Day p.i	Avg # of apoptotic cells
PD2	PBS	0.9±0.7	PD2	PBS	0.9±0.7

	WA			CB	
A.	**MPXV**		**B.**	**MPXV**	
PD11	Day 4	1±0.6	PD25	Day 4	6.2±4.5
PD12	Day 4	0.7±0.6	PD26	Day 4	1.1±0.7
PD13	Day 6	4.4±2.0	PD27	Day 6	4.6±3.3
PD14	Day 6	5.3±2.9	PD28	Day 6	2.8±1.8
PD15	Day 9	10.1±11.0	PD29	Day 9	7.9±5.0
PD16	Day 9	0.8±1.0	PD30	Day 9	4.7±3.6
PD21	Day 12	6.9±4.0	PD32	Day 12	3.6±1.3
SPLEEN APOPTOSIS					
PD#	Day p.i.	Avg # of apoptotic cells	PD#	Day p.i	Avg # of apoptotic cells
PD2	PBS	3.4±1.6	PD2	PBS	3.4±1.6
C.	**WA MPXV**		**D.**	**CB MPXV**	
PD11	Day 4	1.6±1.0	PD25	Day 4	1.5±1.5
PD12	Day 4	1.4±1.5	PD26	Day 4	2±1.9
PD13	Day 6	10.7±7.8	PD27	Day 6	17.2±10.0
PD14	Day 6	8.7±5.0	PD28	Day 6	12±7.2
PD15	Day 9	17.3±8.4	PD29	Day 9	22.1±8.7
PD16	Day 9	15±4.3	PD30	Day 9	34.9±13
PD21	127	Day 12	14.8±11.1	Day 12	TMTC (>100)

.

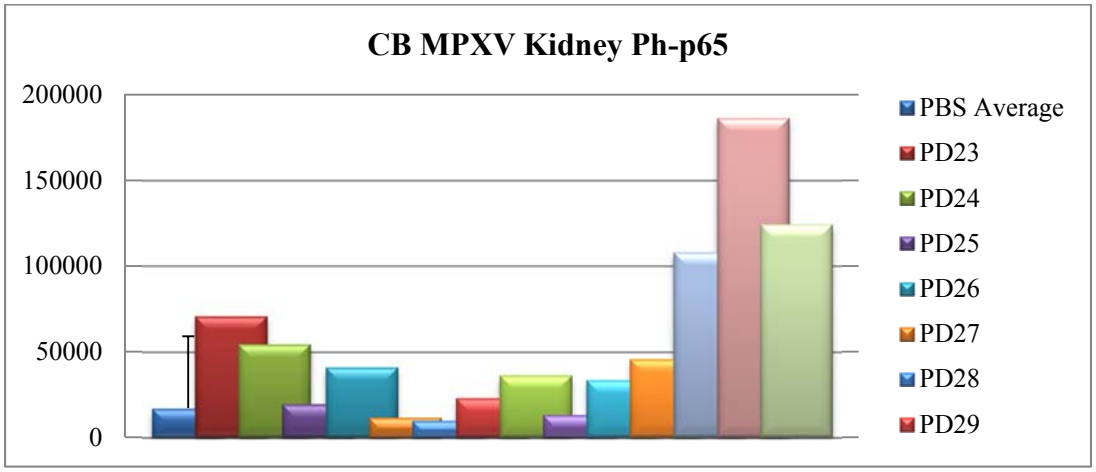

a.

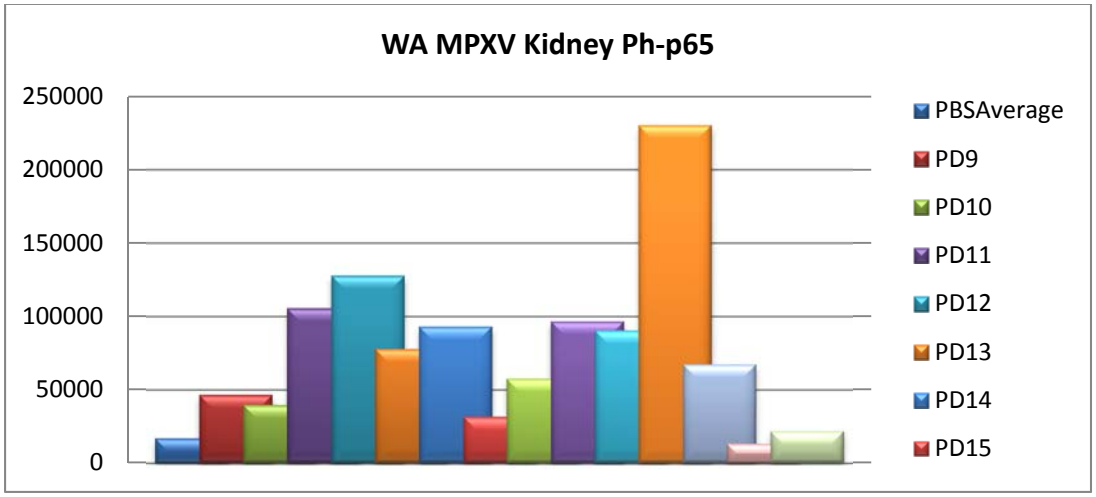

b.

Fig 3.1: Activation of p65 within kidney from MPXV infected prairie dogs. In Congo Basin MPXV infected animals (a), p65 activation (band intensity) tended to rise on days 2-4 p.i., then drop when viable virus was present (days 6-12). At viral clearance on day 17-24 p.i., p65 activation reemerged. This trend was not as evident in Wes African infected animals (b).

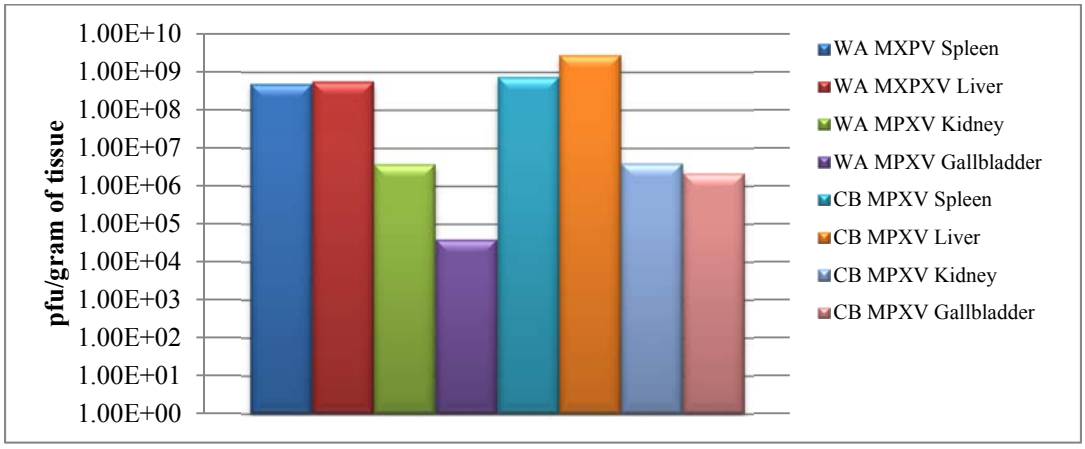

Fig 3.2: Average viral loads in WA and CB MPXV infected prairie dogs.

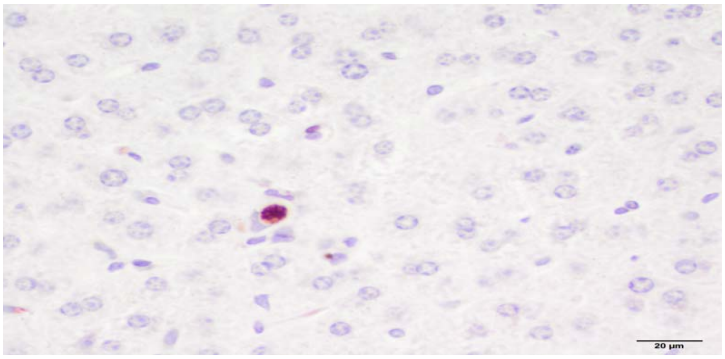

a.

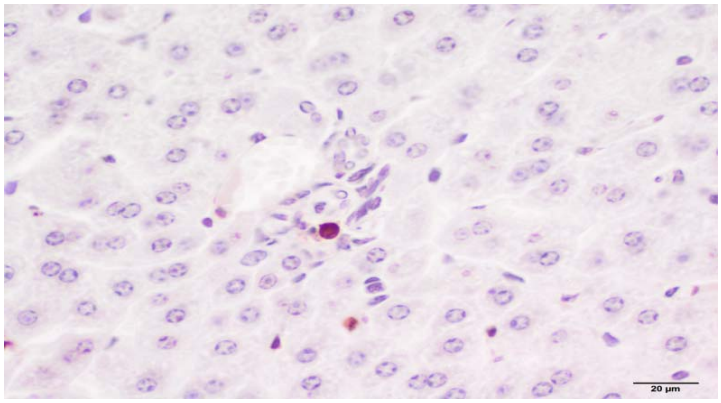

b.

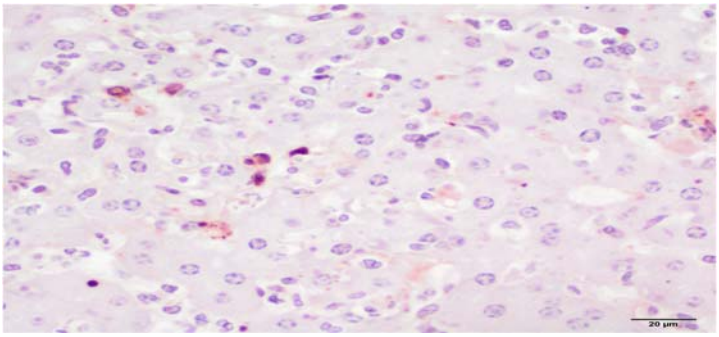

c.

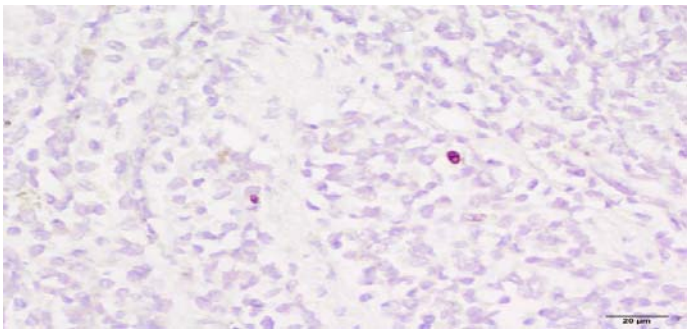

d.

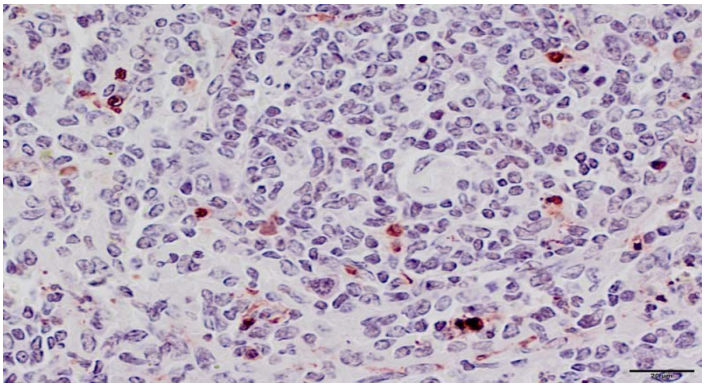

e.

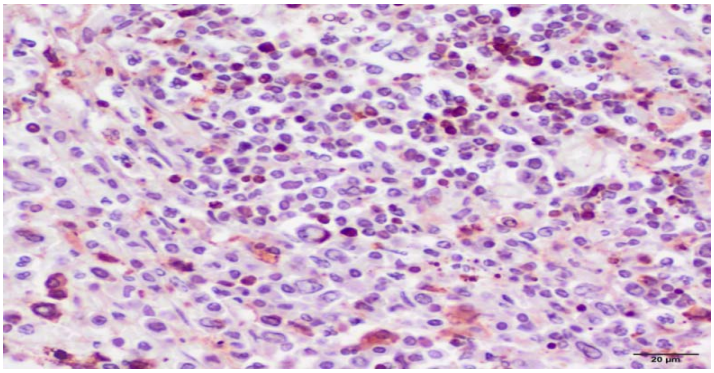

f.

Figure 3.3: Apoptosis within MPXV infected prairie dog liver and spleen. Prairie dogs intranasally challenged ($8x10^3$p.f.u.) with West African WA MPXV were serially sacrificed (days 2, 4, 6, 9, 12, 17 and 24) following challenge. Representative images of

immunohistochemical staining of paraffin-embedded prairie dog liver (a, b, c) and spleen (d, e, f) sections stained with Millipore Apoptosis kit. Apoptotic cells are identified by red-brown staining nucleus. (400x original magnification, scale bar=20 µm, immunoperoxidase method, Vector NovaRed chromogen, hematoxylin counterstain).

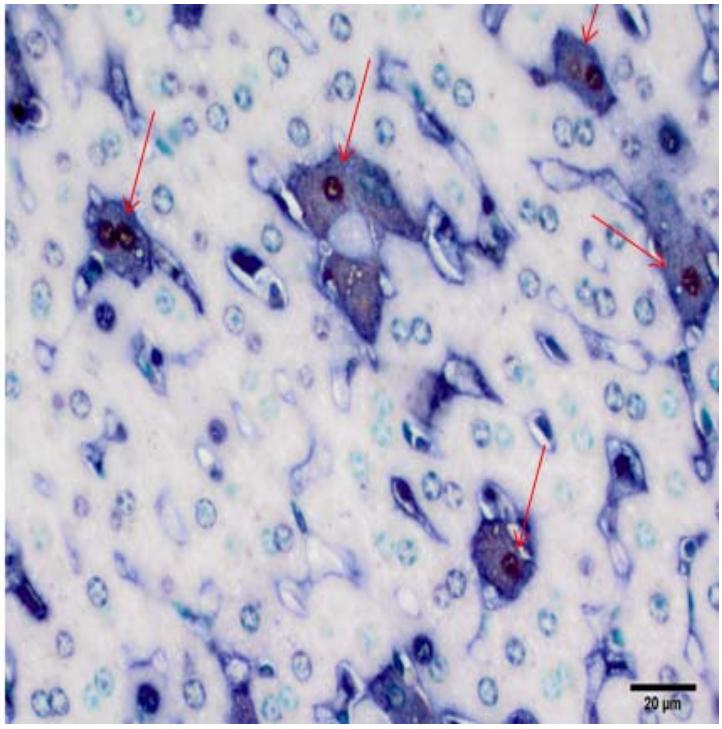

Figure 3.4: Dual viral and apoptosis IHC within representative liver section from Congo Basin MPXV infected prairie dog on day 12 p.i. Apoptotic cells (red-brown nuclei) tended to also stain for poxvirus (blue/black cytoplasmic staining, arrows). (Immunoperoxidase method with Vector Red chromogen, alkaline phosphatase method with BCIP/NBT Chromogen; 400X original magnification, scale bar=20 µm; methyl green counterstain).

CHAPTER 4

THE USE OF ANALGESICS DURING A LOW-DOSE CHALLENGE OF WEST AFRICAN MONKEYPOX VIRUS WITHIN THE PRAIRIE DOG ANIMAL MODEL[3]

[3]C.L. Hutson, T. Nagy, N. Gallardo, , J. Salzer, J. Ayers, J.B. Doty, C.M. Hughes, Y. Nakazawa, P. Hudson, N. Patel, V. Olson, S. Keckler, I.K. Damon, D.S. Carroll. To be submitted to *PlosOne*.

Abstract

Human patients with Monkeypox virus (MPXV) infection report painful signs during the course of the disease; it is therefore reasonable to assume that animals infected with the virus experience some degree of pain. Analgesics are often withheld during challenge studies with the reasoning that viral disease course might be altered. Understanding how analgesic agents affect MPXV disease progression is critical when planning animal studies as well as making recommendations for human infections. In the current study prairie dogs were challenged with a low dose ($4X10^3$ pfu) of West African MPXV and treated with Metacam (NSAID) or Buprenorphine (opioid). Another group of animals was challenged with MPXV and was not treated. Additional groups of animals were treated with Metacam or Buprenorphine, but were not challenged with MPXV. Subsets of animals from each group were serially sacrificed during the course of the study and samples obtained. Disease progression and viral kinetics was similar; with the exception of two unexpected deaths in the Metacam-treated group. There were no histologic lesions directly attributable to analgesic treatment in any of the treatment groups. The findings in the current study will allow us to make more informed decisions concerning the use of analgesics during a MPXV infection.

Introduction

Since the eradication of smallpox (caused by the Orthopoxvirus Variola), the closely related Monkeypox virus (MXPV) has become the most important human health threat within this genus. As evidenced by the 2003 US outbreak, as well as the ongoing outbreaks of MPXV within Africa, there is a continued need to study this important human health threat [1–3]. Additionally, MPXV provides a surrogate for the study of related orthopoxviruses including variola virus. An ideal animal model is one that would emulate key features of human disease

including: utilizing a route of infection that mimics the natural transmission of the pathogen in humans; the ability to obtain disease with an infectious dose equivalent to that causing disease in humans; as well as having a disease course, morbidity and mortality similar to what is observed with human disease. Previous studies of the prairie dog MPXV model showed after intranasal or scarification challenge with a reasonable challenge dose, animals developed disease that closely resembled human monkeypox, including a protracted incubation period before the development of generalized lesions [4]. Additionally, these studies have shown that the prairie dog model is valuable for the comparison of disease attributable to the two MPXV clades, primarily by differences in mortality and level of morbidity.

Human patients with MXPV infection report painful signs during the course of disease including headache, sore throat, back pain and mouth sores [5]. Therefore it is likely that animals infected with MXPV experience some degree of pain, especially during robust infections. However analgesics are often withheld during challenge studies with the reasoning that viral disease course might be altered. Non-steroidal anti-inflammatory drugs (NSAIDs) are commonly prescribed to alleviate pain. These include salicylates, NSAIDs, and glucocorticoids to name a few. Metacam is commonly prescribed by veterinarians and falls into the NSAID category. However NSAIDs have been shown to inhibit the nuclear factor kappa-light-chain-enhancer of activated B cells pathway (NF-κB) which is the primary regulator of inflammation and plays a key role in regulating the immune response to different types of infection, including viral infection [6]. Orthopoxviruses, have been shown to encode multiple proteins that act in various ways to prevent NF-κB activity. The ability of orthopoxviruses to modulate NF-κB activation likely plays an important role in the ability of these viruses to cause disease, and therefore the utilization of substances that inhibit NF-κB activation (such as NSAIDS) would

very likely change the normal virus .[7] Opioids are also a common pain-reliving type of drug used to alleviate human and animal suffering. The justification for not using opioids during a viral challenge study is that these drugs have been shown to have multiple adverse effects that may exacerbate the morbidity of infected animals and may complicate the assessment of the immune response to the virus in an animal model. MPXV infection can cause respiratory distress which could be confused with the depression of respiratory function which can occur with opioid analgesics. In addition, opioid analgesics in rats have been shown to cause temperature deregulation and respiratory depression which could affect the safety of the animals during anesthesia and would also affect the behavior and eating habits of the animals. In addition, these animal experiments also seek to understand the immune response of the animals to the viral infection and opioid based analgesics could compromise the analysis of the immune response. Lastly, MPXV can affect liver function and this could be exacerbated by opioid use as these drugs are metabolized in the liver.

In the current study prairie dogs were challenged with a low dose ($4X10^3$ pfu) of West African MPXV and treated with Metacam (NSAID) or Buprenorphine (opioid). Our studies provide evidence against the use of Metacam during a MPXV infection. However only subtle differences were observed when comparing Buprenorphine treated MPXV infected animals to MPXV controls after 21 days of opioid treatment; at earlier points in the study, there were no differences between these two groups. It is therefore likely that the use of Buprenorphine for short-term pain relief during a WA MPXV infection would result in no changes to viral pathogenicity. Such findings will be critical when making recommendations for pain relief during future animal challenge studies.

Materials and Methods

Animals

Wild-caught, juvenile black-tailed prairie dogs (PDs ;*Cynomys ludovicianus*) were obtained from Texas. At time of infection, animals were approximately 8 months old and had been prescreened by a veterinarian, determined to be in good health status and found negative for the presence of anti-orthopoxvirus antibodies. A sterile PIT tag was injected subcutaneously at the base of the neck for animal identification and non-invasive recording of body temperature. The average starting weight for animals was 446 grams (range 360-620). During experimental infections animals were housed individually in large HEPA-filtered ventilated cages rack system within an animal Biological Safety Level-3 (ABSL-3) animal room. Animals were cared for in accordance with CDC Institutional Animal Care and Use Committee (IACUC) guidelines under an approved protocol (2367HUTPRAC). In addition to PD chow and hay, animals were provided with monkey biscuits, mixed nuts and approved fruit and vegetables for added dietary enrichment and measurement of appetence.

Analgesics

The drug Meloxicam (Metacam) is a non-steroidal anti-inflammatory drug (NSAID) that is used in both veterinary and human medicine for pain relief. Metacam inhibits both COX-1 and COX-2. Metacam was given to animals by a subcutaneous injection at 4mg/kg (Metacam) once a day. Volume of drug administered was based on weight of each animal and the total volume administered at each treatment was between 0.5-1.5mL. This dosing regimen was based on studies with Metacam in rats. Animals that were given Metacam were dosed from day 3 through day 21 post infection; or until the animal's predetermined day of euthanasia.

The drug Buprenorphine is an opioid analgesics used in both veterinary and human medicine for pain relief. Buprenorphine is 25-50 times more potent than morphine and may be associated with less respiratory depression than other opioids. Buprenorphine was given by the subcutaneous injection at 0.1mg/kg every 12 hours. Volume of drug administered was based on weight of each animal and the total volume administered at each treatment was between 0.5-1.5mL. This dosing regimen was based on studies with Buprenorphine in rats. Animals that were given Buprenorphine were dosed from day 3 through day 24 post infection; or until the animal's predetermined day of euthanasia.

Animal Groups

Animals were divided into 5 experimental groups. On day 0, animals (n=25) were challenged with Monkeypox virus (MPXV) ($5X10^3$ pfu in 10ul via an intranasal challenge). This dosage was based on previous studies, utilizing a dose that resulted in 100% morbidity with no mortality within the prairie dog MPXV model. 5 animals were challenged with MPXV as described below to serve as positive controls. 10 challenged animals were treated once a day with Metacam. 10 challenged animals were treated twice a day with Buprenorphine. Additionally, 14 animals were used as treatment controls; they were uninfected but treated with appropriate analgesic (Metacam or buprenorphine) for comparison of blood chemistries values, clinical signs as well as pathological examination of tissues collected during necropsy. On sample days (see below), the animals were administered the appropriate drug once while under anesthesia during sampling and additionally for Buprenorphine, once without anesthesia while being held by the scruff of the neck with bite-proof gloves. This is due to the belief that anesthetizing animals twice a day is not conducive to the animals' health and may have a negative impact on disease progression. On non-sample days, animals receiving analgesic

treatment were appropriately dosed daily with Metacam and every 12 hours with Buprenorphine if not sacrificed (either under anesthesia or while being held by the scruff of the neck with bite-proof gloves, being consistent throughout the study). On sample days 4, 6, 9 and 12 two challenged/treated animals, one treatment control animal and one challenge control animal from each group were humanely sacrificed while under anesthesia as shown in table 1 (these time points were based on earlier studies within this model). Other animals that were not sacrificed were weighed, checked for lesions (and other signs of morbidity) and had blood and oral swabs taken also while under anesthesia. Animals that are not euthanized by day 12 were also sampled as described above on day 17. A pain scale scoring system has been established for the MPXV prairie dog model and was utilized during the study to increase animal monitoring, administer subcutaneous fluids and/or humanely euthanize an animal if it met the corresponding criteria. All animals that survived infection were humanely euthanized 24 days post infection. After death/euthanasia, all animals underwent a complete necropsy as described below.

Virus

The MPXV strain used to challenge animals, MPXV-USA-2003-044, was isolated during the 2003 U.S. outbreak [2,8]. The virus has been fully sequenced and underwent 2 passages in African green monkey kidney cells (BSC-40) prior to seed pool production; sucrose-cushion purified preparations of virus were used for animal challenges.

Animal inoculation

Inocula dosages ($4X10^3$ plaque forming units [pfu]) were calculated based on the morbidity and mortality rates observed in the authors' previous studies with this animal model. Briefly, a challenge dose of $6X10^3$ pfu WA MPXV o resulted in disease morbidity including skin lesions and viral shedding identified in oral cavity samples in 100% of animals with 25%

mortality [9]. As our goal was to achieve morbidity with no mortality, we challenged animals with a slightly lower dose in the current study. The viral strain stock was diluted in phosphate-buffered saline (PBS). Inocula titers were immediately re-confirmed by standard plaque assay (as described below). Animals were infected by an intranasal (IN) route of inoculation while under general anesthesia using 5% isoflurane administered through a VetEquip Incorporated vaporizer. Animals were inoculated with a total volume of 10ul (5ul in each nostril). Additionally, 14 animals were mock infected with PBS to serve as analgesic controls.

Observations and sampling

For all 24 days of study post-infection, individual animals were observed for signs of morbidity, fever, malaise (inappetence, decreased activity, recumbence with reluctance to move, etc.) and clinical lesions, including rash. On scheduled euthanasia days (4, 6, 9 and 12 post infection (pi)) and day 17 pi; oropharyngeal swabs, blood weights, and lesion counts were collected from all animals while under general anesthesia (as described above), before subsets of animals were sacrificed by humane euthanasia. For those animals euthanized, blood and necropsy samples were also collected. Strict euthanasia criteria were applied throughout the study as follows: any animal that became unresponsive to touch, lost 25% or more starting body weight, or accrued a total score of 10 on the following scale was humanely euthanized; decreased activity (2 points); lethargy, unsteady gait, inappetence (3 points each); labored breathing and recumbence (5 points each).

Necropsy and tissue specimen collection

Necropsies on all animals were performed according to IACUC standards in an ABSL-3 laboratory and utilizing full ABSL-3 personal protective equipment (PPE). Complete

necropsies were performed after euthanasia with duplicate sets of tissues taken. Instruments were cleaned and decontaminated with 5% Microchem and 70% ethanol between collections of each tissue. One set of tissues were frozen at -70°C prior to further processing. The other tissue set including the head was placed into 10% buffered formalin solution for histologic evaluation (see below). Oral and ocular swabs were collected with sterile individual Dacron swabs and stored frozen without diluent. Serum was separated from whole blood and processed for serology and clinical chemistry levels (see below). Tissues and swabs were subsequently processed and further prepared for DNA analysis, virus isolation, and western blot (see below).

Sample preparation for PCR and viral growth

Sample processing was performed under BSL-2 conditions with BSL-3 work practices. The BioRobot EZ-1 Workstation (Qiagen) was used for genomic DNA extraction of all blood, swab and tissue samples. Samples were incubated at 55ºC for an hour to inactivate viable virus particles prior to DNA extraction. For whole blood samples, 100ul was used for DNA extraction, and the remaining blood was used for tissue culture propagation. For each swab collected, 400ul of PBS was added. The swab extraction tube systems (SETS) (Roche) protocol was used to recover sample from the swab. DNA was extracted from 100ul of the swab lysate. The remaining swab eluate was used for virus isolation. For tissue preparation, 1ml aliquots of PBS and SPEX bead (SPEX Sample Prep) were prepared. The PBS/bead aliquot was then poured into a tube containing the individual tissue sample. The GenoGrinder 2000 (SPEX Sample Prep) was used following the manufacturer's instructions to create a tissue homogenate. 100ul of the homogenate was extracted for DNA isolation. The remaining homogenate was used for virus isolation.

Real-time PCR analysis

Samples were tested by real-time PCR using forward and reverse primers and probes complimentary to the conserved non-variola orthopoxvirus (OPXV) E9L (DNA polymerase) gene [10]. Purified MPXV DNA (10fg – 1ng) was used as standard controls to allow quantification of viral DNA. A positive sample produced CT values (in duplicate) of 37 or below. A weakly positive sample displayed CT values 38-39 (duplicates).

Virus-tissue infectivity

All samples were stored at -70°C until virus isolation was attempted. Previous analyses demonstrated that real-time PCR detection of MPXV DNA detects trace amounts of MPXV DNA [1]. Therefore, specimens were first tested for presence of OPXV DNA by PCR and, if positive, were subsequently evaluated for viable virus by tissue culture propagation. Each swab or tissue sample was titrated in duplicate using 10 fold dilutions of swab eluate or tissue slurry on BSC-40 cell monolayers, incubated at 35.5° C and 6% CO_2 for 72 hours, and subsequently stained with crystal violet and formalin to visualize plaques. Titers were expressed as p.f.u. per milliliter of blood or swab eluate; or p.f.u. per gram of tissues.

Serologic analysis

A modified ELISA was used for analysis of anti-OPXV immunoglobulin types M and G in separated serum as previously described in detail [4,11] .

High content screening-green fluorescent protein (HCS-GFP) neutralization assay

Beginning on day 9 pi, serum samples were further tested with the HCS-GFP neutralization assay as described in Keckler et al. In brief, serum samples were serially diluted from 1:40 to 1:1280 and then neutralizing antibody (NAb) titers against vaccinia virus were measured using a GFP based assay. The HCS-GFP assay detects the percentage of GFP-

producing responder cells (R), and this value is then normalized to control wells to produce the relative percent responders (RPR) titer. The reported values in this manuscript are 50% RPR titers that are equivalent to the serum dilution that neutralizes 50% of viral infection (ID_{50}) in a traditional plaque reduction neutralization titer (PRNT) assay. The 50% RPR titer was calculated using a modified variable slope sigmoidal equation (Hill equation, Levenberg Marquardt algorithm) and Prism 5.0 software (GraphPad) with goodness of fit to this sigmoidal curve (represented by R^2; all R^2 values considered positive were above 0.9000) calculated by the least-squares method.

Blood chemistry values

Serum was separated from whole blood, transferred to a clean tube and stored at -20ºC prior to analysis. The Piccolo blood chemistry analyzer (Abaxis) was utilized to determine the following blood chemistry profiles: sodium (NA), globulin (GLOB), potassium (K), glucose (GLU), calcium (CA), blood urea nitrogen (BUN), creatinine (CRE), alkaline phosphatase (ALP), alanine aminotransferase (ALT), amylase (AMY), phosphours (PHOS), total bilirubin (TBIL), albumin (ALB), and total protein (TP).

Histopathologic evaluation

After euthanasia, a necropsy was performed and tissues were taken as described above. Pieces of each tissue were fixed in 10% neutral-buffered formalin for at least 48 hours and then transferred to 70% ethanol for routine processing to create paraffin block which were subsequently sectioned at 3 μm. Animal heads were decalcified using standard techniques. Routine hematoxylin-eosin (H&E) stains were performed for histopathological evaluation.

Statistical analyses

As data were not normally distributed, nonparametric statistical analyses were used (Lehman, 1975). The Wilcoxon rank-sum test was utilized to compare the blood chemistry percent change (Percent change from day zero value to day 9) for each group of animals. A p-value of <= 0.05 was considered statistically significant. Data analysis was performed using SAS v9.3

Results

Clinical observations (Table 3.2)

Metacam treated control animals tolerated the NSAID analgesic with minimal clinical signs (Table 3.2a). Animals in this treatment group lost less than 5% of their weight appetence/activity remained constant throughout the study. The only side-effect due to the daily subcutaneous injection was a lesion that formed on the dorsum between the shoulder blades of three animals (PD12006 after 6 days of Metacam treatment, PD12036 after 18 days of Metacam treatment and PD12057 after 12 days of Metacam treatment). Necropsy results were grossly normal, with the exception of 1/3 of the animals euthanized at day 24 (PD12057) which had an enlarged liver with a prominent reticular pattern.

Similarly the Buprenorphine treated control animals appeared to tolerate the opioid analgesic with no clinical signs; animals in this treatment group lost less than 8% of their weigh and appetence/activity remained constant throughout the study (Table 3.2b). No respiratory depression or other clinical signs were observed. Upon necropsy, the liver of 4/7 animals was friable and/or discolored, otherwise necropsy results were grossly normal.

MPXV control animals had a similar disease presentation as has previously been characterized in this animal model [4,9]. Prairie dogs euthanized on day 4 and 6 pi did not show

clinical signs of disease (Table 3.2c). The animal euthanized on day 9 pi (PD12014) presented with ruffled fur and displayed respiratory depression while under anesthesia. Upon necropsy of this animal, numerous gross lesions attributable to MPXV infection were observed and are summarized in Table 3.2c. The two remaining MPXV control animals presented with cutaneous MPXV lesions on day 11 pi (PD12011) and day 14 pi (PD12034). As this was a low-dose challenge with the less virulent West African MPXV strain, numbers of cutaneous lesions were minimal (Table 3.2c). PD12011 was euthanized as planned on day 12 pi and with the exception of the cutaneous lesions and nasal discharge, no other clinical signs or abnormal necropsy findings were seen. PD12034 was euthanized 24 days pi after recovering from MPXV challenge. During the course of infection, in addition to cutaneous lesions, respiratory depression under anesthesia, nasal discharge and ruffled fur were observed. Additionally this animal lost 13.7% of its body weight and inappetence was noted during the course of infection.

Clinical findings in animals challenged with MPXV and treated with Metacam beginning on day 3 pi are summarized in Table 3.2d. PD12112 unexpectedly died on day 4 pi after one day of Metacam treatment, while under anesthesia during routine sampling. This animal was noted to have mild lymphadenopathy, which is a symptom not typically observed in MPXV infected prairie dogs until day 9 or later pi. Because of the unscheduled death of PD12112, only one animal was euthanized on day 6 pi and it was clinically normal. The two animals in this group that were euthanized as scheduled on day 9 pi had numerous clinical signs attributed to MPXV infection. PD12037 had one MPXV lesion on the tongue, ruffled fur, and a slightly bloated abdomen as well as gross lesions observed during necropsy that were attributable to MPXV infection (Table 3.2d). PD12038 was also euthanized on day 9 pi; this animal had one cutaneous lesion on the paw as well as mild lymphadenopathy. On day 12pi, PD12078 was euthanized as

planned. Although this animal had only developed 2 MXPV lesions (inner mouth), it did have more severe clinical signs than the MXPV control animals including a bloody nose, gastrointestinal bloat, and urine matted/ruffled fur. Inappetence was noted during the course of infection and 10.3% weight loss occurred in this animal. Gross necropsy findings were also extensive in this animal and are summarized in Table 3.2d. PD12024 was euthanized on day 12 pi; however this animal was unsuccessfully challenged as evidenced by no immune response and all tissue samples testing negative for viral DNA. Because this animal model has a steep dose-response, we have seen similarly unsuccessful experimental infections when using a low challenge dose [12]. PD12114 was scheduled for euthanasia on day 24 pi, however due to weight loss (28.4%) and measures of morbidity, this animal was euthanized on day 18 pi. This animal first developed cutaneous lesions on day 12 pi and had a total of 18 lesions at time of euthanasia. Clinical signs included respiratory depression under anesthesia, dehydration, gastrointestinal bloat, nasal discharge/blood, and lethargy. In addition, numerous gross lesions were seen upon necropsy and are summarized in 3.2d. Similar to the Metacam treatment controls, the two animals euthanized on day 24 pi in this group (PD12096 and PD 12059) had lesions on the dorsum due to daily subcutaneous administration of the analgesic. By day 24 pi, these two animals had recovered from infection. Cutaneous lesion development was minimal; PD12059 only developed 1 MPXV lesion in the mouth during the course of infection but had several clinical signs including gastrointestinal bloat, nasal discharge, respiratory depression while under anesthesia, and dehydration. PD12096 only developed 8 MXPV lesions during the study and had minimal weight loss and clinical signs. At time of necropsy on day 24 pi, there were no gross findings.

Clinical findings in animals challenged with MPXV and treated with Buprenorphine beginning on day 3 pi are summarized in Table 3.2e. Until day 12 pi, no animals in this group had clinical signs of MPXV infection. Only two animals in the MPXV challenged/ Buprenorphine treated group developed cutaneous lesions; PD12049 and PD12091 both had lesions by day 12 pi. PD12049 and PD12119 were euthanized on day 12 pi and had moderate weight loss during the course of infection (19.1% and 18.4% respectively). Both of these animals had respiratory depression under anesthesia, nasal discharge, and additionally for PD12119, facial edema and ruffled fur. Several gross lesions were seen upon necropsy of these two animals as summarized in Table 3.2e. PD12091 was euthanized 24 days pi. This animal only developed 6 cutaneous lesions, had minimal weight loss during the study (4.6%), respiratory depression and lesions in the liver and spleen were seen during necropsy. As seen in the other animal during this study (PD12024), PD12079 was unsuccessfully challenged as evidenced by no immune response and all tissue samples testing negative for viral DNA.

Blood chemistry results

Although there were some significant findings in blood chemistry values when comparing the groups, none of these was due to treatment with either Metacam or Buprenorphine, but rather due to viral infection (Table 3.3). Although not enough animals for statistical comparisons, when comparing the mean % change on day 24 pi, uninfected animals treated with Metacam had decreased ALB and increased BUN compared to PBS animals; buprenorphine treated animals had increased ALT values compared to PBS animals (data not shown).

Antibody response (Table 3.4)

Serum from challenged animals was tested by ELISA for antibody production. Additionally, beginning on day 9 pi, serum samples were further tested for neutralization titers. Because the numbers of animals are low, we can only look at trends in the data. Animals between the three groups mounted a measureable immune response between days 9-12 pi, similar to our other studies with this animal model (Hutson et al. 2015 submitted for publication). In previous studies with MPXV in the prairie dog, it has been consistently shown that cutaneous lesions and antibody production (captured by ELISA) occur simultaneously. However in the current study, one MPXV/Buprenorphine animal (PD12091) and two MPXV/Metacam animals (PD12078, PD12096) developed lesions on day 12 but were negative by ELISA, although these animals did have neutralizing titers at this time (data not shown). The ELISA values on day 12, 17 and 24 pi were similar between the MPXV control animals and the MPXV challenged animals and those challenged animals treated with either Metacam or Buprenorphine (Table 3.4). On day 12 and 17 pi the neutralization titers were also similar between the three groups. However, comparing the groups on day 24 pi, the MPXV control animal had a neutralizing titer that was more than 10000 times that of the animals treated with Metacam or Buprenorphine (Table 3.4). However because the numbers of animals are so small in each group, we cannot make any definitive conclusions.

Kinetic of viral spread

Table 3.5 summarizes the presence of viral DNA, viable virus and peak viral load within the different groups of animals. In the MPXV control animals, viral DNA was first detected on day 4 pi in the blood, lungs, stomach and liver. Viable virus was present from the majority of samples collected from this group of animals beginning on day 6 pi. By day 24 only the nasal cavity had viable virus remaining however viral DNA was still detectible in all tissues collected,

except the blood. When looking at the peak viral load for each tissue throughout the study, we saw a range of $1X10^2$ pfu (blood) to the spleen having the highest peak viral load at $2x10^9$ pfu on day 9 pi from the MXPV control animals. The nasal cavity and salivary glands/submandibular lymph nodes had similarly high loads ($5X10^7$ pfu and $3X10^7$ pfu respectively) on day 9 pi from this group of animals.

Viral DNA was detectable in more tissues on day 4 pi in the MXPV challenged animals treated with Metacam; oral swabs, nasal tissue, salivary gland/submandibular lymph node, liver, small intestine, mesenteric lymph node, and stomach were all positive for viral DNA in this group of animals (Table 3.5). Additionally on day 4, PD12112 that unexpectedly died while under anesthesia and presented with lymphadenopathy had viable virus detected in the salivary gland/submandibular lymph node tissue. This was earlier than our MPXV positive controls and a previous serial sacrifice study with WA MPXV (Hutson et al. 2015). The other tissues were all positive for virus beginning by day 6 or 9 pi, except for the blood (viremia from this group was not captured). By day 24, only the nasal cavity was still positive for viable virus, however viral DNA remained in all tissues except the blood (as was seen in the positive controls). The minimum peak viral load was from the brain $1X10^2$ pfu (day 18) from the Metacam/MPXV challenged animals. The tongue had the highest viral load in this group of animals ($5X10^7$ pfu on day 12 pi) followed by the skin lesion ($2X10^7$ pfu on day 18 pi) and the spleen and nasal cavity on day 9 pi ($9X10^6$ pfu and $6X10^6$ pfu respectively).

There was also slightly more tissues positive for viral DNA on day 4 pi in the MXPV challenged animals treated with Buprenrophine compared to the MPXV control animals; blood, salivary glands/submandibular lymph node, spleen, liver, mesenteric lymph node and stomach were positive for viral DNA (Table 3.5). In this group of animals, there was no viable virus

present in any tissues on day 24 pi, although viral DNA was still detected in several tissues. Viable virus was not detected in the stomach form any animals of the Buprenorphine, MPXV challenged animals. The tissue with the lowest peak viral load was the skin lesion on day 12 pi ($8X10^2$ pfu). The highest peak viral load was seen in the nasal cavity on day 12 pi ($2X10^8$ pfu) followed by the tongue ($3X10^6$ pfu on day 12) and spleen ($5X10^5$ pfu day 6).

Pathology findings

Previously, we have fully described the pathogenesis of MPXV within the prairie dog animal model (serial sacrifice study) between days 2-24 pi. Based on those studies in which pathological changes due to viral infection were first observed primarily on day 9 pi and because we wanted to look for pathologic changes after long term treatment of prairie dogs with an NSAID or opioid, we performed histologic evaluations on animals euthanized between days 9-24 pi.

Metacam treated controls

After 9 days of NSAID treatment, there were no pathological changes observed within the animal euthanized (12021) with the exception of diffuse glycogen vacuolation within hepatocytes. Animal 12006 that was euthanized on day 12 within the Metacam treated control group was also normal within most tissues examined. The stomach of this animal had multifocal moderate lymphoplasmacytic infiltrates within the lamina propria and submucosa. This lesion was similar to those seen in dogs and humans as a result of Helicobacter infections of the stomach. This lesion could also represent a residual inflammatory reaction to gastric parasitic (helminth) infections. Whatever the exact cause, the gastric inflammatory infiltrates were most likely not related to the NSAID treatment. This animal also had an injection site reaction from

the daily SQ administration of Metacam. The epidermis had a locally extensive sub-corneal pustule and the dermis contained a perivascular to interstitial, mostly neutrophilic inflammatory infiltrate. There was degeneration, necrosis, with mild neutrophilic and histiocytic inflammation and regeneration in the underlying cutaneous muscle. The surrounding soft tissues were normal. The three animals euthanized after 21 days of Metacam treatment (prairie dogs 12029, 12036 and 12057) had various lesions, none of which was attributable directly to NSAID treatment (with the exception of the injection site). These three animals had sub-mucosal lymphoplasmacytic and histiocytic inflammatory foci in the stomach mucosa. In addition, animal 12029 had a slight increase in the number of lymphocytes and plasma cells within the lamina propria of the duodenum. Moreover, the glycogen vacuolation within the liver section from this animal was diffuse and marked. Additionally there was slight growth of yeast (*Candida* spp.) in the esophageal mucosa. In animal 12036, glycogen vacuolation in the liver section was diffuse and moderate. Focal, moderate bronchus- associated lymphoid tissue (BALT) hyperplasia was seen within the lung. Also a single submucosal lymphocytic inflammatory focus was seen in the submucosa of the esophagus. Animal 12057 had diffuse and moderate glycogen vacuolation of the hepatocytes. Additionally, in the liver, multifocal mild portal infiltrates of lymphoid cells were observed and the Kupffer cells were prominent. At the injection site, the ulcer extended to the panniculus and is covered with a seroceullular crust and numerous neutrophils. The muscle has undergone degeneration and necrosis where injection of Metacam occurred.

Buprenorphine treated controls

After 9 days of opioid treatment, there were only non-significant pathological findings and none were attributed to treatment in animal 12072. In the stomach of this animal, two small

lymphoid nodules were observed in the mucosa. Similar to the Metacam treated animals, glycogen vacuolation was observed (for this animal it was moderate and mostly periportal to midzonal within the hepatic lobules). In the lungs, occasional small granulomas were seen with histiocytes and neutrophils within). Most likely, these granulomas formed as a reaction to either inhaled foreign bodies or to migrating parasites. Nevertheless, neither foreign bodies nor parasites were found within these granulomas. The esophagus from the animal euthanized on day 9 had small bacterial colonies within the cornified layer without an inflammatory reaction. A bilateral impaction of feed material in the root of the molars with neutrophilic inflammation and bone remodeling unilaterally was also seen. The animal euthanized after 12 days of Buprenorphine treatment (12045) only had minimal and non-significant histologic lesions. The hepatocytes within all zones of the hepatic lobules had mild and diffuse glycogen vacuolation. Multifocal, mild, superficial esophagitis with multifocal erosions were observed. Inflammatory infiltrate consisted of numerous neutrophils, either singly or in small clusters, were present in the superficial layers of the esophageal epithelium. In these areas where neutrophils are the esophageal epithelium is extensively vacuolated and/or focally eroded. Small numbers of bacteria are seen attached to the epithelial surface throughout. The three animals treated with Buprenorphine for 24 days before euthanasia (12055, 12071, 12046) had various, minimal and non-significant histological lesions. None of these lesions were compatible with or attributable to the treatment with Buprenorphine. Animal 12055 had periportal and moderate hepatocytic vacuolation. Bacteria were observed on the mucosal surface of the esophagus in this animal. Animal 12071 had mild, focal periportal mixed (lymphoplasmacytic, histiocytic, and neutrophilic) inflammatory infiltrate as well as focal hepatic necrosis with associated, mostly neutrophilic inflammatory infiltrate. The kidney of this animal had focal mild interstitial

nephritis. Prominent BALT was observed in the lung section. In animal 12046 the stomach had a single prominent sub-mucosal lymphoid nodule. Hepatocytic glycogen vacuolation was moderate and diffuse. In the kidney, there was a focus of interstitial nephritis with associated tubular degeneration and regeneration. The esophagus from this animal had scattered, small mixed inflammatory infiltrate consisting of lymphoplasmacytes and histiocytes. Nodules were seen in the submucosa (prob. Prior damage to esophageal lining). Focally the infiltrate extends into the basal layers of the epithelium. This animal also had unilateral impacted feed material within a root of a molar tooth.

MPXV positive control animals

The MPXV challenged animal 12014 that was euthanized on day 9 p.i. exhibited histologic lesions attributable to MPXV infection. Unilateral moderate nutrophilic rhinitis was observed in this animal. Additionally the submandibular lymph nodes had multifocal necrosis as did the spleen which had multifocal, widespread necrosis both in the white and red pulp (affecting primarily red pulp). The liver had minimal, multifocal hepatic necrosis with associated, mostly neutrophilic inflammatory infiltrate. In the lung one Langhans type giant cell was seen in the alveolar septum. Incidental findings in this animal included a lymphoid nodule in the submucosa of the stomach. Animal 12011 was euthanized on day 12 p.i. and had the following histological lesions. It had a bilateral, severe, necrotizing, and purulent rhinitis with osteolysis in the nasal turbinates. Additionally there was necrosis of the nasal associated lymphoid tissue (NALT) and adjacent soft tissues. The submandibular lymph node and mesenteric lymph node displayed prominent germinal centers in the lymphoid follicles. Lymphoplasmacytic inflammatory infiltrates were seen in the mucosa, as well as in the submucosa of the stomach. The duodenum had mildly increased numbers of lymphocytes and

plasma cells in the lamina propria. In the liver rare, small neutrophilic inflammatory foci were observed and the Kupffer and endothelial cells were also prominent. The trachea had focal, mild infiltrate (lymphocytes, plasma cells and lesser numbers of histiocytes) in the submucosa. There was diffuse and mild hepatocytic glycogen vacuolation throughout the liver. Animal 12034 was euthanized 24 days p.i. and had minimal histological lesions. There was residual mild, diffuse lymphoplasmacytic bilateral rhinitis with mucosal necrosis of NALT. The liver had multifocal lymphoplasmacytic infiltrates in scattered portal triads. The heart from this animal had a focal myocardial necrosis and associated mixed (neutrophilic, histiocytic, and lymphocytic) inflammatory infiltrate. The kidney had focal mixed inflammatory infiltrate primarily lymphoplasmacytic with lesser number of neutrophils in the sub-capsule. A focal collection of alveolar macrophages were observed within the lung. There was diffuse and mild hepatocytic glycogen vacuolation throughout the liver. There were also scattered bacterial colonies in the cornified layer of the esophagus (without any inflammatory reaction).

Metacam treated MPXV challenged animals

Animals challenged with MPXV and treated with Metacam for 9 days before euthanasia (Prairie dogs 12037 and 12038) exhibited histological lesions characteristic for pox viral infection similar to those seen in the MPXV positive control animal on day 9. Animals 12037 had neutrophilia in the capillaries within the nasal mucosa with neutrophils traversing the nasal mucosa. The submandibular lymph node appeared normal, however the spleen had focal, minimal necrosis and single-cell necrosis was seen in the white pulp. Additionally the white pulp was slightly hyperplastic. The stomach had a single submucosal infiltrate consisting of lymphocytes, plasma cells and some histiocytes. Neutrophils in the alveolar capillaries were present in slightly elevated numbers (pulonary neutrophilia) and there was slight alveolar

histiocytosis as well. There was diffuse and mild hepatocytic glycogen vacuolation throughout the liver. Animal 12038 also had several lesions characteristic of MPXV infection, primarily bilateral neutrophilic and necrotizing rhinitis as well as NALT necrosis (with obliteration of the NALT). Additionally, multifocal necrotizing lymphadenitis was observed in the submandibular lymph node. There was diffuse and mild hepatocytic glycogen vacuolation throughout the liver. Animal 12078 was challenged with MPXV and treated with Metacam 12 days before euthanasia. Similar pathological changes as the MPXV positive control euthanized 12 days pi were seen in this animal including bilateral neutrophilic rhinitis with NALT necrosis. The mesenteric lymph node displayed lymphadenitis characterized by macrophages and some neutrophils. Mild submucosal lymphoplasmacytic and histiocytic inflammatory infiltrate was seen in the submocosa focally in the trachea. Multiple minute foci of hepatic necrosis with associated inflammatory infiltrates (mostly neutrophils) were observed in the liver, as well as prominent and hypertrophied Kupffer and endothelial cells. A submucosal lymphoid follicle with focal and mild inflammation in the muscle coat was observed in the stomach; infiltrate was perivascular lymphoplasmacytic and histiocytic. The kidney displayed mild chronic interstitial nephritis (most likely pre-existing inflammation not related to NSAID treatment or viral infection). When the brain was examined, minimal lymphoplasmacytic inflammation was seen in the choroid plexus. Animal 12114 was euthanized 18 days pi due to measures of morbidity meeting euthanasia criteria. Examination of the submandibular lymph node revealed acute multifocal necrosis. Fibrin on the capuslar surface of the spleen with small numbers of entrapped neutrophils was seen (a reflection of peritinities in the liver). Mesenteric fat necrosis with severe nutrophilic inflammatory infiltrate and some lymphocytes and macrophages as well as areas of mineralization were also seen. The liver displayed several lesions including prominent Kupffer

cells. Capsular cells were also prominent with a band of neutrophils under the capsular region. Focally, fibrin with embedded neutrophils covered the liver capsule (peritonitis) . Sinusoids had moderately increased numbers of neutrophils (sinus neutrophilia). Grossly visible fibrin on the surface of the liver was associated with large numbers of entrapped neutrophils. In the kidney there were also occasional necrotic tubules in the deep medulla as well as focal mineralization in the medulla adjacent to the renal pelvis. The skin from the injection site of this animal had necrotizing myositis. Two animals (12096 and 12059) were challenged with MPXV and treated with Metacam for 21 days. These animals were euthanized at day 24 pi. Animal 12096 had minimal histologic lesions including slight lymphoid depletion in the spleen, and mild multifocal lymphoplasmacytic and histiocytic infiltrate in the mucosa of the stomach. Additional findings included mildly increased numbers of lymphocytes and plasma cells in the lamina propria of the duodenum. The kidney from this animal was observed to have tubular fat vacuolation and multifocal tubular lipidosis in the cortex. Also scattered and mild histiocytic and neutrophilic interstitial infiltrates at the corticomedullary junction of the kidney were seen. All other examined tissues, including the nasal cavity, were normal. Animal 12059 had necrotizing and neutrophilic rhinitis (residual lesions due to intranasal infection with MPXV). The mesenteric lymph node had focal, mild necotizing lymphanitis. There was diffuse and mild hepatocytic glycogen vacuolation throughout the liver. The gallbladder had scattered lymphocytes and plasma cells in the submucosa.

Buprenorphine treated MPXV challenged animals

Two animals (12115 and 12085) that were challenged with MPXV and treated with the opioid buprenorphine were sacrificed 9 days pi. With the exception of the lung which had moderate neutrophila in blood vessels and diffuse and mild hepatocytic glycogen vacuolation

throughout the liver, all other examined tissues were histologically normal. Additionally to the histologic lesions above, animal 12115 had histologic lesions characteristic of pox viral infection; minimal multifocal neutrophilic infiltrate was observed in the nasal cavity. Animals 12049 and 12119 were challenged with MPXV and treated with buprenorphine 12 days before euthanasia. Animal 12049 had bilateral, moderate to marked purulent rhinitis with osteolysis and necrosis of NALT. A single necrotic peyers patch lymphoid was seen in the small intestine. Multiple minute foci of hepatocellular necrosis was observed in the liver, as well as moderately prominent Kupffer's and endothelial cells. The kidney had occasional faint hyaline casts in the tubules. Subepithelial mixed inflammatory infiltrate (lymphocytes, plasma cells, and neutrophils) was observed in the esophagus. This animal also had a focal subcorneal neutrophilic pustule that extended into the superficial dermis and the adjacent underlying dermis had dense diffuse neutrophila and lymphoplasmacytic inflammatory infiltrate. Animal 12119 also had severe bilateral neutrophilic and necrotizing rhinitis. Additionally there was necrosis of the NALT (and intralesional bacterial cocci) as well as unilateral dental pulp necrosis. The submandibular lymph node had necrosis with scattered Langhans type giant cells. Diffuse and mild hepatocytic glycogen vacuolation was seen throughout the liver. Additionally, Kupffer's cells were prominent and there was moderate sinusoidal neutrophilia. The kidney had multifocal, chronic interstitial nephritis with radiating bands of fibrosis (residual scar from prior interstitial nephritis). A focal submucosal collection of lymphocytes and plasma cells was seen in the trachea. Animal 12091 was challenged with MPXV and treated with buprenorphine for 24 days before being euthanized. Histological lesions in this animal were minimal. There was diffuse and mild hepatocytic glycogen vacuolation throughout the liver. The duodenum had mildly increased numbers of lymphocytes and plasma cells in the lamina propria. Focal

submucosal collections of lymphocytes and plasma cells were seen in the trachea. Multifocal, moderate mineralization was seen in the kidney (at the corticomedullary junction). Additionally mild, multifocal chronic interstitial nephritis was observed in the kidney of this animal.

Discussion

Overall animals tolerated both Buprenorphine and Metacam for this extended period very well, providing valuable information that both of these analgesics can be safely utilized within this non-standard laboratory animal species. Respiratory depression has been associated with the use of opioids as has gastritis with NSAIDs; based on animal observation, weight monitoring and necropsy observations, neither of these side effects occurred in treated prairie dogs. With the exception of the lesion on the dorsum from Metacam injections, no other adverse clinical signs were observed during the course of the study in either Metacam or Buprenorphine control animals. Histologic evaluation of Metacam controls revealed various lesions, however none were directly attributable to NSAID treatment. One of the animals in the Metacam control group euthanized on day 24 had multifocal mild portal infiltrates of lymphoid cells observed in the liver and prominent Kupffer cells. Prominent Kupffer cells has been attributed to NSAID toxicity in rats [13] , however since only one animal presented with this finding, we cannot definitively say if the NSAID treatment was the cause. Similarly the Buprenorphine treated controls had numerous lesions upon histologic exam, but none were compatible with or attributable to the treatment with Buprenorphine. Two of the Buprenorphine treatment animals euthanized on day 24 pi had mild interstitial nephritis, and additionally one of these had tubular degeneration and regeneration. As kidney toxicity is not a known side-effect during Buprenorphine treatment, these were likely incidental findings specific to these two animals.

MPXV control animals had a typical disease progression associated with a low-dose challenge of West African MPXV [9]. Although clinical signs and cutaneous MPXV lesions was minimal, tissue tropism of the virus was extensive with viable virus detected in all tested tissues and viral loads reaching as high as $2X10^8$ pfu/gram of tissue. The MPXV challenged/Metacam treated animals had a similar disease progression as the MPXV control animals; however subtle increases in disease severity were noted. In this animal group, there were two unexpected deaths, one of these occurring on day 4 pi. This animal also had viable virus detected upon necropsy at day 4 pi as well as lymphadenopathy at time of death; both of which do not typically occur in these animals challenged with WA MPXV until day 6-9 pi. However because this animal had only been treated with Metacam on one day prior to death, we cannot be sure that the differences seen were due to Metacam treatment, or just differences in this particular animal. The other unexpected death in the MPXV/Metacam group was an animal that had to be euthanized on day 18 pi due to weight loss and measures of morbidity. Additionally in this group, there were more animals that developed cutaneous lesions and more severe clinical signs in some animals (gastrointestinal bloat, bloody nose, dehydration and lethargy) compared to the MPXV control animals. Although these findings suggest higher morbidity in those MPXV challenged animals that were treated with Metacam, the tissue tropism and peak viral loads within tissues were similar to the MXPV control group of animals. Those animals challenged with MXPV and treated with Buprenrophine for the course of the study also had a similar disease progression compared to MPXV challenged control animals. In this group of animals, no clinical signs were observed until day 12 pi and only two animals developed cutaneous MPXV lesions. There were no unexpected deaths in the MPXV/Buprenorphine group and the tissue tropism and peak viral load was similar to the MXPV control animals. Histologic examination

of animals in the three MPXV challenged groups revealed pathologic lesions attributable to viral infection. However there was no indication that treatment with Metacam or Buprenorphine exacerbated the viral-attributed lesions.

Only MPXV positive controls (n=1), Buprenorphine/MPXV animals (n=2) and Metacam/MPXV animals (n=3) had weight loss >or equal to 10%; therefore weight loss was most likely caused by the virus not drug treatments. Although there was nothing statistically significant on day 9 pi to indicate a change in blood chemistry values caused by either analgesic, when comparing the mean % change on day 24 pi, uninfected animals treated with Metacam had decreased ALB and increased BUN compared to PBS animals; buprenorphine treated animals had increased ALT values compared to PBS animals, which could indicate changes in liver function. When we compared antibody response, ELISA results were similar between the three groups of animals, however the neutralization titers on day 24 were dramatically lower in those animals challenged with MPXV and treated with Buprenorphine or Metacam compared to the MPXV control animals. Additionally in the current study, one MPXV/Buprenorphine animal and two MPXV/Metacam animals developed lesions on day 12 but were negative by ELISA, although these animals did have neutralizing titers at this time. Taken together this could indicate a delay in immune response (most likely the neutralization is due to IgM antibodies, which we have hypothesized our ELISA assay does not adequately capture (unlike IgG antibodies)) and/or that the animals were not mounting a robust immune response due to daily administration of these analgesic agents. However because our animal numbers were small, we cannot definitively conclude this.

The study had several limitations, primarily that the numbers in each study group were low. Because the prairie dog is a relatively large laboratory animal that has to be individually

caged, and we are limited by the amount of cage space available within our BSL3 animal laboratories, we are restricted to doing smaller groups of animal numbers. Additionally because these studies are performed under BSL3 conditions including full BSL3 PPE, in order to safely execute these studies we limit the number of animals so that personnel are not working within the BSL3 laboratories for extended hours. Because we had two animals that were unsuccessfully challenged we had a further decrease in our animal numbers. There are several possible explanations for why these animals were not infected after experimental inoculation. Although the animals are completely anesthetized during inoculation, it is possible that the virus was not efficiently delivered via intranasal challenge. We have previously seen a steep dose response in this animal model, even half a log lower than the intended viral inoculation could result in little or no disease. This steep dose response was noted in a previous study in which $6X10^3$ pfu of each MPXV clade resulted in overt MPXV disease in all four animals [9]. However, in the same study, approximately one log lower dose of $6X10^2$ pfu resulted in only one of the four challenged animals becoming infected for each clade. If the intended inoculation was efficiently given, another possibility is that this animal's innate immune system was able to effectively clear the virus before the adaptive immune system became involved. Because these are wild/outbred animals, we do observe differences in disease response and progression. Although we had small sample sizes, because we have previously fully characterized this animal model, we do feel that we can gain meaningful data from the current studies when comparing to previous studies. Another limitation is that we only used the less virulent WA MPXV. Therefore it might be worthwhile to do a follow-up study with CB MPXV (which may have some differences in the way it is circumventing the host's immune response compared to WA MPXV). We might therefore have different results with CB MPXV especially with Metacam treatment as it inhibits

the NFkB pathway and we have previously shown that CB MPXV more effectively inhibits this pathway (Hutson et al. 2015 in draft).

In the current study we used a low-dose challenge of WA MPXV and treated groups of animals with either Metacam or Buprenorphine. If either of these analgesics caused an increase in viral pathogenesis we expected to see stark differences in our MPXV challenged/analgesic treated animals compared to the MPXV positive/untreated animals (i.e. earlier and increased cutaneous lesion development, increased morbidity/mortality, and increased viral loads within tissues). However clinical signs between the groups was similar; with the exception of increased trends of morbidity and mortality within the MXPV infected/Metacam treated animals. Based on these observations, as well as the indications of immune suppression, and decreased liver function at day 24 pi, it would not be recommended to give either of these analgesics (especially at the high analgesic dose utilized) for an extended period during a viral infection as was done for the current study (18 days for Metacam and 21 days for Buprenorphine). Evidence against the use of Metacam during a MPXV infection was stronger (particularly given the fact that one Metacam/MPXV challenged animal died during anesthesia and had earlier viable virus after only one day of treatment). However because the differences we observed were so subtle comparing Buprenorphine treated MPXV infected animals to MPXV controls, it is likely the use of this analgesic for short-term pain relief (i.e. less than 7 days) during a WA MPXV infection would result in little differences in pathogenicity. However to confirm this, additional studies with a larger group of animals would be required.

Reference List

1. Hutson CL, Lee KN, Abel J, Carroll DS, Montgomery JM, Olson VA, Li Y, Davidson W, Hughes C, Dillon M, Spurlock P, Kazmierczak JJ, Austin C, Miser L, Sorhage FE, Howell J, Davis JP, Reynolds MG, Braden Z, Karem KL, Damon IK, Regnery RL (2007) Monkeypox zoonotic associations: insights from laboratory evaluation of animals associated with the multi-state US outbreak. Am J Trop Med Hyg 76: 757-768.

2. Reed KD, Melski JW, Graham MB, Regnery RL, Sotir MJ, Wegner MV, Kazmierczak JJ, Stratman EJ, Li Y, Fairley JA, Swain GR, Olson VA, Sargent EK, Kehl SC, Frace MA, Kline R, Foldy SL, Davis JP, Damon IK (2004) The detection of monkeypox in humans in the Western Hemisphere. N Engl J Med 350: 342-350.

3. Rimoin AW, Kisalu N, Kebela-Ilunga B, Mukaba T, Wright LL, Formenty P, Wolfe ND, Shongo RL, Tshioko F, Okitolonda E, Muyembe JJ, Ryder RW, Meyer H (2007) Endemic human monkeypox, Democratic Republic of Congo, 2001-2004. Emerg Infect Dis 13: 934-937.

4. Hutson CL, Olson VA, Carroll DS, Abel JA, Hughes CM, Braden ZH, Weiss S, Self J, Osorio JE, Hudson PN, Dillon M, Karem KL, Damon IK, Regnery RL (2009) A prairie dog animal model of systemic orthopoxvirus disease using West African and Congo Basin strains of monkeypox virus. J Gen Virol 90: 323-333.

5. Huhn GD, Bauer AM, Yorita K, Graham MB, Sejvar J, Likos A, Damon IK, Reynolds MG, Kuehnert MJ (2005) Clinical characteristics of human monkeypox, and risk factors for severe disease. Clin Infect Dis 41: 1742-1751.

6. Kopp E, Ghosh S (1994) Inhibition of NF-kappa B by sodium salicylate and aspirin. Science 265: 956-959.

7. D'Acquisto F, May MJ, Ghosh S (2002) Inhibition of nuclear factor kappa B (NF-B): an emerging theme in anti-inflammatory therapies. Mol Interv 2: 22-35. 10.1124/mi.2.1.22 [doi];2/1/22 [pii].

8. Likos AM, Sammons SA, Olson VA, Frace AM, Li Y, Olsen-Rasmussen M, Davidson W, Galloway R, Khristova ML, Reynolds MG, Zhao H, Carroll DS, Curns A, Formenty P, Esposito JJ, Regnery RL, Damon IK (2005) A tale of two clades: monkeypox viruses. J Gen Virol 86: 2661-2672.

9. Hutson CL, Carroll DS, Self J, Weiss S, Hughes CM, Braden Z, Olson VA, Smith SK, Karem KL, Regnery RL, Damon IK (2010) Dosage comparison of Congo Basin and West African strains of monkeypox virus using a prairie dog animal model of systemic orthopoxvirus disease. Virology 402: 72-82.

10. Li Y, Olson VA, Laue T, Laker MT, Damon IK (2006) Detection of monkeypox virus with real-time PCR assays. J Clin Virol 36: 194-203.

11. Karem KL, Reynolds M, Braden Z, Lou G, Bernard N, Patton J, Damon IK (2005) characterization of acute-phase humoral immunity to monkeypox: use of immunoglobulin M enzyme-linked immunosorbent assay for detection of monkeypox infection during the 2003 North American outbreak. Clin Diagn Lab Immunol 12: 867-872.

12. Hutson CL (2013) Transmissibility of the monkeypox virus clades via respiratory transmission: investigation using the prairie dog-monkeypox virus challenge system.

13. Abatan MO, Lateef I, Taiwo VO (2006) Toxic Effects of Non-Steroidal Anti-Inflammatory Agents in Rats. African Juornal of Biomedical Research 9: 219-223.

Table 4.1: **Animal groups and numbers sacrificed on days post infection.**

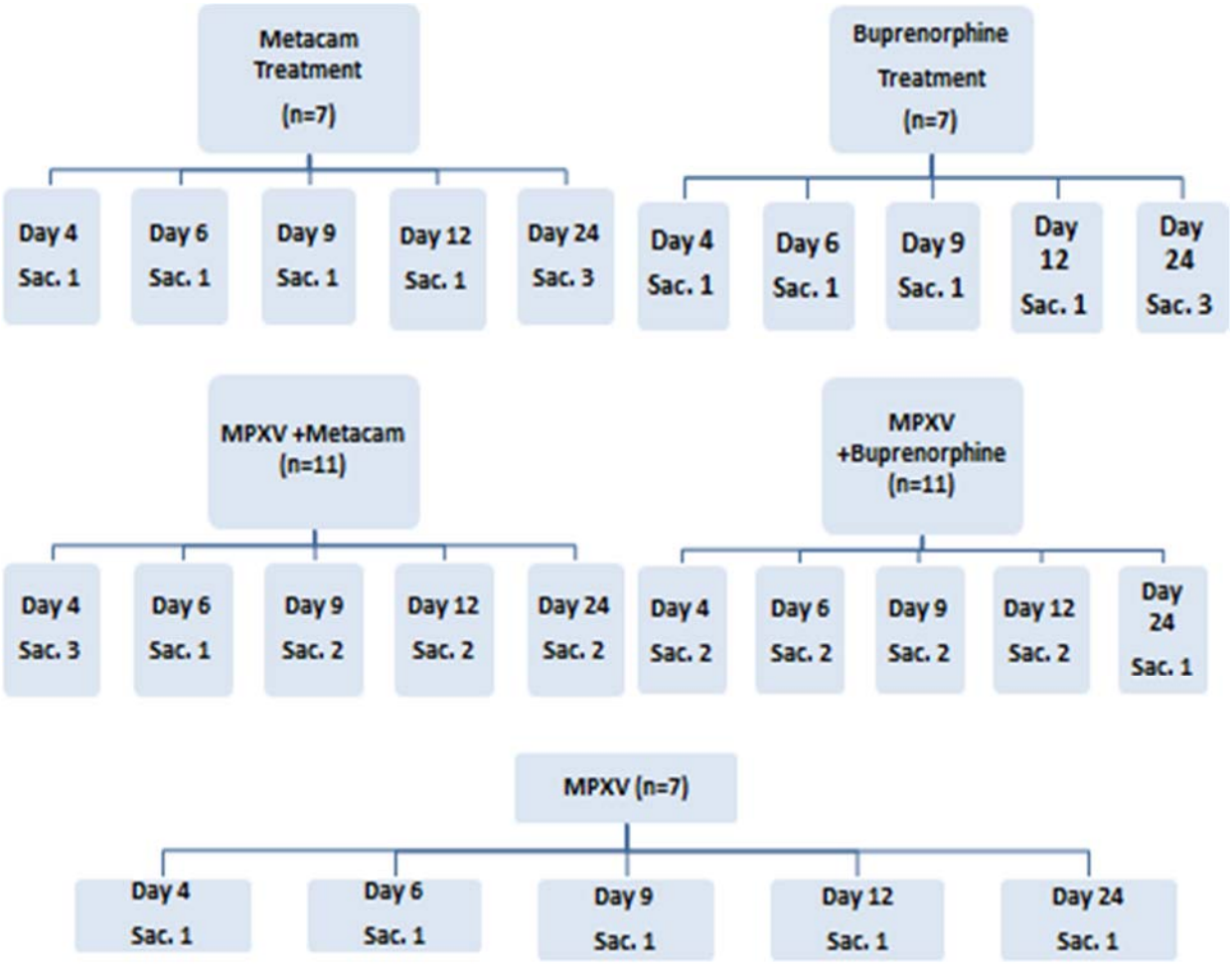

Table 4.2: Clinical and laboratory findings in prairie dogs treated with Metacam (A), treated with Buprenorphine (B), challenged with monkeypox virus (MXPV; C), challenged with MXPV and treated with Metacam (D), challenged with MPXV and treated with Buprenorphine (E). Legend: R.D.: Respiratory depression while under anesthesia; N.O.: nothing observed; N.E. not examined; ɨ: Unscheduled death; ɷ Unsuccessfully infected; ◊ Excluding viral load in lesions.

A. Metacam Controls				
Sacrifice Day p.i.	Prairie dog Number	Maximum Weight loss (%)	Clinical Signs During Course of Study	Gross Pathology
4	12019	0	N.O.	N.O.
6	12017	4.1	N.O.	N.O.
9	12021	1.7	N.O.	N.O.
12	12006	0	Lesion on dorsum from metacam tx	N.O.
24	12029	2.7	N.O.	N.O.
	12036	1.1	Lesion on dorsum from metacam tx	N.O.
	12057	0	Lesion on dorsum from metacam tx	Liver enlarged and pale w/prominent reticular pattern.

B. Buprenorphine Controls				
Sacrifice Day p.i.	Prairie dog Number	Maximum Weight loss (%)	Clinical Signs During Course of Study	Gross Pathology
4	12056	0.6	N.O.	N.O.

6	12001	7.9	N.O.	Slightly friable. Liver, bloody at cut surface
9	12072	4.2	N.O.	N.O.
12	12045	4.2	N.O.	N.O.
24	12055	0	N.O.	Liver is light brown w/nutmeg appearance. Very friable.
	12071	2.4	N.O.	Liver slightly pliable; bleeding on surface.
	12046	3.8	N.O.	Surface of liver adjacent to diaphragm had white multi-focal discoloration.

C. MPXV Controls

Sacrifice Day p.i.	Prairie dog Number	Maximum # of lesions observed	Maximum Weight loss (%)	OPXV Antibodies Detected	Clinical Symptoms During Course of Study	Gross Pathology	Tissue Viral DNA (#positive/#tested)	Viable Virus (#positive/ #tested)	Highest Viral Load at Necropsy
4	12028	0	3.3	N.O.	N.O.	N.O.	4/12	0/12	
6	12058	0	2.4	N.O.	N.O.	N.O.	10/11	8/11	6X10^5 Spleen

9	12014	0	4.2	Neg.	R.D, ruffled fur	Mild lymphadenopathy; gallbladder moderately enlarged; spleen moderately enlarged with a finely nodular appearance of small white lesions; mesentery lymph node slightly enlarged; small intestine thin walled and yellow/mucousy substance	12/12	11/12	1.7X10^8 Spleen
12	12011	2	1.7	Pos.	Nasal discharge	N.O.	11/11	8/11	1.9X10^7 Nasal
24	12034	13	13.7	Pos.	RD, nasal discharge, ruffled fur	Firm and pale brown liver with rounded edges	12/12	1/12	3.4X10^4 Nasal

D. MPXV + Metacam

Sacrifice Day p.i.	Prairie dog Number	Max # of lesions observed	MaxWeight loss (%)	OPXV Antibodies Detected	Clinical Signs During Course of Study	Gross Pathology	Tissue Viral DNA (#positive/#tested)	Tissue Viable Virus (#positive/ #tested)	Highest Viral Load (pfu/gram)/ tissue type◊
4	12027	0	0	N.E.	N.O.	N.O.	5/12	0/12	
	12004	0	4.8	N.E.	N.O.	N.O.	5/12	0/12	
	12112ŧ	0	1.1	N.E.	N.O.	Mild lymphadenopathy	5/12	1/12	2.8X 10^2 SM LN
6	12077	0	8.5	Neg	N.O.	N.O.	11/12	3/12	2.2X 10^4 Spleen
9	12037	1	9.5	Neg.	Ruffled fur, mild bloat in abdomen.	Spleen faintly mottled-possible early internal lesions; possible mild mesenteric ln enlargement; lungs have dark mottling all lobes.	11/12	9/12	1.7X 10^7 Tongue
	12038	1	6.9	Neg.	N.O.	Mild lymphadenopathy.	10/11	8/11	5.8X 10^6 Nasal

	12024ϕ	0	0	Neg.	----	----	----		
12/18	12078	2	10.3	Neg.	Bloated. Ruffled fur. Bloody nose. Urine matted fur.	Mild lymphadenopathy. A few scattered small white nodules on liver. Gallbladder slightly enlarged; Colon moderately gas filled. Linear blood clot in trachea, lungs mottled and hemorrhagic.	12/12	9/12	5.1X 10^7 Tongue
	12114ɪ	18	28.4	Pos	RD, dehydration, bloated, nasal discharge, bloody nose, lethargic.	Mesenteric area covered with yellowish fluid. Friable spleen and abdominal fat. Hepatomegaly and friable liver. Intestinal adhesions.	12/13	10/13	3.1X 10^6 Nasal
24	12096	8	2.2	Pos	Lesion on dorsum from metacam tx . RD	N.O.	10/12	1/12	4.6X 10^2 Nasal

	12059	1	6.1	Pos	Lesion on dorsum from metacam tx . Bloating, nasal discharge, RD, dehydration.	N.O.	11/12	0/12	

E. MPXV + Buprenrophine

Sacrifice Day p.i.	Prairie dog Number	Max # of lesions observed	Max Weight loss (%)	OPXV Antibodies Detected	Clinical Signs During Course of Study	Gross Pathology	Tissue Viral DNA (#positive/#tested)	Viable Virus (#positive/ #tested)	Highest Viral Load at Necropsy
4	12002	0	9.2	Neg.	N.O.	N.O.	4/12	0/12	
	12064	0	6	Neg.	N.O.	N.O.	4/12	0/12	
6	12092	0	2.7	Neg.	N.O.	N.O.	10/12	6/12	2X10^6 Tongue
	12025	**0**	7.7	Neg.	N.O.	N.O.	11/12	1/12	6.2X10^2 Nasal
9	12115	0	3.9	Neg.	N.O.	N.O.	10/12	5/12	6.8X10^5 Small intestine
	12085	0	8.1	Neg.	N.O.	N.O.	9/12	2/12	2.9X10^5 Spleen
12	12049	3	19.1	Pos.	RD, nasal discharge.	Lymphadenopathy. Left kidney possibly dilated.	10/11	8/11	1.9X10^8 Nasal
	12119	0	18.4	Pos.	RD, nasal discharge, facial edema, ruffled fur.	Lymphadenopathy. Lungs have liquid foam on cut surface. Right lung dark and brown on dorsal surface. Liver-friable/ pale. Gas and	12/12	3/12	8.5X10^5 Nasal

						liquid in jejunum.			
24	12091	6	4.6	Pos.	RD.	Liver has nutmeg appearance, areas of discoloration and hepatomegaly). Spleen congested.	3/12	0/12	
	12079ø	----	3.2	Neg.	----	----	----		

Table 4.3: Statistical comparison of blood chemistry values from groups of prairie dogs. Yellow highlighting indicates statistical significance.

ALB

	Metacam+	BUP+	None+	Metacam-	BUP-	None-
Metacam+	---					
BUP+	0.78	---				
None+	1	0.63	---			
Metacam-	0.78	0.74	0.86	---		
BUP-	0.83	0.91	0.79	0.73	---	
None-	0.286	0.6	0.4	0.4	0.44	---

ALP

	Metacam+	BUP+	None+	Metacam-	BUP-	None-
Metacam+	---					
BUP+	0.19	---				
None+	0.79	0.11	---			
Metacam-	0.73	0.03	0.63	---		
BUP-	0.06	0.41	0.036	0.016	---	
None-	0.57	0.8	0.4	0.27	0.19	---

ALT

	Metacam+	BUP+	None+	Metacam-	BUP-	None-
Metacam+	---					
BUP+	0.91	---				
None+	1	0.86	---			
Metacam-	0.19	0.74	0.23	---		
BUP-	0.032	0.29	0.036	0.73	---	
None-	0.38	0.8	0.4	0.8	0.38	---

AMY

	Metacam+	BUP+	None+	Metacam-	BUP-	None-
Metacam+	---					
BUP+	0.56	---				
None+	0.39	0.63	---			
Metacam-	0.91	0.89	0.86	---		
BUP-	0.42	0.56	0.79	0.91	---	
None-	0.19	0.27	0.8	0.53	0.57	---

BUN

	Metacam+	BUP+	None+	Metacam-	BUP-	None-
Metacam+	---					
BUP+	0.91	---				
None+	0.04	0.06	---			
Metacam-	0.08	0.11	0.06	---		
BUP-	0.15	0.02	0.04	0.91	---	
None-	0.1	0.13	0.2	0.13	0.1	---

CA

	Metacam+	BUP+	None+	Metacam-	BUP-	None-
Metacam+	---					
BUP+	0.06	---				
None+	1	0.23	---			
Metacam-	0.9	0.11	1	---		
BUP-	1	0.11	1	0.91	---	
None-	0.57	0.8	0.8	0.53	0.57	---

CRE

GLOB

	Metacam+	BUP+	None+	Metacam-	BUP-	None-
Metacam+	---					
BUP+	0.52	---				
None+	0.25	0.29	---			
Metacam-	0.18	0.09	0.09	---		
BUP-	0.69	0.37	0.21	0.52	---	
None-	0.19	0.2	0.8	0.13	0.14	---

	Metacam+	BUP+	None+	Metacam-	BUP-	None-
Metacam+	---					
BUP+	1	---				
None+	0.54	0.63	---			
Metacam-	0.02	0.03	0.06	---		
BUP-	0.38	0.41	0.25	1	---	
None-	0.81	1	1	0.2	0.38	---

GLU

	Metacam+	BUP+	None+	Metacam-	BUP-	None-
Metacam+	---					
BUP+	0.29	---				
None+	0.79	0.23	---			
Metacam-	0.41	0.06	1	---		
BUP-	0.84	0.11	0.57	0.56	---	
None-	0.19	0.13	0.8	0.8	0.1	---

K

	Metacam+	BUP+	None+	Metacam-	BUP-	None-
Metacam+	---					
BUP+	0.19	---				
None+	0.25	0.11	---			
Metacam-	1	0.49	1	---		
BUP-	0.42	0.78	0.04	0.56	---	
None-	0.86	0.53	0.8	0.8	0.57	---

NA

	Metacam+	BUP+	None+	Metacam-	BUP-	None-
Metacam+	---					
BUP+	0.91	---				
None+	0.57	0.63	---			
Metacam-	0.56	0.69	1	---		
BUP-	0.42	0.41	0.04	0.06	---	
None-	0.57	1	0.8	0.53	1	---

PHOS

	Metacam+	BUP+	None+	Metacam-	BUP-	None-
Metacam+	---					
BUP+	0.19	---				
None+	1	0.4	---			
Metacam-	0.19	0.03	0.4	---		
BUP-	1	0.41	0.79	0.19	---	
None-	0.57	0.13	0.4	0.8	0.57	---

TBIL

Metacam+	BUP+	None+	Metacam-	BUP-	None-

TP

Metacam+	BUP+	None+	Metacam-	BUP-	None-

Metacam+	---					
BUP+	0.76	---				
None+	0.54	0.77	---			
Metacam-	1	0.66	0.29	---		
BUP-	0.76	1	0.38	0.17	---	
None-	1	0.93	1	1	1	---

Metacam+	---					
BUP+	0.41	---				
None+	0.25	0.4	---			
Metacam-	0.73	0.69	0.4	---		
BUP-	1	0.56	0.39	0.73	---	
None-	0.38	0.8	1	0.53	0.48	---

Table 4.4: Comparison of ELISA and neutralization titers in prairie dog serum.

	MPXV	MPXV +Metacam	MPXV + Buprenorphine
Day 12 Avg ELISA	0.384932 (n=2)	0.191386 (n=3)	0.091053 (n=3)
Day 17 ELISA	0.642148 (n=1)	0.676553 (average; n=3)	0.677219 (n=1)
Day 24 ELISA	1.383719 (n=1)	1.081969 (average; n=2)	1.157219 (n=1)
Day 12 Avg. 50% RPR	198.82 (n=2)	283.57 (n=3)	290.67 (n=3)
Day 17 50% RPR	93.07 (n=1)	348.7 (average; n=3)	279.7 (n=1)
Day 24 50% RPR	21750000 (n=1)	949.5 (average; n=2)	385.8 (n=1)

Table 4.5: Kinetics of MPXV viral spread within prairie dogs challenged with MPXV and not treated with analgesic, treated with Metacam, or treated with Buprenorphine. Peak viral load provided in pfu/gram of tissue. ND: No positive samples detected

Tissue Sample	**West Africa MPXV (+ controls)**			**WA MPXV+ Metacam**			**WA MPXV+ Buprenorphine**		
	DNA presence (days)	**Virus presence (days)**	**Peak viral load value (day)**	**DNA presence (days)**	**Virus presence (days)**	**Peak viral load value (day)**	**DNA viral presence value (days)**	**Virus presence (days)**	**Peak load (day)**
Oral Swab	6-17	6-17	$2X10^6$ (9)	4-24	6-21	$5X10^7$ (12)	6-24	6-12	$3X10^5$ (12)
Blood	4-17	9	$1X10^2$ (9)	6-17/18	ND	ND	4-17	ND	ND
Nasal cavity	6-24	6-24	$5X10^7$ (9)	4-24	9-24	$6X10^6$ (9)	6-12	6-12	$2X10^8$ (12)
Salivary glands/SM lymph nodes	6-24	6-12	$3X10^7$ (9)	4-24	4-18	$2X10^5$ (9)	4-12	6-12	$1X10^5$ (12)
Spleen	6-24	6-12	$2X10^8$ (9)	4-24	6-9	$9X10^6$ (9)	4-24	6-12	$3X10^5$ (6)

Tongue	6-24	6-12	$9X10^6$ (9)	6-24	6-18	$5X10^7$ (12)	6-24	6-12	$3X10^6$ (12)
Lungs	4-24	6-9	$5X10^4$ (9)	6-24	9-18	$6X10^5$ (9)	6-12	9-12	$4X10^4$ (12)
Liver	4-24	6-12	$7X10^6$ (9)	4-24	9-12	$6X10^4$ (9)	4-12	12	$2X10^4$ (12)
Small Intestine	6-24	6-12	$2X10^4$ (9)	4-24	9-18	$5X10^5$ (12)	6-12	6-9	$7X10^5$ (9)
Mesenteric LN	6-24	6-12	$3X10^6$ (9)	4-24	6-12	$7X10^3$ (9)	4-12	6-12	$5X10^4$ (6)
Belly skin/lesion	9-24	12	$1X10^6$ (12)	6-24	9-18	$2X10^7$ (18)	12-24	12	$8X10^2$ (12)
Stomach	4-24	9-12	$5X10^3$ (9)	4-24	9-18	$2X10^5$ (9)	4-24	ND	ND
Brain	6-24	9	$2X10^2$ (9)	9-24	9,18	$1X10^2$ (18)	6,12	12	$7X10^3$ (12)

CHAPTER 5

CONCLUSIONS

Monkeypox virus (MPXV) is considered endemic within Africa where it causes sporadic outbreaks of human disease. In 2003, an outbreak of human monkeypox occurred in the US after the importation of infected African rodents. Since the eradication of smallpox (an orthopoxvirus closely related to monkeypox) and cessation of routine smallpox vaccination, there is an increasing population of unvaccinated people that are at risk for orthopoxvirus diseases. As evidenced by continued outbreaks of monkeypox within Africa, the US outbreak, as well as the increased at-risk population, there is a continued need to study this important public health threat, and to have relevant animal models for testing of next-generation vaccines and therapeutics. We have shown through the current and previous studies that Congo Basin MPXV infected prairie dogs consistently shed slightly larger loads of viable virus compared to West African MXPV. Additionally through the current study, we see that Congo Basin MXPV infected animals have a slightly earlier viral kinetics time-line, however West African MXPV infected prairie dogs seem to shed virus for a slightly longer period of time. Furthermore we were able to completely describe the pathology of the MPXV infection within this animal model at key days after infection. Such data will be critical in future studies designed at evaluating anti-virals and vaccines against a MPXV challenge in the prairie dog.

Using the prairie dog MPXV model, we were able to show that when cells are undergoing apoptosis, they generally co-localize with the virus suggesting that the viral invasion of these cells triggers the apoptotic response. Based on our study, there is suggestion that CB MXPV

causes more apoptosis within the spleen compared to WA MPXV, however apoptosis in the liver is most likely being inhibited by both viruses. Although much work has been done looking at how poxviruses inhibit the host immune system in vitro, there is less data from in vivo studies Through our work, we were able to compare protein levels of key subunits involved in pathways upstream of NFkB activation (TLR and RLR pathways) as well as the NFkB pathway during *a in vivo* MPXV infection as well as the amount of apoptosis caused by each MPXV clade. The findings from our studies suggest that there are differences in the amount of apoptosis and NFkB activation and viral suppression dependent on the tissue type infected as well as the viral clade. The ability of Congo Basin MPXV to suppress NFkB activation in more of the tissues we analysed than the West African MPXV clade, suggests that viral inhibition of NFkB may be more important than apoptosis inhibition in regard to viral pathogenicity and virulence.

Importantly, through the use of this animal model we were able to compare the effect of analgesics on a MPXV infection *in vivo*. To do so, we used a low-dose challenge of WA MPXV and treated groups of animals with either Metacam or Buprenorphine. If either of these analgesics caused an increase in viral pathogenesis we expected to see stark differences in our MPXV challenged/analgesic treated animals compared to the MPXV positive/untreated animals (i.e. earlier and increased cutaneous lesion development, increased morbidity/mortality, increased viral loads within tissues). However clinical signs and molecular results between the groups was similar; with the exception of increased trends of morbidity and mortality within the MXPV infected/Metacam treated animals. Based on these observations, as well as the indications of immune suppression, and decreased liver function at day 24 pi, it would not be recommended to give either of these analgesics (especially at the high analgesic dose utilized) for an extended period during a viral infection as was done for the current study (18 days for Metacam and 21

days for Buprenorphine). Evidence against the use of Metacam during a MPXV infection was stronger (particularly given the fact that one Metacam/MPXV challenged animal died during anesthesia and had earlier viable virus after only one day of treatment). However because the differences we observed were so subtle comparing Buprenorphine treated MPXV infected animals to MPXV controls, it is likely the use of this analgesic for short-term pain relief (i.e. less than 7 days) during a WA MPXV infection would result in little differences in pathogenicity. However to confirm this, additional studies with a larger group of animals would be required.

These studies had several limitations, primarily that the numbers in each animal study were low. Because the prairie dog is a relatively large laboratory animal that has to be individually caged, and we are limited by the amount of cage space available within our BSL3 animal laboratories, we are restricted to doing smaller groups of animal numbers. Additionally because these studies are performed under BSL3 conditions including full BSL3 PPE, in order to safely execute these studies we limit the number of animals so that personnel are not working within the BSL3 laboratories for extended hours. Although we had small sample sizes, because we have previously characterized this animal model, we do feel that we can gain meaningful data from the current studies, especially when comparing to previous studies. Additionally the data on the viral inhibition of apoptosis and NFkB activation does not provide definitive proof that MPXV inhibits both of these pathways, but instead suggests that there are differences between tissues and between MPXV clades. This could be specific to this animal model, or a good representation of the complex interplay between the host immune response to viral invasion. Because of this, it is important to utilize this data along with *in vitro* studies as well as additional animal studies to more fully explain the findings from our prairie dog MPXV studies.

Future studies with this animal model would be benefited through the use of *in vivo* imaging techniques. In vivo imaging techniques offer significant advantages over conventional pathogenesis studies including the ability to visualize viral spread and tissue tropism in living animals; obtaining additional data such as previously unidentified sites of viral replication and modes of viral spread; faster and more economical data acquisition and quantification as images can be quantified within minutes after imaging; and significant ethical advantages since experiments can be carried out with fewer animals. Utilization of this novel research will be of great benefit to scientific findings as well as animal welfare . As our studies were lacking in animal numbers, using the in vivo imager would allow us to increase the knowledge gained from the previous studies, while gaining new knowledge not previously obtained. Additionally, it would be beneficial to do a follow-up study with analgesic treatment of Congo Basin MPXV infected animals as the current study utilized West African MPXV during comparisons of analgesic use. Because there may be differences in the way the two viral clades are circumventing the host's immune response, we might observe different results with Congo Basin MPXV, especially with Metacam treatment as it inhibits the NFkB pathway.

Through our current studies, we have again shown that the prairie dog MPXV model is a relevant model for the study of systemic orthopoxvirus disease. The prairie dog model will continue to be important in the testing of novel therapeutics and next generation vaccines and thus our results are important for future studies. Additionally the results suggesting that Congo Basin MPXV is more efficient at inhibiting NFkB compared to West African MPXV, lays the path ahead for future *in vitro* and *in vivo* studies to explore this finding. Taken together, these findings allow for further characterization of differences between MPXV clade pathogenesis, including identifying early sites during viral replication, cellular response to viral infection and

mechanisms the virus uses to evade the immune response. Furthermore we have provided evidence against the use of NSAIDs during prairie dog MPXV challenge studies, and alternatively data that supports of the use of the opioid Buprenorphine. This data will be critical when planning future studies to alleviate pain and suffering of the animals that are challenged with West African MPXV.